

# **A Closed Loop Recycling Process for the End-of-Life Electric Vehicle Li-ion Batteries**

---

A Dissertation

Submitted to the Faculty

of the

WORCESTER POLYTECHNIC INSTITUTE

---

*In partial fulfillment*

*of the requirements for the*

**Degree of Doctor of Philosophy**

*in*

**Materials Science and Engineering**

---

by

**Mengyuan Chen**

May 2020

Approved by:

---

Dr. Yan Wang, Advisor, Professor, Mechanical Engineering

---

Dr. Brajendra Mishra, Head of the Materials Science and Engineering Program

## Abstract

Lithium-ion batteries (LIBs) play a significant role in our highly electrified world and will continue to lead technology innovations. Millions of vehicles are equipped with or directly powered by LIBs, mitigating environmental pollution and reducing energy use. This rapidly increasing use of LIBs in vehicles will introduce a large quantity of spent LIBs within an 8- to 10-year span and proper handling of end-of-life (EOL) vehicle LIBs is required. Over the last several years, the Worcester Polytechnic Institute (WPI) team in the Department of Mechanical Engineering has developed a closed-loop lithium ion battery recycling process and it has been demonstrated that the recovered NMC 111 has similar or better electrochemical properties than the commercial control powder with both coin cells and pouch cells, which have been independently tested by A123 Systems and Argonne National Laboratory. In addition, the different chemical compositions of the incoming recycling streams were shown to have little observed effects on the recovered precursor and resultant cathode material. Therefore, the WPI-developed process applies to different spent Li-ion battery waste streams and is, therefore, general.

During the last few years, industry has the tendency to employ higher-nickel and lower-cobalt cathode material since it can provide higher capacity and energy density and lower cost. However, higher-nickel cathode material has the intrinsic unstable properties and surface modifications can be applied to slow down its degradation. Here, two facile scalable  $\text{Al}_2\text{O}_3$  coating methods (dry coating and wet coating) were applied to recycled NMC 622 and the resultants were systematically studied. The Al-rich layer from the dry coating process imparted improved structural and thermal stability in accelerated cycling performed at 45 °C between 3.0 and 4.3 V, and the capacity retention of pouch cells with dry coated NMC 622 (D-NMC) cathode increased from 83% to 91% compared to Al-free NMC 622 after 300 cycles. However, for wet coated NMC 622 (W-NMC),

the increased surface area accompanying by formation of NiO rock-salt like structure could have negative impacts on the cycling performance.

There exist three challenges for current LIBs' recycling research. First of all, most of the research is done in lab-scale and the scale-up ability needs to be proven. The scale-up ability of our recycling process has been verified by our scale-up experiments. The second challenge resides in the flexibility, here once again, with our intentionally designed experiments that having various incoming chemistries, the flexibility is validated. The last challenge is the lack of reliable testing because most of the testing is conducted with coin cells. Coin cells are relatively simple format and lacks persuasion. Here, with various industrial-level cell formats that ranging from coin cell, single layer pouch cell, 1Ah cell and 11Ah cell, a reliable and trustworthy testing is established. With this validation, the hesitation of recruiting recycled materials into industry shouldn't exist.

## **Acknowledgements**

I would like to express my deep gratitude to my advisor, Prof. Yan Wang, for his persistent support and professional guidance. He disciplines himself with high standards and shows me all the excellent qualities a researcher should have. He will be a role model I am following in my careers.

I am honored to have Professor Brajendra Mishra, Professor Jianyu Liang, Professor Yu Zhong, Dr. Eric Gratz as committee members. Thanks for their help, encouragement and guidance during my graduate studies. Special thanks to Professor Richard D. Sisson, who is always there and provides great help to me. His generosity and kindness make MSE department look like a big family for all of us. I want to thank Dr. Boquan Li for his continuous help and technical guidance with XRD, SEM equipment. Many thanks to Rita Shilansky, who treats me as a sincere friend, gave me generous help and constant care.

I would like to thank all the collaborator and partners in this USABC recycling project. Paul Gionet, Ian O'Connor, Leslie Pinnell, Dennis Bullen, Jun Wang from A123 Systems; David Robertson from ANL; Eric Gratz, Zhangfeng Zheng, Qing Yin from Battery Resourcers; Renata Arsenault from Ford. Special thanks to Renata Arsenault for helping revising literatures.

I would like to thank my colleagues in Electrochemical Energy Laboratory, Zhangfeng Zheng, Qiang Wang, Bin Chen, Ruihan Zhang, Sungyool Bong, Jin Liu, Yubin Zhang, Xiaotu Ma, Yangtao Liu, Qing Yin, Azhari Luqman, Panawan Vanaphuti, Zifei Meng, Chao Shen, Dapeng Xu, Jiayu Cao, Yadong Zheng, Jinzhao Fu, Jiajun Chen, Zeyi Yao, Yilun Tang, who have been helping me a lot in the labs.

I thank my parents, boyfriend and friend for their unconditional love and care. Without their support, I won't achieve anything.

I acknowledge the financial support of the Department of Energy, the National Energy Technology Laboratory under award number DE-EE0006250 with the United States Advanced Battery Consortium LLC (USABC LLC).

#### Disclaimer

This report was prepared as an account of work sponsored by an agency of the United States Government and USABC, LLC. Neither the USABC, LLC, the United States Government, nor any agency thereof, nor any of their employees, makes any warranty, expresses, implies, or assumes any legal liability or responsibility for the accuracy, completeness, or usefulness of any information, apparatus, product, or process disclosed or represents that its use would not infringe privately owned rights. Reference herein to any specific commercial product, process, or service by trade name, trademark, manufacturer, or otherwise does not necessarily constitute or imply its endorsement, recommendation, or favoring by the United States Government or any agency thereof. The views and opinions of authors expressed herein do not necessarily state or reflect those of the United States Government or any agency thereof or those of USABC, LLC.

## Table of Contents

Abstract .....	I
Acknowledgements.....	III
Table of Contents .....	V
Chapter 1 Introduction of Recycling End-of-Life Electric Vehicle Lithium-Ion Batteries.....	1
Chapter 2. Closed Loop Recycling of Electric Vehicle Batteries to Enable Ultrahigh Quality Cathode Powder .....	49
Chapter 3. High Performance Cathode Recovery from Different Electric Vehicle Recycling Streams.....	75
Chapter 4. Systematic Comparison of Al <sup>3+</sup> Modified NMC 622 from Recycling Process .....	93
Chapter 5. Systematic Electrochemical Comparisons between Recycled NMC Powder with Commercially Controlled Powder .....	115
Chapter 6. Summary and Recommendations for Future Work.....	143
Chapter 7. Publications and Presentations .....	147

# **Chapter 1 Introduction of Recycling End-of-Life Electric Vehicle Lithium-Ion Batteries**

## **Abstract**

Lithium-ion batteries (LIBs) play a significant role in our highly electrified world and will continue to lead technology innovations. Millions of vehicles are equipped with or directly powered by LIBs, mitigating environmental pollution and reducing energy use. This rapidly increasing use of LIBs in vehicles will introduce a large quantity of spent LIBs within an 8–10-year span. Proper handling of end-of-life (EOL) vehicle LIBs is required, and multiple options should be considered. This paper demonstrates that the necessity for EOL recycling is underpinned by leveraging fluctuating material costs, uneven distribution and production, and the transport situation. From a life-cycle perspective, remanufacturing and repurposing extend the life of LIBs, and industrial demonstrations indicate that this is feasible. Recycling is the ultimate option for handling EOL LIBs, and recent advancements both in research and industry regarding pyrometallurgical, hydrometallurgical, and direct recycling are summarized. Currently, none of the current battery recycling technologies is ideal, and challenges must be overcome. This article is anticipated as a starting point for a more sophisticated study of recycling, and it suggests potential improvements in the process through mutual efforts from academia, industry, and governments.

## **Scope and Method of This Introduction**

In this introduction, the needs and options to address end-of-life (EOL) lithium-ion batteries (LIBs) are first discussed. Furthermore, the current status of LIB recycling, including academic innovations and industrial demonstrations, are systematically reviewed, focusing on

pyrometallurgical, hydrometallurgical, and direct recycling methods. The challenges facing current recycling technologies are analyzed, along with potential suggestions or solutions. This study was conducted by establishing scope and approach, searching related literature and industry demonstrations, screening for inclusion, and providing insights. In addition, experts and industry representatives were interviewed to validate the accuracy of this study.

## **1. Needs**

LIBs currently dominate the market for electric vehicles (EVs), due to their high energy and power density, and long life-span, combined with sweeping cost reductions over the last decade. Millions of electric and hybrid vehicles that are powered by LIBs have been sold to date, and this number is projected to increase significantly in the coming years with the continued electrification of the automobile industry. According to Avicenne Energy,<sup>1</sup> LIBs represent the highest growth and the major portion of industry investments. For example, worldwide, LIBs sales have increased by an average of 16% per year from 1996 to 2016. In 2016, the global LIBs market was over \$20 billion at cell level. By 2025, it is projected to reach ~\$40 billion, of which more than \$15 billion will be from the hybrid and electric vehicle (xEV) market. In the United States, there will be 1.4 million EV sales in 2035, as forecast by the U.S. Energy Information Administration (EIA). This high demand for LIBs by the EV market will translate into a large number of spent LIB packs, estimated at 1 million in 2030, and 1.9 million in 2040. The cumulative EOL LIB packs generated between 2015 and 2040 will be as many as 21 million.<sup>2</sup> Although the LIBs in these vehicles are expected to last at least 8-10 years, EOL options must be considered now to ensure infrastructure readiness when recycling needs reach greater volume. In fact, LIBs recycling is critical for several key reasons: buffering the uncertainties associated with fluctuating material costs, rebalancing the

uneven distribution and production sourcing of strategic materials, and addressing transport situation.

### **1.1 Fluctuating Material Costs**

LIB costs have decreased by a factor of 5 over the past ten years (~\$1,000/kWh in 2005 to ~\$200/kWh in 2016).<sup>3</sup> This is primarily a result of ever-increasing manufacturing scale. However, material costs have been fluctuating significantly in the last few years. For example, the price of lithium increased 3-4 fold (~ \$5/kg in 2010 to ~\$20/kg in 2017) and dropped back to ~\$10/kg at the end of 2018.<sup>4,5</sup> Since early 2017, the price of cobalt has tripled (from \$30/kg to \$90/kg in March 2018), and dropped back to less than \$40/kg in early 2019.<sup>6</sup>

### **1.2 Uneven Distribution and Production**

The production of the main materials used in lithium ion batteries is dominated by a few countries, shown in **Figure 1**.<sup>7</sup> More than half of the cobalt used is from the Congo.<sup>8</sup> Australia and Chile control ~80% of lithium production, while China controls ~70% of graphite production.

### **1.3 Transport Situation**

LIBs are classified as category 9 hazardous materials, due to their unstable thermal and electrical qualities,<sup>9</sup> and because of the risk of thermal runaway if improperly handled during transportation. LIBs must undergo and pass a suite of national and/or international tests prior to shipment by road, sea, or air. Having local and mature recycling facilities has many advantages (economic, access to strategic materials, etc.) over shipping batteries to countries with less stringent regulations that govern transport and recycling.

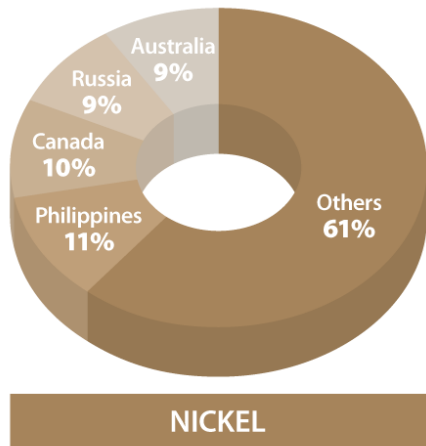
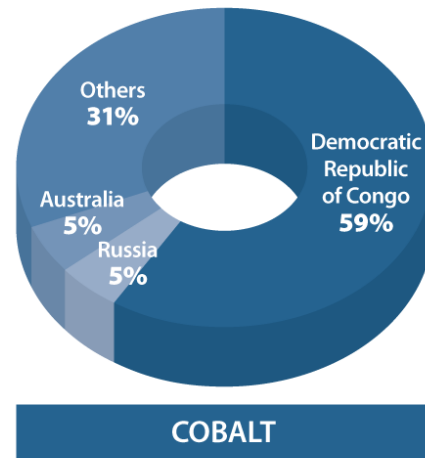
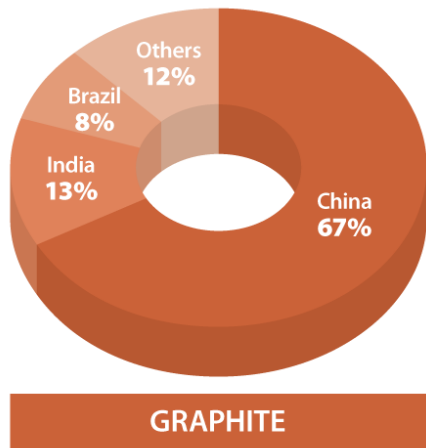
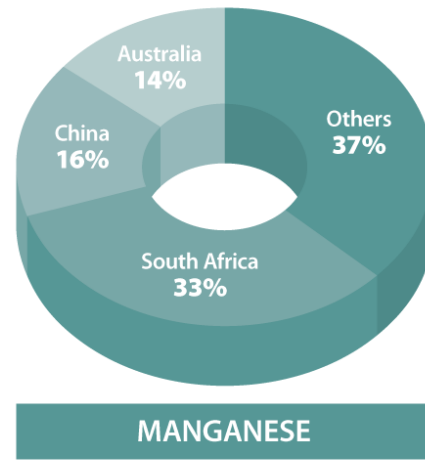
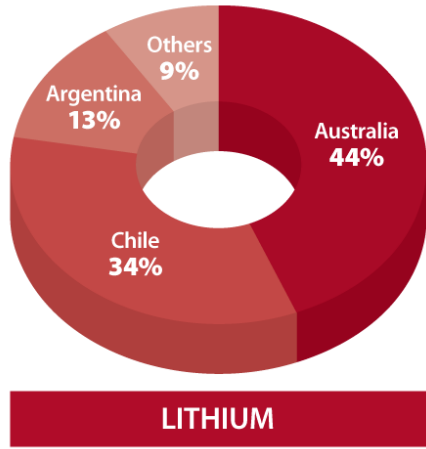


**Figure 1: Global production of main lithium ion battery materials.** Lithium, graphite, nickel, manganese, and cobalt represent the five key elements of current LIBs. The global production is unevenly distributed and dominated by a few countries.

Reconciling the projected exponential growth in the demand for EV batteries, the possibility of fluctuating prices for lithium and cobalt, and unsustainable production of strategic materials poses a serious supply concern for the EV industry. Therefore, EOL options for EV LIBs must be addressed with appropriate urgency. For example, given the high costs of transporting spent LIBs, resulting from their hazardous materials classification, it would be ideal if LIBs could be recycled or rendered inert locally.

## **2. Options for end-of-life EV batteries**

There are three possible options for EOL EV batteries, depending upon their design, quality, and state of health (SOH): remanufacturing, repurposing, and recycling. Remanufacturing and repurposing extend the usage of LIBs, while recycling closes the loop. To capture the maximum value of LIBs, the ideal scenario would involve remanufacturing or repurposing first, followed by recycling.<sup>10,11</sup> Remanufacturing is the most desirable EOL scenario in terms of maximizing the value and minimizing life-cycle energy consumption and emissions; however, this option is the most stringent in terms of battery quality requirements. Going directly from first life use (in-vehicle) to recycling is less desirable from a life-cycle standpoint, because of insufficient benefit, uncertainty about performance, and the unavoidable material and energy losses that occur in the process. However, recycling is beneficial because LIBs become part of the circular economy instead of becoming waste. That said, recycling returns valuable materials back into the value

chain promptly, partially mitigating the need for extraction of new resources. Repurposing batteries for a non-automotive (second life) use lies between these two scenarios, in terms of desirability. However, considering the scalability and ease of processing, recycling is probably the simplest and certainly the most broadly applicable solution for EOL EV batteries. It should be noted that, even if batteries are first remanufactured or repurposed, they will ultimately be recycled. The first two options only delay the recycling horizon. In this introduction, recycling is the main focus of analysis.

## **2.1 Remanufacturing**

Remanufacturing refers to refurbishing EV batteries and deploying them in their original (automotive) applications. This requires that the EV batteries have acceptable SOH and meet all OEM-specified requirements for power, energy, cycle life, etc. According to the United States Advanced Battery Consortium (USABC), batteries are generally not suitable for EV use when the delivered capacity or power of a cell, module, or pack is less than 80% of its original rated value.<sup>12</sup> Examination of the entire battery pack could show that only a small percentage of cells failed to hold the required capacity, and abandoning the entire battery pack represents an incomplete usage. The idea behind remanufacturing is to replace inferior cells or modules in the packs and return the remanufactured battery packs for use in EVs.

### **Industry demonstrations**

The number of EOL vehicle LIBs is likely to reach ~50% of the demand for new vehicle LIBs between the year of 2020 and 2033, and according to the cost-benefit analysis by Foster, remanufacturing spent LIBs saves 40% of the cost of using new batteries.<sup>13</sup> Remanufacturing LIBs

involves diagnosis, partial disassembly of battery packs, replacement of damaged cells or modules within the battery packs, and then reassembly into new battery packs.

Spiers New Technologies (SNT), a US-based startup located in Oklahoma, offers 4R services (repair, remanufacturing, refurbishing, and repurposing) for vehicle original equipment manufacturers (OEMs), including Nissan and General Motors. Characterized and sorted using SNT's comprehensive diagnostic evaluations, EOL vehicle battery packs may be remanufactured to their original use (per OEM specifications) or be repurposed to second-life redeployment in an alternate application. In May 2018, SNT announced its new production center at Ede in the Netherlands and launched remanufacturing services for the rapidly growing European automotive and energy markets. Looking ahead, SNT is actively promoting market development in China, hoping to provide remanufacturing services to the largest xEV market worldwide.

Global Battery Solutions (formerly Sybesma's Electronics) has been repairing electronics since 1958, and recently the company stepped into the field of repairing xEV's LIBs in western Michigan. Global Battery Solutions offers repair, remanufacturing, repurposing, and recycling, depending on the status of the degraded LIBs. The company states that remanufactured batteries can cut replacement cost by over 70%, and these remanufactured cells have started to be used by BAE Corporation.

## **2.2 Repurposing**

Repurposing is another option for EOL batteries, whereby batteries are reconfigured for 'second life' use in less-stressful applications (such as stationary storage), thus extracting more value by extending their useful lifetime beyond their automotive 'first life' usage. In the case where a pack is unable to hold a desired capacity, for example 80%, remanufacturing seems economically

unfavorable, and repurposing becomes a viable path. Repurposing not only requires replacing damaged cells or modules but also requires reconfiguring the modules or packs, including establishing a new battery management systems (BMS), to accommodate a non-vehicle application. However, repurposing faces numerous challenges, including reliably grading the EOL packs or modules, dealing with the many different designs and performance metrics, liability, and the cost of reconfiguration, which must compete with new, cheaper batteries. For example, the original xEV manufacturer has the responsibility to offer vehicle-use qualified LIBs. However, the risks and liability of using batteries in non-original functions are not well defined. If repurposing is to make a significant impact, liability standards need to be developed.<sup>14</sup> Prospects for battery repurposing require feasible economics and an underlying business case. Testing, grading, and repackaging are the main cost contributors for repurposing EOL batteries, and costs could be minimized by exploiting more advanced technologies. For example, BMS could be used to transmit SOH information and thus expedite testing and grading operations. Also, service-based business models could facilitate increased usage of repurposed batteries by minimizing consumers' concerns regarding depleted capacity.<sup>15</sup> Customers intuitively distrust degraded batteries, but that uncertainty can be obviated if the manufacturer delivered more value-added services, such as a warranty, consulting, installation and maintenance for repurposed batteries.<sup>16</sup>

### **Industry demonstrations**

Repurposed EOL batteries can be employed in various second-use systems, such as peak shaving, backup, frequency regulation, renewables integration, and EV charging.<sup>17</sup> Differentiated by power and time scale, EOL batteries are repurposed for optimal alignment with the technical requirements of second-use applications.<sup>14</sup> In one example, Nissan's repurposed EV LIBs are used in the xStorage System: xStorage Home is an integrated solar and home energy storage system; xStorage

Building is a robust solution to efficiently power businesses that have high energy-consumption demands.<sup>11</sup> As the largest energy storage system manufactured by second-life LIBs in Europe (4MW; 4MWh), xStorage Building uses 280 Nissan LEAF batteries and has been used as back-up power in Amsterdam ArenA, home to the AFC Ajax football team and a world-famous entertainment venue.<sup>18</sup> In another example, General Motors utilized five repurposed Chevrolet Volt batteries in tandem with solar arrays and wind turbines, to power GM's Enterprise Data Center in Milford, Michigan.<sup>19</sup> Deployment in the charging infrastructure is another option for repurposed EOL batteries and, to demonstrate this potential application, Renault EOL EV batteries were installed on highways in Belgium and Germany in August 2017.<sup>19</sup>

### **2.3 Recycling**

Recycling is the third option, which can and must accommodate battery packs of all designs and states of health. However, the multiplicity of material chemistries used in today's EV LIBs increases recycling complexity, presenting a few technical and economic hurdles that must be addressed to enable efficient, large-scale automotive battery recycling. First, LIB packs are complex structures, comprised of multiple modules, in which numerous pouch, prismatic, or cylindrical cells are connected in a variety of parallel-series configurations (welding, wire bonding, and mechanical joining are common joining techniques used within LIB cells, modules, and packs).<sup>20</sup> The respective architectures of LIB packs, modules, and cells vary significantly from manufacturer to manufacturer. Within the cells, the chemical composition of active materials also varies among manufacturers and continues to evolve. Cathode materials in xEVs can be any one of or a mixture of  $\text{LiCoO}_2$  (LCO),  $\text{LiNi}_x\text{Mn}_y\text{Co}_z\text{O}_2$  (NMC,  $x+y+z=1$ ),  $\text{LiFePO}_4$  (LFP),  $\text{LiMn}_2\text{O}_4$  (LMO), and  $\text{LiNi}_x\text{Co}_y\text{Al}_z\text{O}_2$  (NCA,  $x+y+z=1$ ), and manufacturers are moving increasingly toward higher nickel/lower cobalt chemistries, in response to cost and availability concerns. This leads to

a weakening of existing battery recycling business models, which depend largely on the recovery of high-value cobalt.<sup>21</sup> The cathode material represents the highest value in the LIB, and, as such, recovering cathode as the final recycling process output is economically desirable. Of course, recycling more battery materials such as the anode, foils, and electrolyte further augments recycling process margins, thereby enhancing the sustainability of the recycling ecosystem.

Recycling has been successfully implemented for EOL lead-acid and nickel metal hydride (NiMH) batteries. For example, the recycling rates of lead-acid batteries in both the United States and Europe approach 100%. Collection is ensured via a value-driven model, which does not yet exist for LIB technology. Recycling rates of small-format LIBs (in the consumer electronics industry) have been reported as low, suffering from low collection rates. As noted, LIB technology faces more recycling-related challenges than its lead-acid or NiMH predecessors. First, at least five different cathode chemistries are being widely used in commercial LIBs, with many EV batteries also using mixed cathodes (a mixture of two or three cathode materials in a single cell). The vast research efforts presently directed at cathode materials are certain to produce an even more variable supply chain for recyclers to process. Because the supply chain for recyclers fluctuates significantly and includes LIBs with many different cathode (and other) materials, if a recycler cannot recover pure and consistent material, the recoverable value will be low and inconsistent. Since cathode materials account for ~40% of the material value in typical LIBs, recycling the cathode materials is especially important for optimal economics. The three different battery recycling technologies are shown in **Figure 2**: a) Pyrometallurgical processes, b) Hydrometallurgical processes, and c) Direct recycling processes. The first two methods are established and starting to operate at industrial scales, and the third is presently at the lab/pilot

scale. Novel approaches in all three categories are the subject of extensive development in industry and academia.

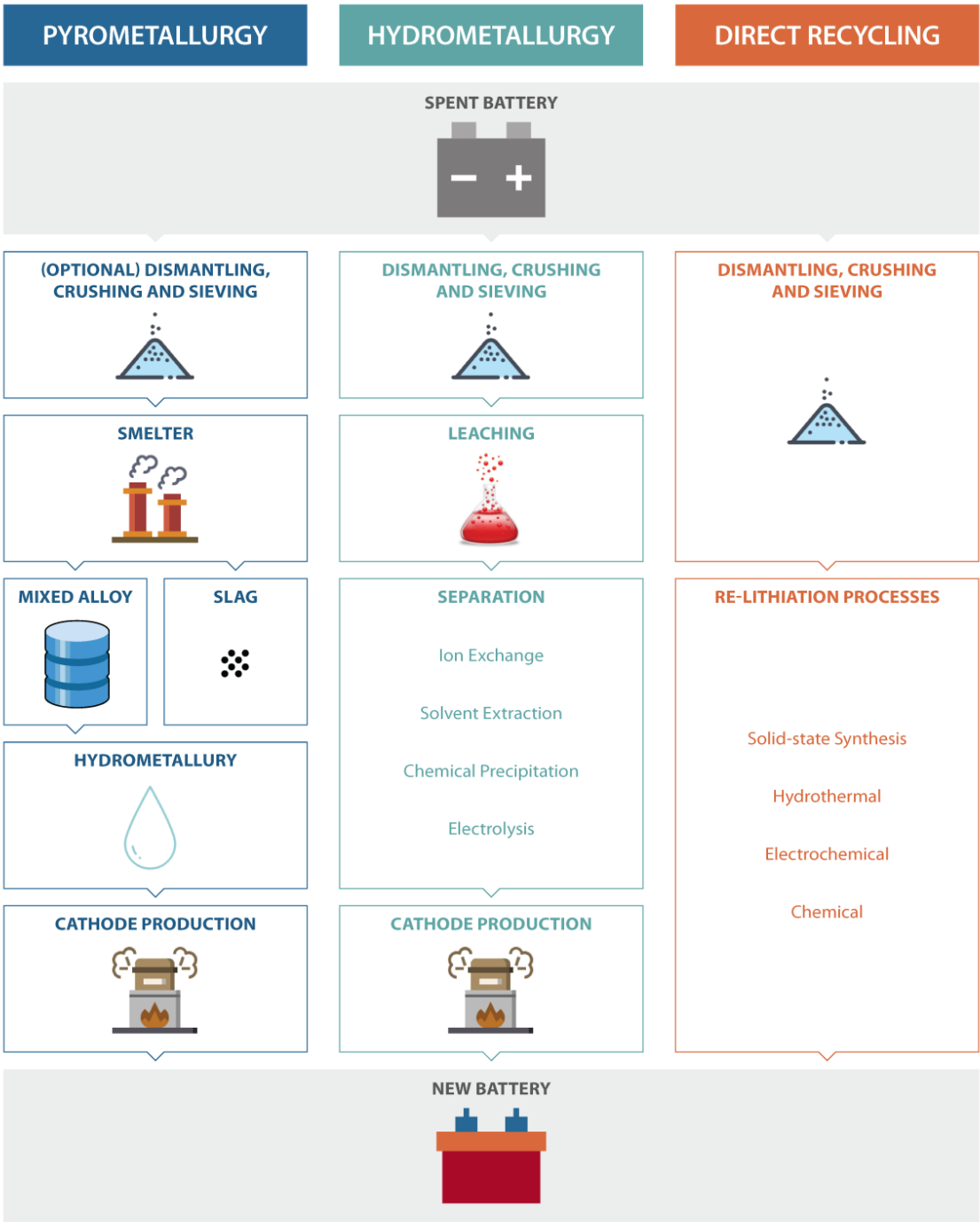


**Figure 2. Different Recycling Technologies.** Currently there are three major LIB-recycling processes including pyrometallurgy, hydrometallurgy, and direct recycling. Pyrometallurgical process is a high-temperature smelting process, which usually involves burning and subsequent separation. Hydrometallurgical process is achieved using aqueous chemistry, via leaching in acids (or bases) and subsequent concentration and purification. Direct recycling directly harvests and recovers active materials of LIBs, while retaining their original compound structure. Pyrometallurgy and hydrometallurgy are being operated at industrial level, and direct recycling is at lab and pilot scale.

### **2.3.1 The Pyrometallurgical Process**

The Pyrometallurgical Process is a high-temperature smelting process, which usually involves two steps.<sup>22</sup> First, LIBs are burned in a smelter, where compounds are broken down and organic materials, such as plastic and the separator, are burnt away. Then, new alloys are generated through carbon reduction.<sup>23</sup> In the subsequent steps (often hydrometallurgical), metal alloys are further separated to recover pure materials. In this process, only expensive metals (cobalt (Co), nickel (Ni), and copper (Cu)) are recovered with greatest efficiency. The anode, electrolyte, and plastics are oxidized and supply energy for the process. Lithium is entrained in the slag fraction and can be recovered with added processing (which comes with associated cost and energy), and lithium's recent increase in value has made its recovery feasible for some recyclers. Aluminum serves as a reductant in the furnace and decreases the need for fuel. Pyrometallurgical processes have generated relatively successful business models to date, due to the high cobalt content of lithium ion batteries that are used in portable electronics. However, as EV batteries trend toward lower

cobalt content, the business models will become less attractive. The main advantages of pyrometallurgical processes are: 1) a simple and mature process, 2) sorting and size reduction are not necessary - a mixture of LIBs and NiMH batteries can be recycled, 3) the output consists of basic, elemental ‘building blocks’ that can be used in synthesizing new cathode materials of many different chemistries. The main disadvantages are: 1) CO<sub>2</sub> generation and high energy consumption during the smelting process, 2) the alloy requires further processing, which increases the total recycling cost, 3) many of the materials in LIBs are not recovered (e.g., plastics, graphite, aluminum). The process recovers Co and Ni from the cathode materials and Cu from the anode current collector, which only account for ~30 wt% in LIBs for electronics, and 4) the business model may not work well for EV batteries, due to the low Co concentration. In addition, industry is moving towards reduced cobalt or, ultimately, cobalt-free cathode materials.

### **Recent progress**

Pyrometallurgical processes prevail widely in industry because of their simplicity and high productivity; some of the technical advancements are shown in **Table 1**. In general, slag systems can be designed to optimize recovery efficiencies of metals in LIBs during the smelting reduction processes. CaO-SiO<sub>2</sub>-Al<sub>2</sub>O<sub>3</sub> and FeO-SiO<sub>2</sub>-Al<sub>2</sub>O<sub>3</sub> were primarily employed as slag systems in pyrometallurgical processes, whereas the recovery of manganese and lithium was low.<sup>22</sup> Lately, Ren et al. adopted a novel slag system (MnO-SiO<sub>2</sub>-Al<sub>2</sub>O<sub>3</sub>) and preferentially recovered manganese and lithium. Co-Ni-Cu-Fe alloy and lithium containing manganese-rich slag were produced, and with the further leaching of the manganese-rich slag, the recovery rates of Mn and Li reached 79.86% and 94.85%.<sup>24</sup> Lithium exists in slag as compound and is hard to be recycled by pyrometallurgy, due to its high melting/boiling point. Recently, Dang et al. proposed to recover lithium from slag by evaporation during chlorination roasting, and they found the best chlorine

donor, donor dosage, roasting temperature, and time by experimenting on the simulated slag, resulting in a lithium recovery efficiency of 97.45%.<sup>25</sup>

In-situ reduction roasting attracts significant research interest and is being studied in the laboratory. The ‘in situ’ means that no other additives are needed in this process, and spent batteries can be directly transformed into useful goods via pyrolysis.<sup>26-28</sup> Spent battery systems whose cathode is  $\text{LiCoO}_2$  and  $\text{LiMn}_2\text{O}_4$  have been tested through in-situ recovery.<sup>26,28</sup> In the process of oxygen-free roasting, mixed electrode materials were transformed to  $\text{Li}_2\text{CO}_3$  and metal/metal oxide without any additives.<sup>26,28</sup> Lithium is released from the oxygen framework within the electrode crystal structure and converted to  $\text{Li}_2\text{CO}_3$ . Afterwards, Mao and Xiao provided a theoretical analysis of in-situ recovery and developed a collapsing model, in which graphite, having a stronger affinity to oxygen than lithium and cobalt, causes the collapse of oxygen octahedrons and the transformation of Li to  $\text{Li}_2\text{CO}_3$ .<sup>27,29</sup> They found that burning graphite promoted the pyrolysis of lithium cobalt oxide, due to the coupling reaction between them. Consequently, the decomposition temperature of lithium cobalt oxide decreased from 1,436K to 1,173K. The coupling reaction and collapsing model explained the underlying principles of in-situ recovery, guiding related development efforts in academia and industry.<sup>29</sup>

**Table 1: Technical advancements in pyrometallurgical recycling processes in recent literature**

<b>Pyrometallurgical process</b>	<b>Product and efficiency</b>	<b>Significance</b>
<ul style="list-style-type: none"> <li>• Slag system: <math>\text{MnO-SiO}_2\text{-Al}_2\text{O}_3</math></li> <li>• Smelting condition: 1475 °C, 30 mins</li> </ul>	<ul style="list-style-type: none"> <li>• Co-Ni-Cu-Fe alloy and lithium containing Mn-rich slag</li> <li>• Recovery efficiencies of Co, Ni and Cu: 99.79%, 99.30% and 99.30%</li> <li>• Leaching efficiencies of Mn and Li: 79.86% and 94.85%</li> </ul>	Preferential recovery of Mn and Li based on the novel slag system <sup>24</sup>

<ul style="list-style-type: none"> <li>• Simulated slag: SiO<sub>2</sub>-CaO-Al<sub>2</sub>O<sub>3</sub>-Li<sub>2</sub>O</li> <li>• Chlorination roasting condition: 1000 °C, 90 mins</li> </ul>	<ul style="list-style-type: none"> <li>• LiCl</li> <li>• Recovery efficiencies of Li from slag: 97.45%</li> </ul>	Innovative method to recycle lithium from slag pyrometallurgically <sup>25</sup>
<ul style="list-style-type: none"> <li>• Oxygen-free roasting: 1000 °C, 30 mins</li> <li>• Wet magnetic separation</li> </ul>	<ul style="list-style-type: none"> <li>• Co, Li<sub>2</sub>CO<sub>3</sub>, C</li> <li>• Recovery efficiencies of Co, Li and graphite: 95.72%, 98.93% and 91.05%</li> </ul>	In situ recycling of cobalt, Li <sub>2</sub> CO <sub>3</sub> and graphite in LCO/C battery system <sup>26</sup>
<ul style="list-style-type: none"> <li>• 973 K, 30 mins</li> <li>• Vacuum condition (&lt;1kPa)</li> </ul>	<ul style="list-style-type: none"> <li>• Li<sub>2</sub>CO<sub>3</sub></li> <li>• Recovery efficiency and purity of Li: 81.90% and 99.7%</li> </ul>	In situ recycling of Li <sub>2</sub> CO <sub>3</sub> from spent LCO/LMO/NMC <sup>27</sup>
<ul style="list-style-type: none"> <li>• Oxygen-free roasting: 1073 K, 45 mins</li> </ul>	<ul style="list-style-type: none"> <li>• Li<sub>2</sub>CO<sub>3</sub> and Mn<sub>3</sub>O<sub>4</sub></li> <li>• Recovery efficiency of Li: 91.30%</li> <li>• Purity of Mn: 95.11%</li> </ul>	In situ recycling of Li <sub>2</sub> CO <sub>3</sub> and Mn <sub>3</sub> O <sub>4</sub> in LMO/C battery system <sup>28</sup>
<ul style="list-style-type: none"> <li>• Reduction roasting: 650 °C, 3 hrs, 19.9% carbon dosage</li> <li>• Carbonated water leaching and acid leaching</li> </ul>	<ul style="list-style-type: none"> <li>• Li<sub>2</sub>CO<sub>3</sub>, NiSO<sub>4</sub>, CoSO<sub>4</sub> and MnSO<sub>4</sub></li> <li>• Water leaching efficiency of Li: 84.7%</li> <li>• Acid leaching efficiency of Ni, Mn and Co: &gt;99%</li> </ul>	A simple and efficient reduction roasting process to recover a NMC/C battery system <sup>30</sup>

## Industry demonstrations

In industry, Umicore utilizes the pyrometallurgical process to recycle LIBs. With the use of an ultra-high temperature (UHT) method, Umicore can handle 7,000 metric tons per year, and dangerous pretreatment can be eliminated. The UHT process generates a high-value alloy (Co, Ni, Cu) and slag for construction additives. Further separation or purification steps involve hydrometallurgical techniques (leaching, solvent extraction, precipitation) to produce new cathode materials, such as LCO and NMC. Previously, the lithium reportedly existed in the slag, which is used largely for construction,<sup>22,31,32</sup> but recently, Umicore has demonstrated that, with further processing, the slag from Li-ion batteries can be integrated into standard Li-recovery flowsheets, through cooperation with external partners.<sup>33</sup>

Accurec utilizes vacuum thermal recycling (VTR) to treat LIBs, although VTR was originally developed for precious metal recovery. The combined pyrometallurgical and hydrometallurgical process (EcoBatRec) was finalized in 2016. Spent LIBs are firstly treated mechanically (disassembly) to remove electronic fractions and plastic covers, and then VTR (distillation and pyrolysis) is performed to extract the electrolyte condensate. After crushing, classification, and sorting, Al, Cu, and steel are recovered by sieving, magnetic separation, and air separation, while the electrode materials are agglomerated to pellets with binder and converted into a Co-based alloy by smelting.<sup>21,22,31,34-36</sup> Lithium containing slag (also produced in this process) can be leached out by acid and converted to lithium carbonate/chloride.<sup>31</sup>

Sony/Sumitomo in Japan recycles spent LIBs using a combined pyrometallurgical and hydrometallurgical processes. At the Sony plant, during a calcination at 1,000 °C, plastics and electrolyte are burned off, leaving metallic parts and active materials. Fe, Cu, and Al can be separated magnetically, while active materials are sent to Sumitomo for further hydrometallurgical recycling, where cobalt is recovered as cobalt oxide. The recovered cobalt oxide has high purity and can be used for the fabrication of new cathode materials.<sup>31,34,35,37</sup> Recently, Sumitomo announced its first practical method to recover copper by pyrometallurgy and nickel by hydrometallurgy.<sup>38,39</sup> With the utilization of this processing flow, more value is extracted from spent LIBs, and the depletion of resources is further addressed.

The pyrometallurgical processes of Inmetco and Glencore (formerly Xstrata Nickel) were not originally designed for lithium ion batteries, and consequently some of the materials, including lithium, are not recovered. Inmetco utilizes a direct-reduced iron process to treat LIB waste, and the recovered Co, Ni, and Fe are used for the production of an iron-based alloy.<sup>22,31,37,40</sup> Glencore processes batteries as secondary feedstock in the extractive routes of Co, Ni, and Cu. With an

added hydrometallurgical process, valued metals such as nickel, cobalt, and copper are recovered.<sup>21,22,31,35,37,41</sup>

### **2.3.2 The Hydrometallurgical Process**

In this process, material recovery is achieved using aqueous chemistry, via leaching in acids (or bases) and subsequent concentration and purification. For LIBs, ions in solution are separated with various technologies (ion exchange, solvent extraction, chemical precipitation, electrolysis, etc.) and precipitated as different compounds.<sup>42</sup> The main advantages of the hydrometallurgical process are: 1) high purity materials can be generated, 2) most LIB constituents can be recovered, 3) low temperature operation, and 4) lower CO<sub>2</sub> emissions as compared with the pyrometallurgical process.<sup>43</sup> The main disadvantages of the hydrometallurgical processes include: 1) a need for sorting, which requires increased storage space and adds to process cost and complexity, 2) the challenge of separating some elements (Co, Ni, Mn, Fe, Cu, Al) in the solution, due to their similar properties, which can lead to higher costs, 3) the expense of waste water treatment and associated costs.

#### **Recent progress**

Some technical hydrometallurgical improvements regarding leaching, solvent extraction, chemical precipitation, and sol-gel, reported in recent literatures, are listed in **Table 2**.

#### **Leaching**

Leaching dissolves the metals present in EOL LIBs, and the subsequent leachate undergoes further treatment to separate metal ions and produce final products.

**Alkali leaching:** Alkali leaching has attracted attention due to its selective leaching and the resulting potential to avoid costly separation or purification steps. An ammonia-based system is used because it can form stable ammonia complexes with metals, such as Ni, Co, and Cu. Zheng and Chen utilized ammonia and/or ammonium sulphate as a leaching solution, and sulphites as the reducing agent. The overall leaching efficiencies of Ni, Co and Li were high in both studies and are summarized in **Table 2**; Mn showed different leaching behavior.<sup>44,45</sup> Chen found that the leaching efficiency of Mn was largely dependent on the concentration of  $(\text{NH}_4)_2\text{SO}_3$ , with an optimal concentration of 0.75M.<sup>45</sup>

**Acid leaching:** Acid leaching remains prevalent because of its high recovery efficiency. With the use of acid in leaching, strong inorganic leaching may cause secondary pollution (excess acid solution and hazardous gas emission), while organic leaching offers similar leaching efficiency with biodegradable properties. Acid leaching agents include HCl,  $\text{H}_2\text{SO}_4$ , and  $\text{HNO}_3$ , and organic leaching agents consist of citric acid, ascorbic acid, oxalic acid, and formic acid.

Barik and He obtained a leaching efficiency of over 99% by utilizing dense HCl and  $\text{H}_2\text{SO}_4\text{-H}_2\text{O}_2$  systems, respectively, when dissolving Co, Mn, and Li. Manganese was further separated by adding sodium hypochlorite in Barik's work.<sup>46,47</sup> Instead of using excess acid, Li et al. recovered  $\text{LiFePO}_4$  in a low-concentration leaching solution of sulfuric acid and hydrogen peroxide. After operating at  $60^\circ\text{C}$  for 2hrs, 96.85% Li, 0.027% Fe, and 1.95% P were recovered in the leachate. Subsequently, 95.56% Li was recycled as  $\text{Li}_3\text{PO}_4$  with the addition of  $\text{Na}_3\text{PO}_4$ , and the leaching residue was recovered as  $\text{FePO}_4$ , through burning off the carbon slag.<sup>48</sup> The reduced usage of inorganic acid in the process leads to a simultaneous decrease in the amount of secondary waste and overall cost.

Organic acid leaching can reach efficiencies similar to inorganic acid leaching, and in milder environments. Gao et al. introduced formic acid into their closed-loop recycling process to selectively leach lithium ions into solution, while precipitating other metals out for precursor production.<sup>49</sup> In this process,  $\text{Li}_2\text{CO}_3$  was obtained with a purity of 99.9%, after removing metal residues.<sup>49</sup> Zhang et al. developed an innovative method to recycle NMC by oxalic acid leaching. Lithium was dissolved in the solution, whereas Ni, Mn, and Co were precipitated as oxalate. Unlike LCO systems, where the metal oxide can be fully leached out,<sup>50,51</sup> the layered NMC structure still exists after 2 hrs' leaching with oxalic acid. This occurs because reacted NMC oxalate precipitate covers the surface of NMC and hinders a continuous reaction, and the degree of leaching can be controlled by changing the leaching time. Subsequent calcination with  $\text{Li}_2\text{CO}_3$  transformed oxalate precipitates into regenerated NMC, which showed excellent electrochemical performance. At 0.2C, the initial specific discharge capacity was 168mAh/g and was better than that in reported recycled materials (155 mAh/g).<sup>52-54</sup> The specific capacity was 153.7mAh/g after 150 cycles, demonstrating a capacity retention of 91.5%. The promising behavior is attributed to the creation of submicron-sized particles as well voids formed during the regeneration.<sup>55</sup>

**Biobleaching:** Biobleaching is another environmental-friendly method, and it utilizes the acid produced during metabolization of microorganism to leach spent batteries. Generally, bacteria form inorganic acid, while fungi form organic acid. However, biobleaching has the drawback of a long culturing time and the susceptibility to contamination. Bahaloo-Horeh et al. utilized a bio-hydrometallurgical route to leach spent lithium ion batteries, in which *Aspergillus niger* was cultured. With a pulp density of 2% (w/v), 100% Cu and Li, 77% Mn, and 75% Al were recovered, while 64% Co and 54% Ni could be recycled at another experiment setting, with 1% (w/v) pulp

density.<sup>56</sup> This team also stated that citric acid played a more significant role in bioleaching than other organic acid produced by *Aspergillus niger*.<sup>57</sup>

The efficiency of the leaching process is enhanced by reducing agents, since lower valence metals dissolve more readily. The reducing agents include inorganic and organic species and metallic current collectors (Cu, Al); the most commonly used one is hydrogen peroxide. Following leaching, treatment options to separate metals or remove impurities include solvent extraction, chemical precipitation, electrolysis, and ion exchange.

### **Solvent extraction**

The driving mechanism of solvent extraction is the different solubilities of various metal ions in an organic solvent versus an aqueous liquid. This approach has the advantage of short reaction time (around 30mins) and high purity yield of products, but its application is limited by the high cost of solvents and process complexity. To recover the cobalt from spent batteries, Wang et al. used D2EHPA (di-(2-ethylhexyl) phosphoric acid) and PC-88A (2-ethylhexylphosphonic acid mono-2-ethylhexyl ester) to perform the extraction. First, D2EHPA was employed to remove Cu and Mn, then cobalt and nickel were separated by PC-88A. Finally, cobalt was recycled as cobalt oxalate, with a purity of 99.5%.<sup>58</sup> Virolainen et al. separated Li, Ni, and Co successfully from spent battery leachate by extractant-Cyanex 272 (Bis(2,4,4-trimethylpentyl)phosphinic acid). Modified Cyanex 272 by TOA (trioctylamine, a phase modifier), which helps to abate the formation of unwanted organic phases, was utilized to obtain a Li raffinate, whose purity was 99.9%. With

subsequent scrubbing and stripping, a 99.7% Ni aqueous solution and a 99.6% Co organic solution were recovered.<sup>59</sup>

### **Chemical precipitation**

Similar to solvent extraction, chemical reactions can be used to separate metals or remove impurities, and these have the ability to precipitate out diverse metals by strategic tuning of pH numbers. Pinna et al. dissolved Co and Li, using a leaching solution of  $\text{H}_3\text{PO}_4$  and  $\text{H}_2\text{O}_2$ . Then, by adding oxalic acid and NaOH, Co was precipitated out as  $\text{CoC}_2\text{O}_4$ , with an efficiency of 88%, and Li was recovered as  $\text{Li}_3\text{PO}_4$ , at an efficiency of 99%.<sup>60</sup> A lithium ion-sieve (LIS) can selectively absorb lithium with a high capacity and is generally employed in lithium extraction from brine, groundwater, and seawater. Lithium manganese oxide is a good candidate material as a LIS. As demonstrated by Guo et al., recycled  $\text{Li}_2\text{CO}_3$  can be sintered with  $\text{MnCO}_3$  to fabricate LMO for usage as a LIS. The content of  $\text{Na}_2\text{CO}_3$  impurity in raw  $\text{Li}_2\text{CO}_3$  was controlled below 10%, and the Na-doped LMO LIS was shown to be able to resist the Mn corrosion to a level of 21.07%, while maintaining a satisfactory absorption capacity of 40.08 mg/g.<sup>61</sup>

### **Co-precipitation**

Notably, Ni, Mn, and Co share similar properties and thus require complex steps to separate them. An effective approach is to coprecipitate them together and sinter the precursor directly into NMC cathode material. Yang et al. accomplished this goal via the co-extraction and co-precipitation paths and successfully fabricated recycled NMC 111 with good performance. First, a three-stage extraction with an extractant of D2EHPA in kerosene was employed, and 100% Mn, 99% Co, and 85% Ni were co-extracted. Separated Li raffinate was treated with  $\text{Na}_2\text{CO}_3$ , and a purity of 99.2%  $\text{Li}_2\text{CO}_3$  was obtained. Next, transition metals were stripped with 0.5M  $\text{H}_2\text{SO}_4$ , and

$\text{Ni}_{1/3}\text{Mn}_{1/3}\text{Co}_{1/3}(\text{OH})_2$  was produced in a co-precipitation reaction. Lastly, recycled NMC 111 was created through calcination of the mixture of  $\text{Li}_2\text{CO}_3$  and metal hydroxide. Co-extraction and co-precipitation demonstrate a promising path, in which tedious and costly separation steps are obviated, and a high-quality cathode material is produced.<sup>62</sup> A closed-loop LIB recycling process developed by Worcester Polytechnic Institute (WPI) shared the same principle of co-precipitation.<sup>52,63-67</sup> A hydrometallurgical process is implemented, and different cathode materials are dissolved in the leaching solution. Then, impurities in the leachate, including Cu, Fe, and Al, are removed through a series of pH adjustments, leaving the Ni, Mn, Co metal ions. Next, the ratio of Ni, Mn, Co is tailored to the desired ratio, by adding virgin metal sulfates as needed. Subsequently, the adjusted metal sulfate solution undergoes the co-precipitation reaction, and NMC hydroxide precursor powder is produced. After calcination with recovered lithium carbonate, recovered NMC cathode powder is ready for use in ‘new’ batteries, enabling a closed-loop approach. The group has demonstrated that the recovered NMC 111 has similar or better electrochemical properties than the commercial control powder with both coin cells and pouch cells, which have been independently tested by A123 Systems and Argonne National Laboratory.

### **Sol-gel**

Sol-gel synthesis is another approach to synthesize cathode material while avoiding separation steps, and it is generally operated after the ratio of metal ions has been adjusted to the desired number. Initially, metal ions are homogeneously distributed in sol states. Then, by hydrolyzing the mixture of precursors, the sol gradually transforms to a gel state. The generation of final solid cathode powder requires a drying step, to remove any remaining solvent, and an additional sintering step. Li et al. treated spent mixed cathode batteries with citric acid and hydrogen peroxide. Then, recycled NMC 111 was synthesized from leachate, via the sol-gel process, in which citric

acid was the chelating agent. For comparison, virgin NMC 111 was also synthesized by the same sol-gel method but with pure materials. Recycled cathode outperformed the virgin material in cell tests, and it was speculated that this was because trace amounts of Al performed a doping function, which was conducive to stabilizing the structure during the insertion and extraction of Li.<sup>68</sup> This same group also experimented by using the sol-gel method with lactic acid, and the capacity retention of recycled NMC 111 was 96% after 100 cycles at 0.5C.<sup>69</sup>

For most cathode materials, hydrometallurgical recycling processes are economically viable, particularly for cathodes high in cobalt and nickel. For this reason, LFP and LMO pose a challenge for traditional business purposes, due to the low intrinsic value of the cathode material components (Fe and Mn).<sup>70</sup>

**Table 2: Technical advancements in hydrometallurgical recycling processes in recent literature**

<b>Hydrometallurgical process</b>	<b>Experiment condition and efficiency</b>	<b>Significance</b>
Leaching	<ul style="list-style-type: none"> <li>Alkali leaching: <math>\text{NH}_3\text{-(NH}_4)_2\text{SO}_4\text{-Na}_2\text{SO}_3</math></li> <li>Leaching efficiencies of Ni, Co, Mn, and Li: 94.8%, 88.4%, 6.34%, and 96.7%</li> </ul>	Strong selective leaching, in which metal separation (Mn from others) is achieved <sup>44</sup>
	<ul style="list-style-type: none"> <li>Alkali leaching: <math>(\text{NH}_4)_2\text{SO}_4\text{-(NH}_4)_2\text{SO}_3</math></li> <li>Leaching efficiencies of Ni, Co, Mn, and Li: 98%, 81%, 92%, and 98%</li> </ul>	High leaching efficiencies of metals; adjustable leaching behavior of Mn <sup>45</sup>
	<ul style="list-style-type: none"> <li>Inorganic acid leaching: HCl</li> <li>Leaching efficiencies of Co, Mn, and Li in lab scale: 98%, 99% and 99.2%</li> <li>Leaching efficiencies of Co and Mn in pilot scale: 95% and 90%</li> </ul>	A successful transition demonstration from lab to pilot scale <sup>46</sup>
	<ul style="list-style-type: none"> <li>Inorganic acid leaching: <math>\text{H}_2\text{SO}_4\text{-H}_2\text{O}_2</math></li> <li>Leaching efficiencies of Ni, Co, Mn, and Li: 99.7%</li> </ul>	Reveals that leaching mechanism of having

		surface chemical reaction as a limiting step <sup>47</sup>
	<ul style="list-style-type: none"> <li>• Inorganic acid leaching: H<sub>2</sub>SO<sub>4</sub>-H<sub>2</sub>O<sub>2</sub></li> <li>• Leaching efficiencies of Li, Fe, and P: 96.85%, 0.027%, and 1.95%</li> </ul>	Reduced usage of acid leads to a highly selective leaching and effective metal separation <sup>48</sup>
	<ul style="list-style-type: none"> <li>• Organic acid leaching: formic acid-H<sub>2</sub>O<sub>2</sub></li> <li>• Leaching efficiency of Li: 99.93%</li> </ul>	Selective leaching of Li and separation of metals (Li vs. transition metals) <sup>49</sup>
	<ul style="list-style-type: none"> <li>• Organic acid leaching: oxalic acid</li> <li>• Leaching efficiency of Li: 98%</li> </ul>	A simple leaching and filtering process to separate and recover Li and Co from with high efficiency <sup>50</sup>
	<ul style="list-style-type: none"> <li>• Organic acid leaching: oxalic acid</li> <li>• Leaching efficiency of Li: 81%</li> </ul>	Partial leaching introduces voids of cathode particles and helps the electrochemical performance of the resynthesized cathode <sup>55</sup>
	<ul style="list-style-type: none"> <li>• Bioleaching: <i>Aspergillus niger</i></li> <li>• Leaching efficiencies of Cu, Li, Mn, Al, Co, and Ni: 100%, 100%, 77%, 75%, 64%, and 54%</li> </ul>	Enhanced and optimized recycling process with the utilization of <i>Aspergillus niger</i> <sup>56</sup>
	<ul style="list-style-type: none"> <li>• Bioleaching: <i>Aspergillus niger</i></li> <li>• Leaching efficiencies of Cu, Li, Mn, Al, Co, and Ni: 100%, 95%, 70%, 65%, 45%, and 38%</li> </ul>	Citric acid is more effective in leaching behavior, when compared with other organic acid <sup>57</sup>
Solvent extraction	<ul style="list-style-type: none"> <li>• Extractants: D2EHPA and PC-88A</li> <li>• Purity of cobalt oxalate: 99.5%</li> </ul>	Cobalt of high purity is recycled <sup>58</sup>
	<ul style="list-style-type: none"> <li>• Extractants: Cyanex 272 with TOA as phase modifier</li> <li>• Purity of Li raffinate, organic Co solution and aqueous NiSO<sub>4</sub> solution: 99.9%, 99.6% and 99.7%</li> </ul>	Battery-grade materials with high purity requirements are recovered <sup>59</sup>
	<ul style="list-style-type: none"> <li>• Extractants: D2EHPA and Cyanex 272</li> <li>• Purity of cobalt carbonate: 95%</li> </ul>	Spent battery powder is gained from pilot-scale pretreatment; feasibility of this process in industry is proven by the complexity of the treated sample <sup>71</sup>
Chemical precipitation	<ul style="list-style-type: none"> <li>• Precipitants: oxalic acid and H<sub>3</sub>PO<sub>4</sub></li> <li>• Recovery efficiencies of Co and Li: 99% and 88%</li> </ul>	An optimized recycling process that can efficiently recover Co and Li <sup>60</sup>

	<ul style="list-style-type: none"> <li>• Precipitants: <math>\text{Na}_2\text{CO}_3</math> and <math>\text{Na}_3\text{PO}_4</math></li> <li>• Recovery efficiencies of Li as <math>\text{Li}_2\text{CO}_3</math> and <math>\text{Li}_3\text{PO}_4</math>: 74.72% and 92.21%</li> </ul>	The removal of Na impurity in $\text{Li}_2\text{CO}_3$ can be avoided when fabricating LIS <sup>61</sup>
	<ul style="list-style-type: none"> <li>• Precipitants: <math>\text{H}_3\text{PO}_4</math></li> <li>• Recovery efficiencies of Fe and Li: 93.05% and 82.55%</li> </ul>	No secondary waste; a closed-loop recycling process <sup>72</sup>
	<ul style="list-style-type: none"> <li>• Precipitants: <math>\text{NaClO}</math></li> <li>• Recovery efficiencies of Mn: 97.7%</li> </ul>	Selective separation of Mn from Co <sup>46</sup>
	<ul style="list-style-type: none"> <li>• Precipitants: <math>\text{Na}_3\text{PO}_4</math></li> <li>• Recovery efficiencies of Li: 95.56%</li> </ul>	The effective metal separation leads to an easy precipitation <sup>48</sup>
Co-precipitation	<ul style="list-style-type: none"> <li>• Leaching agent: <math>\text{H}_2\text{SO}_4\text{-H}_2\text{O}_2</math></li> <li>• Reagent for the co-extraction of Ni, Mn and Co: D2EHPA in kerosene</li> <li>• Discharge capacity of NMC 111 at 0.5C (2.7-4.3V): 150mAh/g</li> </ul>	Transition metals are co-extracted and co-precipitated; electrochemical performance of recycled cathode is comparable to a pristine cathode <sup>62</sup>
	<ul style="list-style-type: none"> <li>• Leaching agent: <math>\text{H}_2\text{SO}_4\text{-H}_2\text{O}_2</math></li> <li>• Extractant for impurities: copper extractant and phosphate ester</li> <li>• Discharge capacity of NMC 111 at 0.1C (2.7-4.3V): 150.6mAh/g</li> </ul>	Low secondary waste and closed-loop recycling process; a mixture of spent cathode materials are treated <sup>53</sup>
Sol-gel	<ul style="list-style-type: none"> <li>• Leaching and chelating agent: citric acid</li> <li>• Leaching efficiency of Li, Ni, Co, and Mn: 99.1%, 98.7%, 99.8%, and 95.2%</li> <li>• Discharge capacity of NMC 111 at 0.2C (2.8-4.3V): 152.8mAh/g</li> </ul>	Better electrochemical performance than pristine material, due to the stabilization of Al impurity <sup>68</sup>
	<ul style="list-style-type: none"> <li>• Leaching and chelating agent: lactic acid</li> <li>• Leaching efficiency of Li, Ni, Co, and Mn: 97.7%, 98.2%, 98.9%, and 98.4%</li> <li>• 96% capacity retention after 100 cycles at 0.5C</li> </ul>	Better rate and cycle performance than freshly synthesized cathode; lactic acid is proven to be an effective chelating agent for sol-gel method <sup>69</sup>
	<ul style="list-style-type: none"> <li>• Leaching and chelating agent: malic acid</li> <li>• Discharge capacity of NMC 111 at 0.2C (2.75-4.25V): 147.2mAh/g</li> <li>• 95.06% capacity retention after 100 cycles at 0.5C</li> </ul>	Significant enhancement compared with spent material; satisfactory electrochemical performance <sup>73</sup>

## Industry demonstrations

In North America, Retrieiv uses a hydrometallurgical process to recycle LIBs. After the battery packs come in, they are manually dismantled, to the module or cell level, then fed into a flooded hammer-mill (immersed in lithium brine) for crushing, so as to lower the reactivity of the batteries, neutralize the electrolyte, and prevent gas emissions.<sup>22,32,35-37,43,74-76</sup> The Retrieiv process produces three streams of materials: metal solid, metal-enriched liquid, and plastic fluff. The metal solid may contain black mass, Cu and Al foils, and the metal-enriched liquid primarily includes Li ion, which is precipitated and filtered.<sup>77</sup> The filter cake and metal solid are sold to down-stream smelters (Glencore) that are interested in the cobalt or nickel content. Plastics can be directly recycled or disposed. Here, lithium can be recycled as lithium carbonate.<sup>21,22,31,34-36,40,43,74-76,78-80</sup>

Batrec Industrie AG employs a hydrometallurgical process to recycle lithium ion batteries. The used batteries are sorted and crushed in a CO<sub>2</sub> atmosphere, and the released lithium is then neutralized by moist air. Following crushing and neutralization, the protective CO<sub>2</sub> gas is purified in a gas scrubber before being exhausted. The remaining scrap materials are processed in acidified aqueous liquid, and the resultant leaching liquor and solid fraction are separated for further purification.<sup>21,31,34</sup>

Recupyl's hydrometallurgical process for LIB recycling, named Valibat, consists of a mechanical treatment of spent batteries, implemented under an inert gas mixture (CO<sub>2</sub>), and the physical separation of steel, copper, and plastics. Subsequent leaching of the fine powders yields an alkali solution of lithium, mixed metal oxides, and carbon. Lithium is precipitated out as Li<sub>2</sub>CO<sub>3</sub> or Li<sub>3</sub>PO<sub>4</sub>, and metal oxides undergo a second leaching. After the Cu and other impurities are removed, NaClO is added in order to precipitate cobalt as cobalt (III) hydroxide.<sup>34</sup>

The LithoRec project, funded by the German Federal Ministry of Environment, aimed to develop an economically viable and ecological beneficial recycling process with high recycling rates. Active materials that separated in the recycling stream are sent to Albemarle Germany GmbH (Rockwood Lithium GmbH) for hydrometallurgical treatment, and the recovered lithium and transition metal salts can be used for the synthesis of new cathode material.<sup>37,75,76,81</sup>

The hydrometallurgical process is also primarily deployed in China. As a leading battery recycling enterprise, Brunp processes spent LIBs by acid leaching (sulfuric acid and hydrogen peroxide), and the produced metal hydroxides can be utilized for cathode fabrication.<sup>31,82-85</sup> Other major LIB recyclers (GEM, GHTECH, TES-AMM China, and Highpower International) also adopted a similar route to recycle LIBs.

SungEel HiTech is a hydrometallurgical recycling facility located in South Korea and offers the capability of recovering Ni, Mn, Co, Li and Cu from spent LIBs. The recovered materials (metal sulfate and lithium phosphate) are supplied to LIB manufacturers to synthesize new batteries.<sup>86</sup>

Battery Resourcers, located in Worcester, MA, has developed a closed-loop process to recycle LIBs. Here, a hydrometallurgical process is utilized to dissolve the cathode powder. The leaching solution is used to synthesize different  $\text{LiNi}_x\text{Mn}_y\text{Co}_z\text{O}_2$  (NMC). SMCC and American Manganese are also actively developing a hydrometallurgical process in order to recycle LIBs.

### **2.3.3 The Direct Recycling Process**

Direct recycling is a recovery method proposed to directly harvest and recover active materials of LIBs, while retaining their original compound structure.<sup>87,88</sup> In this process, battery constituents are separated, primarily using physical separation methods, magnetic separation, and a moderate thermal processing, in order to avoid chemical breakdown of the active materials, which are the

main recovery ‘target’. The active materials are purified, and both surface and bulk defects are repaired by re-lithiation or hydrothermal processes. However, cathodes may be a mixture of more than one active materials, and separating them may not be economically or technically feasible. Furthermore, inputs containing multiple NMC chemistries cannot yet be separated, and thus present significant sorting challenges. The main advantages of the direct recycling approach include: 1) a relatively simple process, 2) active materials could be directly reused after regeneration, 3) significantly lower emissions and less secondary pollution, in comparison with pyrometallurgy and hydrometallurgy.<sup>43</sup> The main disadvantages of the direct recycling process include: 1) requires a rigorous sorting/pre-processing, based on exact active material chemistry, 2) it is a challenge to guarantee consistent high purity and pristine crystal structure, which may not meet rigorous standards required by the battery industry, 3) an unproven technology that, thus far, exists only at lab scale, 4) significant sensitivity to input stream variations, 5) an inflexible process: What goes in comes out, and thus the process may not be appropriate to meet the reality of changing cathode chemistry (active materials recovered at EOL will be ‘old technology’ and may no longer be relevant). In the near term, this technology is more likely to be adopted by battery manufacturers for recycling electrode scrap, where the chemistry is known and current.

### **Recent progress**

Direct recycling processes can restore the structure of active materials directly and some recent technical innovations are mentioned in **Table 3**. Capacity degradation of spent LIBs is associated with lithium loss due to the thickening of the solid-electrolyte interface (SEI) and undesired phase change.<sup>88</sup> In earlier studies of direct-recycling, researchers principally focused on relithiation to regenerate cathode materials. Solid-phase sintering with a lithium source is a versatile tool to supplement deficiency. Song et al. doped spent  $\text{LiFePO}_4$  (LFP) materials with new LFP, at a ratio

of 3:7 and calcinated at 700 °C. Results showed that the recycled LFP offered a discharge capacity of 144 mAh/g (commercial LFP: ~150mAh/g).<sup>89</sup>  $\text{Li}_2\text{CO}_3$  can also be added and mixed with the spent cathode to compensate for lithium loss. Li et al. regenerated spent LFP, by calcinating it with  $\text{Li}_2\text{CO}_3$  for 1 hour, at 650 °C. The end product delivered a high first-discharge capacity of 147.3 mAh/g and kept a capacity retention of 95.32% after 100 cycles (commercial LFP requirement: >92.43%).<sup>90</sup> A key challenge for the direct recycling approach relates to the levels of impurities. While aluminum and copper have been shown to improve the electrochemical performance of regenerated cathode material, there remains a threshold impurity limit. Chen et al. verified this conclusion when regenerating  $\text{LiCoO}_2$  by direct recycling with solid-state sintering. With an Al content less than 0.4wt%, or Cu content less than 0.6wt%, the electrochemical reaction was not hindered by impurities but, in fact, improved. With an optimal quantity of  $\text{Li}_2\text{CO}_3$ , followed by a heat treatment at 850 °C, the regenerated cathode displayed a good discharge capacity of 150.3 mAh/g (commercial LCO: ~150mAh/g) and a capacity retention of 93.2% after 100 cycles.<sup>91</sup>

In addition to the aforementioned solid-state sintering, relithiation can also be achieved via hydrothermal, electrochemical, and chemical processes. Electrochemical relithiation uses an electrochemical method to restore the cathode powder's lost lithium, whereas the chemical method involves soaking the cathode powder in a solution with an excess lithium source, and the hydrothermal technique employs the same steps as the chemical method but with added thermal treatments. Ganter et al. evaluated the electrochemically and chemically regenerated LFP by SEM, XRD, and electrochemical testing, finding that it exhibited identical performance and characteristics as the new LFP. It can thus be said that both electrochemical and chemical lithiation processes show promising results for future applications.<sup>92</sup> Zhang et al. regenerated  $\text{LiCoO}_2$

hydrothermally, assisted by ultrasound. The repaired LCO had a discharge capacity of 133.5 mAh/g (theoretical capacity: 137mAh/g for  $\text{Li}_{0.5}\text{CoO}_2$ ) and approached the specifications of commercial cathodes. Ultrasonic waves produce cavitation effects and thereby accelerate relithiation.<sup>93</sup> Hydrothermal lithiation can partially restore the structure of the cathode, and when followed by an annealing process, the structure restoration is further enhanced. Shi et al. also successfully regenerated spent  $\text{LiCoO}_2$  cathode by hydrothermal lithiation, followed by short-duration annealing, which resulted in better crystallinity, less cation disordering, and fewer defects. The hydrothermally renovated LCO showed a discharge capacity of 153.1 mAh/g (commercial LCO: ~150 mAh/g) at 0.1C and capacity retention of 91.2% at 1C after 100 cycles. This result was compared with another LCO sample recovered by sole heat treatment (850°C, 12hrs), and the hydrothermally repaired sample showed superior rate capability. Unlike sole heat treatment, where the amount of added lithium sources must first be calculated by testing the level of lithium loss, the proposed hydrothermal method can accommodate any degradation level of spent cathode materials, and the ratio of Li to the delithiated cathode does not have to be tightly controlled.<sup>87</sup> This group also demonstrated its feasibility in direct regeneration of NMC cathode particles. Degradation mechanisms related to cycled NMC cathode materials are complex, compared with LCO, incurring more challenges during the regeneration process. In addition to the lithium loss due to the solid-electrolyte interphase (SEI) formation, spinel and rock salt phase changes also exacerbate this capacity loss. Shi et al. used a hydrothermal treatment, followed by a short annealing, and the recovered NMC cathode was converted back to a layered structure. The rejuvenated NMC cathode exhibited good electrochemical performances, approaching pristine materials, with NMC 111 showing a capacity of 158.4 mAh/g in the first cycle, at 1C, and 122.6 mAh/g after 100 cycles; concurrently, NMC 532 maintained a capacity of 128.3 mAh/g after 100

cycles. In contrast with NMC 111, solid-state regeneration of NMC 532 was more sensitive to oxygen partial pressure and cannot fully recover the desired microphases/layer structure of NMC 532 in air.<sup>88</sup>

**Table 3: Technical advancements in direct recycling processes in recent literature**

<b>Direct recycling process</b>	<b>Performance</b>	<b>Significance</b>
<ul style="list-style-type: none"> <li>Hydrothermal: 220°C 4hrs</li> <li>Short annealing: 800°C 4hrs</li> </ul>	<ul style="list-style-type: none"> <li>LiCoO<sub>2</sub></li> <li>91.2% capacity retention after 100 cycles at 1C (3-4.3V)</li> <li>141.9 mAh/g at 2C and 130.3 mAh/g at 5C</li> </ul>	A nondestructive and simple renovation process; mixed cathode can be processed together <sup>87</sup>
<ul style="list-style-type: none"> <li>Hydrothermal: 220°C 4hrs</li> <li>Short annealing: 850°C 4hrs in O<sub>2</sub></li> </ul>	<ul style="list-style-type: none"> <li>NMC 111: First discharge capacity of 158.4 mAh/g at 1C and 122.6 mAh/g after 100 cycles</li> <li>NMC 532: 128.3 mAh/g after 100 cycles</li> </ul>	Cathode with higher nickel content is more sensitive to oxygen partial pressure during solid state regeneration <sup>88</sup>
<ul style="list-style-type: none"> <li>Solid phase sintering: 700°C 8hrs</li> <li>Doping ratio between spent LFP with new LFP: 3:7</li> </ul>	<ul style="list-style-type: none"> <li>LiFePO<sub>4</sub></li> <li>144 mAh/g at 0.1C (2.5-4.1V)</li> <li>135 mAh/g after 100 cycles</li> </ul>	Simple regeneration process; satisfactory electrochemical performance <sup>89</sup>
<ul style="list-style-type: none"> <li>Solid phase heat treatment: 650°C 1hr under Ar/H<sub>2</sub> flow</li> <li>Li<sub>2</sub>CO<sub>3</sub> as lithium source</li> </ul>	<ul style="list-style-type: none"> <li>LiFePO<sub>4</sub></li> <li>First discharge capacity of 147.3 mAh/g (2.5-4.2V)</li> <li>140.4 mAh/g after 100 cycles at 0.2C and capacity retention is 95.32%</li> </ul>	A green recycling process offering high yields; Impurity phases are fully converted <sup>90</sup>
<ul style="list-style-type: none"> <li>Solid phase sintering: 850°C</li> <li>Li<sub>2</sub>CO<sub>3</sub> as lithium source</li> </ul>	<ul style="list-style-type: none"> <li>LiCoO<sub>2</sub></li> <li>First discharge capacity of 150.3 mAh/g (3.0-4.3V) at 0.1C</li> <li>140.1 mAh/g after 100 cycles</li> </ul>	A high total recovery rate of 95.78%; Undesired phases are converted back to layer structure; Al and Cu impurities favor electrochemical performances <sup>91</sup>
<ul style="list-style-type: none"> <li>Electrochemical: cycle spent cathode coating with pure lithium metal</li> </ul>	<ul style="list-style-type: none"> <li>LiFePO<sub>4</sub></li> <li>150-155 mAh/g</li> </ul>	An innovative electrochemical method to regenerate the cathode; decrease of 50% embodied energy,

<ul style="list-style-type: none"> <li>• Chemical: immerse spent cathode power in lithium containing solution</li> </ul>		compared with virgin material production <sup>92</sup>
<ul style="list-style-type: none"> <li>• Hydrothermal: 80°C 6hrs</li> <li>• Ultrasonic power: 600W</li> </ul>	<ul style="list-style-type: none"> <li>• LiCoO<sub>2</sub></li> <li>• First discharge capacity of 133.5 mAh/g</li> <li>• 99.5% capacity retention after 40 cycles</li> </ul>	Ultrasonic radiation is used to facilitate the renovation process <sup>93</sup>

**Industry demonstrations**

Due to the low intrinsic value of LFP, it is not economically feasible to recycle LFP by hydrometallurgical methods. In industry, utilizing direct recycling to recover LFP can be potentially profitable, as claimed by BYD Co. in China.<sup>70</sup> OnTo Technology, LLC, is located in Bend, Oregon, and recycles LIBs via a direct-recycle methodology at bench scale. EOL LIBs are discharged and opened to harvest the electrode, after which the cathode material is gained by blending the electrode in an aqueous alkaline solution and detaching it from the current collector. With the utilization of hydrothermal and additional heat treatment, the degraded cathode material can be regenerated and used in new cells.<sup>94</sup> The company claims that its recycling process is economically viable and has started working with a US-based EV manufacturer. OnTo Technology also recycles electrolyte, using liquid CO<sub>2</sub>, either by circulating CO<sub>2</sub> or soaking spent batteries in supercritical fluid. After discharging and shredding, 90% of the electrolyte is extracted in 48hrs.<sup>34,95</sup> However, this electrolyte recycling process is not practically adopted, due to its intrinsic high cost. Farasis, a lithium ion battery manufacturer, has also been developing a direct recycling process to recycle LIBs under a USABC contract and has claimed some success in its report included in the Department of Energy Annual Merit Review Report.

**3. Summary, Challenges, and Future Outlook**

The EV LIB market is expected to grow to over \$90B USD by 2026.<sup>96</sup> The rapid, ever-increasing adoption rates of EVs pose a concern for the materials supply chain, as evidenced by the fluctuating price of raw materials, especially lithium and cobalt. There is no doubt that LIB recycling will play an important role in strategic materials supply. The US Department of Energy (DOE) has identified LIB recycling as a critical need, to enable long-term material availability and to stabilize the LIB supply chain. In fact, recycling is viewed as a lever that has the potential to decrease future battery costs and energy use, alleviate pristine material prices, and reduce reliance on imported materials. The DOE recently announced the establishment of a Lithium Ion Recycling Center, ReCell, which will house a multi-institution effort led by Argonne National Laboratory. The objective of the center is to develop a closed-loop recycling R&D process, focused on novel materials and processes, in order to improve the economic viability of battery recycling.

As described above, pyrometallurgical, hydrometallurgical, and direct recycling processes each have their respective advantages and disadvantages. Both pyrometallurgical and hydrometallurgical processes have been commercialized, and their business models depend largely on the high cobalt concentration of LIBs for portable electronics. However, these business models may become increasingly challenging for EV batteries, as they trend towards lower and lower cobalt content. Direct recycling processes remain at the lab-scale level and require further development in order to generate meaningful impact. As such, the need for flexible processing techniques to extract as much material value as possible from current and future generations of batteries is critical to the sustainability of electric vehicles. Unfortunately, none of the above recycling processes presently provides an economic solution to the very dynamic input streams of current and future LIBs, and better recycling technologies are needed. It is widely accepted that a

value-based ‘pull system’, whereby extracted value exceeds recycling costs, is the necessary engine for efficient collection and, in turn, sustainable closed-loop recycling.

Although various battery recycling technologies are available today, as yet none of them offer the perfect solution, and continued efforts are needed. LIBs recycling research must keep pace with rapidly evolving LIB materials research, which is bringing new materials and designs to the market. This requires LIB recycling technologies that are flexible, economically feasible, robust, and which offer high recycling efficiencies. The authors see the following research needs/challenges for various recycling processes. Note: different recycling processes may have the same or similar research needs.

**3.1 Sorting and separation technologies:** The spent LIBs most likely include variations in shape, size, and chemistry. Sorting and separation technologies could increase the efficiency of recycling.

A. LIBs separation, based on different chemistries. Recycling facilities normally receive EOL LIBs without knowing the interior chemical constituents. Proper labeling of LIBs by battery manufacturers would help the separation of LIBs, based on chemistry. Then, single-chemistry LIBs can be sorted and recycled, which is more effective and efficient. For example, Society of Automotive Engineers (SAE) has developed labeling standards (J2936) for LIBs. This standard gives labeling recommendations for energy storage devices including cell, battery, and pack-level products during the entire life spectrum.

B. Material separation. Various chemistries and form factors of spent LIBs make the pretreatment of EOL LIBs challenging. Safe and effective separation of battery components needs to be developed. For example, if cell size and shape are standardized to a few designs, auto-dismantling and separation become more feasible.

**3.2 The Pyrometallurgical process:** The pyrometallurgical process is the most mature technology and has been primarily deployed in Europe and North America.

A. Slag recycle. During the smelting process, most of the materials (graphite, separator, organic electrolyte, plastics) are burned and not recovered. Slag, including lithium, is produced. In most traditional pyrometallurgical processes, the lithium and aluminum in slag is not recovered. However, the gradually increasing price of lithium renders this unsustainable; the lithium must be recovered or not be sent to slag. Developing practical technologies to recover lithium in the slag could be one of the important research directions for the pyrometallurgical process.

B. Adaptation to the rapidly developing LIB industry (high nickel and low cobalt). The LIB industry is evolving very quickly. Trends are moving towards increasingly higher nickel and lower cobalt content cathode materials, with the ultimate objective of ‘no-cobalt’ cathodes. The pyrometallurgical process relies on reasonably high cobalt concentrations for economic feasibility. However, as cobalt concentrations are reduced, the business model will be strained. Innovation is needed to enable pyrometallurgical processors to adapt their business model to emergent generations of LIBs, notably low-cobalt or no-cobalt cathode materials. For example, developing roasting conditions to allow easier purification and separation of different chemicals could be one possible direction. In addition, combining hydrometallurgical processes to allow further purification is another direction (a few companies are beginning to employ this practice).

C. Secondary waste treatment: The waste in the pyrometallurgical process includes gases and solids. Gas (mainly CO<sub>2</sub>) is due to the battery-burning process, and non-recycled materials become slag. In industry, gas is purified before emission. However, CO<sub>2</sub> is emitted directly into the air.

Methods devised to reduce CO<sub>2</sub> emission, recover the solid waste, for example, graphite (in addition to Co, Ni, Cu), or convert that waste into valuable materials will further increase the economic benefits of the pyrometallurgical process.

**3.3 The hydrometallurgical process:** The hydrometallurgical process is also a commercialized technology and has been primarily deployed in China.

A. Recovery of electrolyte and anode. Right now, the major focus in hydrometallurgical processing is the recovery of cathode material, due to its high value. Other materials are not recovered or recycled, given that they are low-value materials. Developing technologies to enable the recovery of the electrolyte and graphite anode as high-value materials will further increase the economic feasibility of the recycling process.

B. Recycling of LiFePO<sub>4</sub> batteries: Many e-buses use LIBs with LiFePO<sub>4</sub> cathodes. Also, some EVs (especially in China) also use LIBs with LiFePO<sub>4</sub> cathodes. Although LiFePO<sub>4</sub> is a relatively expensive material, the intrinsic elements are cheap. In fact, synthesizing LiFePO<sub>4</sub> is very costly. There is no economical way to recycle LiFePO<sub>4</sub> cathode-containing lithium ion batteries, using a hydrometallurgical process. Direct recycling of LiFePO<sub>4</sub>, if shown to be technically feasible, may present a viable solution.

C. Secondary waste treatment: The waste in the hydrometallurgical process is water and chemicals from the leaching step, co-precipitation, and washing, which increase recycling costs. Further research on purifying the waste water, reusing the water, or reducing the amount of water in the process is needed to reduce or eliminate waste water and associated costs.

**3.4 The direct recycling process:** The direct recycling process is still in the laboratory stage and much work needs to be done in order to commercialize it.

A. Pre-processing steps to obtain pure materials: The principle of direct recycling is to directly regenerate and reuse the cathode materials. However, typical LIBs include many different materials (anode, cathode, copper, aluminum, plastics, etc.). Creating a means to effectively and efficiently separate cathode materials from other materials and each other automatically could be one important research area for direct recycling. In addition, the purity of the recovered cathode materials is also a critical research area.

B. Recover other materials in addition to cathode materials: Currently, the direct recycling process is mainly focused on cathode powder, which accounts for 30%-40% of material cost. As with the pyrometallurgical and hydrometallurgical processes, it is also important that the direct recycling process recycle other materials as much as possible.

C. Demonstrate recovered materials at scale: In order for industry to adopt the direct recycling process, the recycling process needs to reach a certain scale to support meaningful impact. In addition, the recovered materials need to be independently tested by industry.

D. Recover mixed cathode materials: The spent LIBs may include different cathode materials. Furthermore, a given battery may use a mixture of cathode chemistries. This is especially challenging for the direct recycling process. Research into how to separate different cathode materials is critical, particularly in view of the many ratios of NMC comingled in the waste stream. Another option is trying to find a scenario in which the mixture can be utilized directly.

E. Combine different recycling processes: Since each recycling process has its advantages and disadvantages, it may be necessary to combine different recycling processes to enable the most effective recycling. For example, the cathode materials can be recovered via the hydrometallurgical process, and other materials can be recovered via a direct recycling process.

In addition to the research needs outlined above, the following areas also need to be addressed.

1. Establish a viable business model: Currently, unlike lead acid batteries, a viable business model has not been established for LIB recycling, due to low collection rates, immature technology, and relatively low volumes, among other reasons. Argonne National Laboratory has developed a recycling strategy assessment tool, which models the economics and environmental impacts of the aforementioned recycling approaches. The model considers each process from the initial point of battery extraction from the vehicle to its final recycling through the user-selected process. The model also offers a comprehensive comparison of different recycling technologies,<sup>97</sup> which helps determine both the economic and environmental impacts of a particular recycling process.

2. Recycling or pretreating locally: Due to the hazardous nature of LIBs, transportation accounts for a large percentage of the recycling cost. **Figure 3** shows the main LIB recycling facilities worldwide. As shown in the figure, recycling facilities are only located in a few countries (United States, Canada, France, Switzerland, Germany, Belgium, China, Japan, South Korea, Singapore). For example, in the United States, LIB recycling facilities are concentrated on the east and west coasts. Spent LIBs in the middle of the country must be transported a great distance in order to be recycled. Once spent LIBs reach sizable volumes, establishing distributed recycling facilities across the country will most likely be justified for optimized economic and logistical gains.

3. Design for remanufacturing/repurposing/recycling: EV battery designs are currently optimized for performance, safety, and cost. Remanufacturing/ repurposing/recycling should play a more significant role in EV pack design.

4. Solid state LIB recycling: In order to further increase the energy density, considerable research and development is being conducted for solid-state LIB. The key challenge for solid-state LIB recycling will be how to properly and safely handle lithium metal. Many steps of the current recycling process are not appropriate for lithium metal -- for example, discharging and shredding. Discharging LIBs using a salt solution is a very common method to release the remaining energy. However, lithium metal can have a very aggressive reaction with water. In addition, lithium metal can easily adhere to the shredder due to its soft nature. Therefore, innovations for recycling solid-state LIBs will be also needed.



**Figure 3: Lithium ion battery recycling facilities worldwide.** The locations of LIBs recycling facilities are listed and marked on the world map. With most of the facilities being concentrated in a few countries or locations within a country, the challenges arise from the transportation when the quantity of spent LIBs becomes significant.

In addition to the technical considerations, collection, storage, logistics, and transportation are also critical in order to develop viable business practices for spent LIBs. Although these are beyond the scope of this paper, the recently announced Recycling Prize (DOE) strives to spur advancements in these enabling areas. Moreover, government policy and regulations also need to be implemented

globally for LIB recycling. The European Union has stringent laws regarding LIB recycling, whereby recycling efficiencies must meet 50% by 2030.<sup>98</sup> In China, after August 2018, all electric vehicles are given a specific ID, which will help track the batteries from first production to second use and, finally, to recycling.<sup>99</sup> However, in the US, there are still no national regulations for the collection and recycling of large-format LIBs. Even though national policies regarding LIBs recycling haven't been established, some existing state policies are intended to promote the sustainability of xEV LIBs. California is a forerunner in promoting vehicle electrification, and it will continue to be a national leader in LIB recycling. In 2016, an EV action plan in California set a new goal to develop new market opportunities for battery recycling.<sup>100,101</sup>

In fact, policy can be initiated for manufacturing LIBs, EOL LIB collection and transportation, recycling processes, and reuse of recycled materials. The manufacturing standardization recommendations could include stipulations regarding module design (energy, size and voltage), the joining mechanism (reversible to enable disassembly of packs), and adhesives, and these could effectively promote the acceptability of recycling. If there are fewer variants, the disassembly and separation processes during recycling would require less labor, and appropriate automation techniques could be developed. Also, regulations covering the entire life span of recycling could be raised, from collection, storage, logistics, and transportation to the actual recycling process in the facility. The principles or targets of policy could include e responsibility for EOL LIBs treatment (manufacturers, distributors), collection rates, and recycling efficiencies.<sup>98</sup> The European Union (EU) has enacted a Union-wide extended producer responsibility (EPR) for LIBs, which requires manufacturers to collect and manage EOL LIBs. Also, a deposit-refund system could encourage users to properly recycle or dispose of EOL batteries.<sup>100,102</sup> The concern regarding recycled material rests on its performance, and long time and reliable testing should be

proposed to foster assurances. Policies and regulations for standardized evaluation of EOL LIBs could facilitate the global use of recycled materials.

## References:

- 1 Pillot, C. in *31st International Battery Seminar & Exhibit*.
- 2 Richa, K. Sustainable management of lithium-ion batteries after use in electric vehicles. (2016).
- 3 Nykvist, B. & Nilsson, M. Rapidly falling costs of battery packs for electric vehicles. *Nature Climate Change* **5**, 329, doi:10.1038/nclimate2564 (2015).
- 4 Mo, Y. J. & Jeon, W. The Impact of Electric Vehicle Demand and Battery Recycling on Price Dynamics of Lithium-Ion Battery Cathode Materials: A Vector Error Correction Model (VECM) Analysis. *Sustainability* **10**, doi:10.3390/su10082870 (2018).
- 5 Daswani, R. & Radford, C. *Fastmarkets MB Lithium*, <<https://www.lme.com/Trading/New-initiatives/Electric-Vehicle-Battery-Materials>> (2018).
- 6 <<http://www.infomine.com/investment/metal-prices/cobalt/>> (2018).
- 7 Steward, D. *Supply-Chain Analysis of Lithium-Ion Battery Material and Impact of Recycling*, <[https://www.energy.gov/sites/prod/files/2018/06/f52/bat372\\_mayyas\\_2018\\_p.pdf](https://www.energy.gov/sites/prod/files/2018/06/f52/bat372_mayyas_2018_p.pdf)> (2018).
- 8 Olivetti, E. A., Ceder, G., Gaustad, G. G. & Fu, X. Lithium-Ion Battery Supply Chain Considerations: Analysis of Potential Bottlenecks in Critical Metals. *Joule* **1**, 229-243, doi:<https://doi.org/10.1016/j.joule.2017.08.019> (2017).
- 9 Huo, H. *et al.* Safety Requirements for Transportation of Lithium Batteries. *Energies* **10**, doi:10.3390/en10060793 (2017).
- 10 de Pauw, I., Bakker, C. & van der Grinten, B. Product design and business model strategies for a circular economy AU - Bocken, Nancy M. P. *Journal of Industrial and Production Engineering* **33**, 308-320, doi:10.1080/21681015.2016.1172124 (2016).
- 11 Olsson, L., Fallahi, S., Schnurr, M., Diener, D. & van Loon, P. Circular Business Models for Extended EV Battery Life. *Batteries* **4**, doi:10.3390/batteries4040057 (2018).
- 12 Hesselbach, J. & Herrmann, C. *Glocalized Solutions for Sustainability in Manufacturing: Proceedings of the 18th CIRP International Conference on Life Cycle Engineering, Technische Universität Braunschweig, Braunschweig, Germany, May 2nd-4th, 2011*. (Springer Science & Business Media, 2011).
- 13 Foster, M., Isely, P., Standridge, C. R. & Hasan, M. M. Feasibility assessment of remanufacturing, repurposing, and recycling of end of vehicle application lithium-ion batteries. *Journal of Industrial Engineering and Management; Vol 7, No 3 (2014)DO - 10.3926/jiem.939* (2014).
- 14 DeRousseau, M., Gully, B., Taylor, C., Apelian, D. & Wang, Y. Repurposing Used Electric Car Batteries: A Review of Options. *JOM* **69**, 1575-1582, doi:10.1007/s11837-017-2368-9 (2017).
- 15 Jiao, D. N. *Second-life Electric Vehicle Batteries 2019-2029*, <<https://www.idtechex.com/research/reports/second-life-electric-vehicle-batteries-2019-2029-000626.asp>> (2018).
- 16 Bräuer, S. *et al.* in *2016 IEEE 18th Conference on Business Informatics (CBI)*. 143-152.
- 17 Recycle spent batteries. *Nature Energy* **4**, 253-253, doi:10.1038/s41560-019-0376-4 (2019).

- 18 *The Mobility House, Nissan and Eaton Provide Efficient Battery Storage for Amsterdam Arena*, <[https://www.mobilityhouse.com/int\\_en/magazine/press-releases/the-mobility-house-provides-energy-solution-in-amsterdam-arena-project.html](https://www.mobilityhouse.com/int_en/magazine/press-releases/the-mobility-house-provides-energy-solution-in-amsterdam-arena-project.html)> (2016).
- 19 *From plug-in cars to plug-in homes – EV batteries get a second life*, <<https://www.automotiveworld.com/articles/plug-cars-plug-homes-ev-batteries-get-second-life/>> (2018).
- 20 Cai, W. *Analysis of Li-Ion Battery Joining Technologies*, <[http://cii-resource.com/cet/fbc-05-04/Presentations/BMF/Cai\\_Wayne.pdf](http://cii-resource.com/cet/fbc-05-04/Presentations/BMF/Cai_Wayne.pdf)> (2017).
- 21 Heelan, J. *et al.* Current and Prospective Li-Ion Battery Recycling and Recovery Processes. *JOM* **68**, 2632-2638, doi:10.1007/s11837-016-1994-y (2016).
- 22 Georgi-Maschler, T., Friedrich, B., Weyhe, R., Heegn, H. & Rutz, M. Development of a recycling process for Li-ion batteries. *Journal of Power Sources* **207**, 173-182, doi:<https://doi.org/10.1016/j.jpowsour.2012.01.152> (2012).
- 23 Gaines, L. The future of automotive lithium-ion battery recycling: Charting a sustainable course. *Sustainable Materials and Technologies* **1-2**, 2-7, doi:<https://doi.org/10.1016/j.susmat.2014.10.001> (2014).
- 24 Guoxing, R. *et al.* in *Advances in Molten Slags, Fluxes, and Salts: Proceedings of the 10th International Conference on Molten Slags, Fluxes and Salts 2016*. (eds Ramana G. Reddy, Pinakin Chaubal, P. Chris Pistorius, & Uday Pal) 211-218 (Springer International Publishing).
- 25 Dang, H. *et al.* Recycled Lithium from Simulated Pyrometallurgical Slag by Chlorination Roasting. *ACS Sustainable Chemistry & Engineering* **6**, 13160-13167, doi:10.1021/acssuschemeng.8b02713 (2018).
- 26 Li, J., Wang, G. & Xu, Z. Environmentally-friendly oxygen-free roasting/wet magnetic separation technology for in situ recycling cobalt, lithium carbonate and graphite from spent LiCoO<sub>2</sub>/graphite lithium batteries. *Journal of Hazardous Materials* **302**, 97-104, doi:<https://doi.org/10.1016/j.jhazmat.2015.09.050> (2016).
- 27 Xiao, J., Li, J. & Xu, Z. Novel Approach for in Situ Recovery of Lithium Carbonate from Spent Lithium Ion Batteries Using Vacuum Metallurgy. *Environmental Science & Technology* **51**, 11960-11966, doi:10.1021/acs.est.7b02561 (2017).
- 28 Xiao, J., Li, J. & Xu, Z. Recycling metals from lithium ion battery by mechanical separation and vacuum metallurgy. *Journal of Hazardous Materials* **338**, 124-131, doi:<https://doi.org/10.1016/j.jhazmat.2017.05.024> (2017).
- 29 Mao, J., Li, J. & Xu, Z. Coupling reactions and collapsing model in the roasting process of recycling metals from LiCoO<sub>2</sub> batteries. *Journal of Cleaner Production* **205**, 923-929, doi:<https://doi.org/10.1016/j.jclepro.2018.09.098> (2018).
- 30 Hu, J., Zhang, J., Li, H., Chen, Y. & Wang, C. A promising approach for the recovery of high value-added metals from spent lithium-ion batteries. *Journal of Power Sources* **351**, 192-199, doi:<https://doi.org/10.1016/j.jpowsour.2017.03.093> (2017).
- 31 Zhang, X. *et al.* Toward sustainable and systematic recycling of spent rechargeable batteries. *Chemical Society Reviews* **47**, 7239-7302, doi:10.1039/C8CS00297E (2018).
- 32 Gaines, L., Sullivan, J., Burnham, A. & Belharouak, I. in *Transportation Research Board 90th Annual Meeting, Washington, DC*. 23-27.
- 33 *Our recycling process*, <<https://csm.unicore.com/en/recycling/battery-recycling/our-recycling-process>> (2019).
- 34 Meshram, P., Pandey, B. D. & Mankhand, T. R. Extraction of lithium from primary and secondary sources by pre-treatment, leaching and separation: A comprehensive review. *Hydrometallurgy* **150**, 192-208, doi:<https://doi.org/10.1016/j.hydromet.2014.10.012> (2014).
- 35 Chagnes, A. & Swiatowska, J. *Lithium process chemistry: Resources, extraction, batteries, and recycling*. (Elsevier, 2015).
- 36 Pistoia, G. *Lithium-ion batteries: advances and applications*. (Newnes, 2013).

- 37 Wang, H. & Friedrich, B. Development of a Highly Efficient Hydrometallurgical Recycling Process for Automotive Li-Ion Batteries. *Journal of Sustainable Metallurgy* **1**, 168-178, doi:10.1007/s40831-015-0016-6 (2015).
- 38 Toto, D. Sumitomo Metal Mining Co. develops recycling process for lithium-ion batteries, <<https://www.recyclingtoday.com/article/japanese-company-develops-lithium-ion-battery-recycling-process/>> (2019).
- 39 Utilizing Unused Resources, Achieving Japan's first "battery to battery" recycling, <[http://www.smm.co.jp/E/csr/activity\\_highlights/persistence/highlights4.html](http://www.smm.co.jp/E/csr/activity_highlights/persistence/highlights4.html)> (2019).
- 40 Saloojee, F. & Lloyd, J. Lithium Battery Recycling Process. *Department of Environmental Affairs Development Bank of South Africa (Project No. DB-074 (RW1/1016)* **1** (2015).
- 41 Zhang, X., Xie, Y., Lin, X., Li, H. & Cao, H. An overview on the processes and technologies for recycling cathodic active materials from spent lithium-ion batteries. *Journal of Material Cycles and Waste Management* **15**, 420-430, doi:10.1007/s10163-013-0140-y (2013).
- 42 Chagnes, A. & Pospiech, B. A brief review on hydrometallurgical technologies for recycling spent lithium-ion batteries. *Journal of Chemical Technology and Biotechnology* **88**, 1191-1199, doi:10.1002/jctb.4053 (2013).
- 43 Ciez, R. E. & Whitacre, J. F. Examining different recycling processes for lithium-ion batteries. *Nature Sustainability* **2**, 148-156, doi:10.1038/s41893-019-0222-5 (2019).
- 44 Zheng, X. *et al.* Spent lithium-ion battery recycling – Reductive ammonia leaching of metals from cathode scrap by sodium sulphite. *Waste Management* **60**, 680-688, doi:<https://doi.org/10.1016/j.wasman.2016.12.007> (2017).
- 45 Chen, Y. *et al.* Thermal treatment and ammoniacal leaching for the recovery of valuable metals from spent lithium-ion batteries. *Waste Management* **75**, 469-476, doi:<https://doi.org/10.1016/j.wasman.2018.02.024> (2018).
- 46 Barik, S. P., Prabakaran, G. & Kumar, L. Leaching and separation of Co and Mn from electrode materials of spent lithium-ion batteries using hydrochloric acid: Laboratory and pilot scale study. *Journal of Cleaner Production* **147**, 37-43, doi:<https://doi.org/10.1016/j.jclepro.2017.01.095> (2017).
- 47 He, L.-P., Sun, S.-Y., Song, X.-F. & Yu, J.-G. Leaching process for recovering valuable metals from the LiNi<sub>1/3</sub>Co<sub>1/3</sub>Mn<sub>1/3</sub>O<sub>2</sub> cathode of lithium-ion batteries. *Waste Management* **64**, 171-181, doi:<https://doi.org/10.1016/j.wasman.2017.02.011> (2017).
- 48 Li, H. *et al.* Recovery of Lithium, Iron, and Phosphorus from Spent LiFePO<sub>4</sub> Batteries Using Stoichiometric Sulfuric Acid Leaching System. *ACS Sustainable Chemistry & Engineering* **5**, 8017-8024, doi:10.1021/acssuschemeng.7b01594 (2017).
- 49 Gao, W. *et al.* Lithium Carbonate Recovery from Cathode Scrap of Spent Lithium-Ion Battery: A Closed-Loop Process. *Environmental Science & Technology* **51**, 1662-1669, doi:10.1021/acs.est.6b03320 (2017).
- 50 Zeng, X., Li, J. & Shen, B. Novel approach to recover cobalt and lithium from spent lithium-ion battery using oxalic acid. *Journal of Hazardous Materials* **295**, 112-118, doi:<https://doi.org/10.1016/j.jhazmat.2015.02.064> (2015).
- 51 Sun, L. & Qiu, K. Organic oxalate as leachant and precipitant for the recovery of valuable metals from spent lithium-ion batteries. *Waste Management* **32**, 1575-1582, doi:<https://doi.org/10.1016/j.wasman.2012.03.027> (2012).
- 52 Sa, Q. *et al.* Synthesis of high performance LiNi<sub>1/3</sub>Mn<sub>1/3</sub>Co<sub>1/3</sub>O<sub>2</sub> from lithium ion battery recovery stream. *Journal of Power Sources* **282**, 140-145, doi:<https://doi.org/10.1016/j.jpowsour.2015.02.046> (2015).
- 53 Zheng, R. *et al.* A closed-loop process for recycling LiNi<sub>x</sub>Co<sub>y</sub>Mn<sub>(1-x-y)</sub>O<sub>2</sub> from mixed cathode materials of lithium-ion batteries. *Green Energy & Environment* **2**, 42-50, doi:<https://doi.org/10.1016/j.gee.2016.11.010> (2017).
- 54 Yao, L., Feng, Y. & Xi, G. A new method for the synthesis of LiNi<sub>1/3</sub>Co<sub>1/3</sub>Mn<sub>1/3</sub>O<sub>2</sub> from waste lithium ion batteries. *RSC Advances* **5**, 44107-44114, doi:10.1039/C4RA16390G (2015).

- 55 Zhang, X. *et al.* Innovative Application of Acid Leaching to Regenerate Li(Ni<sub>1/3</sub>Co<sub>1/3</sub>Mn<sub>1/3</sub>)O<sub>2</sub> Cathodes from Spent Lithium-Ion Batteries. *ACS Sustainable Chemistry & Engineering* **6**, 5959-5968, doi:10.1021/acssuschemeng.7b04373 (2018).
- 56 Bahaloo-Horeh, N. & Mousavi, S. M. Enhanced recovery of valuable metals from spent lithium-ion batteries through optimization of organic acids produced by *Aspergillus niger*. *Waste Management* **60**, 666-679, doi:https://doi.org/10.1016/j.wasman.2016.10.034 (2017).
- 57 Horeh, N. B., Mousavi, S. M. & Shojaosadati, S. A. Bioleaching of valuable metals from spent lithium-ion mobile phone batteries using *Aspergillus niger*. *Journal of Power Sources* **320**, 257-266, doi:https://doi.org/10.1016/j.jpowsour.2016.04.104 (2016).
- 58 Wang, F., Sun, R., Xu, J., Chen, Z. & Kang, M. Recovery of cobalt from spent lithium ion batteries using sulphuric acid leaching followed by solid-liquid separation and solvent extraction. *RSC Advances* **6**, 85303-85311, doi:10.1039/C6RA16801A (2016).
- 59 Virolainen, S., Fallah Fini, M., Laitinen, A. & Sainio, T. Solvent extraction fractionation of Li-ion battery leachate containing Li, Ni, and Co. *Separation and Purification Technology* **179**, 274-282, doi:https://doi.org/10.1016/j.seppur.2017.02.010 (2017).
- 60 Pinna, E. G., Ruiz, M. C., Ojeda, M. W. & Rodriguez, M. H. Cathodes of spent Li-ion batteries: Dissolution with phosphoric acid and recovery of lithium and cobalt from leach liquors. *Hydrometallurgy* **167**, 66-71, doi:https://doi.org/10.1016/j.hydromet.2016.10.024 (2017).
- 61 Guo, X., Cao, X., Huang, G., Tian, Q. & Sun, H. Recovery of lithium from the effluent obtained in the process of spent lithium-ion batteries recycling. *Journal of Environmental Management* **198**, 84-89, doi:https://doi.org/10.1016/j.jenvman.2017.04.062 (2017).
- 62 Yang, Y., Xu, S. & He, Y. Lithium recycling and cathode material regeneration from acid leach liquor of spent lithium-ion battery via facile co-extraction and co-precipitation processes. *Waste Management* **64**, 219-227, doi:https://doi.org/10.1016/j.wasman.2017.03.018 (2017).
- 63 Sa, Q. *et al.* Synthesis of Diverse LiNi<sub>x</sub>Mn<sub>y</sub>Co<sub>z</sub>O<sub>2</sub> Cathode Materials from Lithium Ion Battery Recovery Stream. *Journal of Sustainable Metallurgy* **2**, 248-256, doi:10.1007/s40831-016-0052-x (2016).
- 64 Gratz, E., Sa, Q., Apelian, D. & Wang, Y. A closed loop process for recycling spent lithium ion batteries. *Journal of Power Sources* **262**, 255-262, doi:https://doi.org/10.1016/j.jpowsour.2014.03.126 (2014).
- 65 Zou, H., Gratz, E., Apelian, D. & Wang, Y. A novel method to recycle mixed cathode materials for lithium ion batteries. *Green Chemistry* **15**, 1183-1191, doi:10.1039/C3GC40182K (2013).
- 66 Zheng, Z. *et al.* High Performance Cathode Recovery from Different Electric Vehicle Recycling Streams. *ACS Sustainable Chemistry & Engineering* **6**, 13977-13982, doi:10.1021/acssuschemeng.8b02405 (2018).
- 67 Chen, M. *et al.* Closed Loop Recycling of Electric Vehicle Batteries to Enable Ultra-high Quality Cathode Powder. *Scientific Reports* **9**, 1654, doi:10.1038/s41598-018-38238-3 (2019).
- 68 Li, L. *et al.* Process for recycling mixed-cathode materials from spent lithium-ion batteries and kinetics of leaching. *Waste Management* **71**, 362-371, doi:https://doi.org/10.1016/j.wasman.2017.10.028 (2018).
- 69 Li, L. *et al.* Sustainable Recovery of Cathode Materials from Spent Lithium-Ion Batteries Using Lactic Acid Leaching System. *ACS Sustainable Chemistry & Engineering* **5**, 5224-5233, doi:10.1021/acssuschemeng.7b00571 (2017).
- 70 Gaines, L. Lithium-ion battery recycling processes: Research towards a sustainable course. *Sustainable Materials and Technologies* **17**, e00068, doi:https://doi.org/10.1016/j.susmat.2018.e00068 (2018).
- 71 Pagnanelli, F., Moscardini, E., Altamari, P., Abo Atia, T. & Toro, L. Cobalt products from real waste fractions of end of life lithium ion batteries. *Waste Management* **51**, 214-221, doi:https://doi.org/10.1016/j.wasman.2015.11.003 (2016).

- 72 Yang, Y. *et al.* A Closed-Loop Process for Selective Metal Recovery from Spent Lithium Iron Phosphate Batteries through Mechanochemical Activation. *ACS Sustainable Chemistry & Engineering* **5**, 9972-9980, doi:10.1021/acssuschemeng.7b01914 (2017).
- 73 Yao, L., Yao, H., Xi, G. & Feng, Y. Recycling and synthesis of LiNi<sub>1/3</sub>Co<sub>1/3</sub>Mn<sub>1/3</sub>O<sub>2</sub> from waste lithium ion batteries using d,l-malic acid. *RSC Advances* **6**, 17947-17954, doi:10.1039/C5RA25079J (2016).
- 74 Swain, B. Recovery and recycling of lithium: A review. *Separation and Purification Technology* **172**, 388-403, doi:https://doi.org/10.1016/j.seppur.2016.08.031 (2017).
- 75 Kwade, A. & Diekmann, J. Recycling of lithium-ion batteries. *the LithoRec Way* (2018).
- 76 Diekmann, J. *et al.* Ecological Recycling of Lithium-Ion Batteries from Electric Vehicles with Focus on Mechanical Processes. *Journal of The Electrochemical Society* **164**, A6184-A6191, doi:10.1149/2.0271701jes (2017).
- 77 *Lithium Ion*, <<https://www.retrievtech.com/lithiumion>> (2019).
- 78 Chinyama Luzendu, G. (2016).
- 79 Sonoc, A., Jeswiet, J. & Soo, V. K. Opportunities to Improve Recycling of Automotive Lithium Ion Batteries. *Procedia CIRP* **29**, 752-757, doi:https://doi.org/10.1016/j.procir.2015.02.039 (2015).
- 80 Gaines, L. & Cuenca, R. Costs of lithium-ion batteries for vehicles. (United States, 2000).
- 81 *Recycling of EV-Lithium-Ion-Batteries*, <<http://www.lithorec2.de/index.php/en/>> (2019).
- 82 Zeng, X., Li, J. & Liu, L. Solving spent lithium-ion battery problems in China: Opportunities and challenges. *Renewable and Sustainable Energy Reviews* **52**, 1759-1767, doi:https://doi.org/10.1016/j.rser.2015.08.014 (2015).
- 83 Qiao, Q., Zhao, F., Liu, Z. & Hao, H. Electric vehicle recycling in China: Economic and environmental benefits. *Resources, Conservation and Recycling* **140**, 45-53, doi:https://doi.org/10.1016/j.resconrec.2018.09.003 (2019).
- 84 Li, L. *et al.* The Recycling of Spent Lithium-Ion Batteries: a Review of Current Processes and Technologies. *Electrochemical Energy Reviews* **1**, 461-482, doi:10.1007/s41918-018-0012-1 (2018).
- 85 Gu, F. *et al.* An investigation of the current status of recycling spent lithium-ion batteries from consumer electronics in China. *Journal of Cleaner Production* **161**, 765-780, doi:https://doi.org/10.1016/j.jclepro.2017.05.181 (2017).
- 86 *SungEel HiTech*, <<http://www.sungeelht.com/>> (
- 87 Shi, Y., Chen, G. & Chen, Z. Effective regeneration of LiCoO<sub>2</sub> from spent lithium-ion batteries: a direct approach towards high-performance active particles. *Green Chemistry* **20**, 851-862, doi:10.1039/C7GC02831H (2018).
- 88 Shi, Y., Chen, G., Liu, F., Yue, X. & Chen, Z. Resolving the Compositional and Structural Defects of Degraded LiNi<sub>x</sub>Co<sub>y</sub>Mn<sub>z</sub>O<sub>2</sub> Particles to Directly Regenerate High-Performance Lithium-Ion Battery Cathodes. *ACS Energy Letters* **3**, 1683-1692, doi:10.1021/acsenenergylett.8b00833 (2018).
- 89 Song, X. *et al.* Direct regeneration of cathode materials from spent lithium iron phosphate batteries using a solid phase sintering method. *RSC Advances* **7**, 4783-4790, doi:10.1039/C6RA27210J (2017).
- 90 Li, X., Zhang, J., Song, D., Song, J. & Zhang, L. Direct regeneration of recycled cathode material mixture from scrapped LiFePO<sub>4</sub> batteries. *Journal of Power Sources* **345**, 78-84, doi:https://doi.org/10.1016/j.jpowsour.2017.01.118 (2017).
- 91 Chen, S. *et al.* Renovation of LiCoO<sub>2</sub> with outstanding cycling stability by thermal treatment with Li<sub>2</sub>CO<sub>3</sub> from spent Li-ion batteries. *Journal of Energy Storage* **8**, 262-273, doi:https://doi.org/10.1016/j.est.2016.10.008 (2016).
- 92 Ganter, M. J., Landi, B. J., Babbitt, C. W., Ancil, A. & Gaustad, G. Cathode refunctionalization as a lithium ion battery recycling alternative. *Journal of Power Sources* **256**, 274-280, doi:https://doi.org/10.1016/j.jpowsour.2014.01.078 (2014).

- 93 Zhang, Z. *et al.* Ultrasound-assisted hydrothermal renovation of LiCoO<sub>2</sub> from the cathode of spent lithium-ion batteries. *International Journal of Electrochemical Science* **9**, 3691-3700 (2014).
- 94 Sloop, S. E., Trevey, J. E., Gaines, L., Lerner, M. M. & Xu, W. Advances in Direct Recycling of Lithium-Ion Electrode Materials. *ECS Transactions* **85**, 397-403, doi:10.1149/08513.0397ecst (2018).
- 95 Sloop, S. *Advances in Direct Recycling for Lithium-ion Batteries*, <<https://ndiastorage.blob.core.usgovcloudapi.net/ndia/2017/power/Sloop19264.pdf>> (2017).
- 96 *Global Electric Vehicles Battery Market 2017-2026: EV Battery Market to Reach \$93.94 Billion*, <<https://globenewswire.com/news-release/2018/03/26/1452966/0/en/Global-Electric-Vehicles-Battery-Market-2017-2026-EV-Battery-Market-to-Reach-93-94-Billion.html>> (2018).
- 97 *Closing the loop on battery recycling*, <<https://www.anl.gov/article/closing-the-loop-on-battery-recycling-0>> (2018).
- 98 Green, M. Aspects of Battery Legislation in Recycling and Re-use. *Johnson Matthey Technology Review* **61**, 87-92 (2017).
- 99 Jiao, D. N. *All EV batteries born after August 2018 in China will have unique IDs*, <<https://www.idtechex.com/research/articles/all-ev-batteries-born-after-august-2018-in-china-will-have-unique-ids-00015455.asp>> (2018).
- 100 Murphy, L. *THE ELECTRIFYING PROBLEM OF USED LITHIUM ION BATTERIES: RECOMMENDATIONS FOR LITHIUM ION BATTERY RECYCLING AND DISPOSAL*, <[https://law.ucdavis.edu/centers/environmental/files/2018-Spring-papers/The-Electrifying-Problem-of-Used-Lithium-Ion-Batteries\\_Murphy.pdf](https://law.ucdavis.edu/centers/environmental/files/2018-Spring-papers/The-Electrifying-Problem-of-Used-Lithium-Ion-Batteries_Murphy.pdf)> (2017).
- 101 *2016 ZEV Action Plan*, <[https://www.ca.gov/archive/gov39/wp-content/uploads/2018/01/2016\\_ZEV\\_Action\\_Plan-1.pdf](https://www.ca.gov/archive/gov39/wp-content/uploads/2018/01/2016_ZEV_Action_Plan-1.pdf)> (2019).
- 102 Wang, X., Gaustad, G., Babbitt, C. W. & Richa, K. Economies of scale for future lithium-ion battery recycling infrastructure. *Resources, Conservation and Recycling* **83**, 53-62, doi:<https://doi.org/10.1016/j.resconrec.2013.11.009> (2014).

## **Chapter 2. Closed Loop Recycling of Electric Vehicle Batteries to Enable Ultrahigh Quality Cathode Powder**

### **Abstract**

The lithium-ion battery (LIB) recycling market is becoming increasingly important because of the widespread use of LIBs in every aspect of our lives. Mobile devices and electric cars represent the largest application areas for LIBs. Vigorous innovation in these sectors is spurring continuous deployment of LIB powered devices, and consequently more and more LIBs will become waste as they approach end of life. Considering the significant economic and environmental impacts, recycling is not only necessary, but also urgent. The WPI group has successfully developed a closed-loop recycling process, and has previously demonstrated it on a relatively small scale 1 kg spent batteries per experiment. Here, we show that the closed-loop recycling process can be successfully scaled up to 30 kg of spent LIBs from electric vehicle recycling streams, and the recovered cathode powder shows similar (or better) performance to equivalent commercial powder when evaluated in both coin cells and single layer pouch cells. All of these results demonstrate the closed-loop recycling process has great adaptability and can be further developed into industrial scale.

### **1. Introduction**

With the development of mobile devices and electric cars, the demand of lithium-ion batteries (LIBs) keeps increasing. The market value of global lithium-ion battery was \$29.86 billion in 2017 and estimated to reach \$139.36 billion in 2026<sup>1</sup>. Because of the decreasing cost and increasing efficiency of LIBs, the rechargeable battery market is facing a major transformation. Bernatein

estimates that LIBs will occupy 70% of the rechargeable battery market by 2025<sup>2</sup>. Accordingly, the amount of end-of-life LIBs will rise significantly, lagging only in time. It is known that some countries use unsustainable ways to deal with battery waste such as incinerating or landfilling. The materials' value is lost if no suitable recycling process is applied, and thus valuable resources are lost. Considering both the economical and environmental implications, LIBs entering the waste stream require efficient and environmentally friendly recycling processes<sup>3-6</sup>. Favorable economics would encourage collection, and follow the successful effective recycling precedent set by the lead acid industry.

Currently, recycling approaches can be divided into three main types: pyrometallurgical, hydrometallurgical and direct recycling<sup>7</sup>. Pyrometallurgy uses high temperature to smelt valuable metals in spent LIBs, a temperature above 1000 °C is used to form alloys<sup>8</sup>. High use of energy restrains its lab-scale research, however, pyrometallurgy is widely used in industry because of its simplicity and high productivity. Hydrometallurgy employs chemical process to recycle, multi-step treatments including acid–base leaching, solvent extraction, precipitation and ion exchange and electrolysis are involved due to the chemical complexity of LIB itself<sup>9-17</sup>. Direct recycling recover different materials by physical processes. With minimal destruction, the recovered material retains its crystal structure and has a good electrochemical performance<sup>18</sup>. Pyrometallurgy, hydrometallurgy and direct recycling processes can be combined together to accommodate different incoming chemistry and expected outcome materials.

Over the past few years, many different recycling approaches and methods have been proposed and studied although much of the research is still in the lab scale phase. Ren et al. employed a novel slag system FeO-SiO<sub>2</sub>-Al<sub>2</sub>O<sub>3</sub> to recover spent batteries<sup>8</sup>. In situ recycling was developed by Li et al., they used oxygen-free roasting and wet magnetic separation technique to recover spent

LiCoO<sub>2</sub>/graphite batteries<sup>19</sup>. Tanong et al. tested several leaching reagents – inorganic acids, organic acids, chelating agents and alkaine agents, and found sulfuric acid was the most efficient solution for solubilizing metals from spent batteries<sup>10</sup>. They further optimize the best leaching condition using a three level Box-Behnken design<sup>10</sup>. Zhan et al. used froth flotation technique and separated fine battery electrode materials efficiently<sup>20</sup>. Lien concentrated valuable metals and graphite using membrane technologies<sup>21</sup>. Sonoc et al. firstly employed Donnan dialysis with cation exchange membranes and recovered lithium, transition metals<sup>16</sup>. Meng et al. proposed an electrochemical cathode-reduction method to leach LiCoO<sub>2</sub> from spent LIBs and mechanism was revealed by kinetic analysis<sup>17</sup>. Shi et al. developed a simple process to regenerate spent LiCoO<sub>2</sub> cathode, and the resulting cathode had a high electrochemical performance<sup>18</sup>. In addition, a number of research development specifically related to hydrometallurgical technologies in recent years are listed in **Table 1**. Hydrometallurgical recycling mainly involves leaching, solvent extraction and chemical precipitation. Leaching steps can be divided into alkali leaching and acid leaching, and acid leaching is more favorable because of its higher efficiency. Acid leaching includes inorganic acid and organic acid leaching, and inorganic leaching involves strong acid and can produce secondary pollution, while organic leaching can reach similar efficiency under a milder environment. Another leaching process is bioleaching, and it utilizes the acids generated during microorganisms' metabolism processes. Inorganic acid leaching has the advantages of low cost while organic acid leaching and bioleaching are more environmentally friendly. Solvent extraction is the process that follows leaching and to separate metal ions or to remove impurities, and it is accomplished because of the various distribution of metal ions between organic solvent and aqueous solution. Due to the high purity of products, solvent extraction is adopted in industry. However, there is still room for improvements to eliminate the complex procedures and high cost

of solvent. Chemical precipitation is widely used for separating metals from complex systems due to the varied solubilities at a certain pH. Common precipitants are NaOH, H<sub>2</sub>C<sub>2</sub>O<sub>4</sub>, C<sub>4</sub>H<sub>8</sub>N<sub>2</sub>O<sub>2</sub>, H<sub>3</sub>PO<sub>4</sub>, and Na<sub>2</sub>CO<sub>3</sub>, which can react with transition metal ions or Li<sup>+</sup> and forms insoluble precipitates. Ni, Mn and Co have similar properties and thus can be co-precipitated as hydroxides, which can be further fabricated into cathode. As such, complex separation steps are avoided and all the values can be recovered. In addition to the primary chemical processes discussed above, other recycling techniques including electrolysis, ion exchange and sol-gel processes are also studied for recycling. However, most of these processes only use single stream of spent batteries for recycling experiments. The produced materials are normally evaluated in the university lab.

**Table 1: List of hydrometallurgical technologies development in the literature**

Process	Development	Authors and year
Leaching	<ul style="list-style-type: none"> <li>Alkali leaching-NH<sub>3</sub>, (NH<sub>4</sub>)<sub>2</sub>SO<sub>4</sub>, Na<sub>2</sub>SO<sub>3</sub></li> <li>Leaching efficiencies of Co, Ni and Li-over 98%</li> </ul>	Zheng et al., 2017 <sup>41</sup>
	<ul style="list-style-type: none"> <li>Inorganic acid leaching-HCl</li> <li>Leaching efficiencies of Co and Mn-over 99%</li> </ul>	Barik et al., 2017 <sup>42</sup>
	<ul style="list-style-type: none"> <li>Organic acid leaching-Lactic acid</li> <li>Leaching efficiencies of Li, Ni, Co and Mn-over 97%</li> </ul>	Li et al., 2017 <sup>43</sup>
	<ul style="list-style-type: none"> <li>Bioleaching- organic acids produced by <i>Aspergillus niger</i></li> <li>Leaching efficiencies of Cu and Li-100%</li> </ul>	Bahaloo-Horeh et al., 2017 <sup>44</sup>
Solvent extraction	<ul style="list-style-type: none"> <li>Solvent extractants-Cyanex 272 and PC-88A</li> <li>Purities of Li, Ni and Co-99.9%, 99.7% and 99.6%</li> </ul>	Virolainen et al., 2017 <sup>45</sup>
	<ul style="list-style-type: none"> <li>Solvent extractants-D2EHPA in kerosene</li> <li>Purities of Li as Li<sub>2</sub>CO<sub>3</sub>-99.25%</li> </ul>	Yang et al., 2017 <sup>46</sup>
Chemical precipitation	<ul style="list-style-type: none"> <li>Precipitants and Precipitates-H<sub>3</sub>PO<sub>4</sub> and Li<sub>3</sub>PO<sub>4</sub>, H<sub>2</sub>C<sub>2</sub>O<sub>4</sub> and CoC<sub>2</sub>O<sub>4</sub></li> <li>Recovery efficiencies of Li and Co-88% and 99%</li> </ul>	Pinna et al., 2017 <sup>13</sup>
	<ul style="list-style-type: none"> <li>Precipitants and Precipitates-H<sub>3</sub>PO<sub>4</sub> and Li<sub>3</sub>PO<sub>4</sub>, H<sub>2</sub>C<sub>2</sub>O<sub>4</sub> and CoC<sub>2</sub>O<sub>4</sub>, C<sub>4</sub>H<sub>8</sub>N<sub>2</sub>O<sub>2</sub> and Ni(C<sub>4</sub>H<sub>6</sub>N<sub>2</sub>O<sub>2</sub>)<sub>2</sub></li> </ul>	Chen et al., 2016 <sup>47</sup>

	<ul style="list-style-type: none"> <li>• Recovery efficiencies of Li, Ni and Co-93%, 96% and 97%</li> </ul>	
	<ul style="list-style-type: none"> <li>• Precipitants and Precipitates-NaOH and <math>\text{Ni}_x\text{MnyCo}_z(\text{OH})_2</math></li> </ul>	Yang et al., 2016 <sup>48</sup>

Our group has developed a lab-scale and highly efficient closed-loop recycling process previously, which combines hydrometallurgical and direct recycling processes<sup>22-26</sup>. The inorganic acid leaching and co-precipitation reaction in our closed-loop recycling process are the typical hydrometallurgical processes. While different from industrial available hydrometallurgical recycling processes, in which the recovered materials are meal oxides or raw metal alloys, our closed-loop recycling process produced industrial-grade cathode material directly from recycling stream. However, not restricted to the success of recycling in lab scale, this closed-loop recycling process can be transferred into industrial scale and it paved a path to commercially recycle LIBs in a more economic and environmental friendly way. The main and exclusive advantages of our recycling process are as follow: (1) it can accommodate a wide range of incoming LIB chemistry feed. EV batteries from General Motors, Ford and Fiat Chrysler Automobiles were used to demonstrate this flexibility. (2) the recovered cathode material has equal or, in some instances, better electrochemical performance compared with commercial cathode material. (3) the electrochemical results haven been proved by both WPI and A123 Systems independently. (4) the recycling process has been scaled up to 30 kg spent batteries per experiment. Battery Resourcers is further scaling up the recycling work to 0.5ton spent lithium ion batteries per day.

Our previous work has focused primarily on the recycling of electronics battery waste and experiments were conducted up to a maximum scale of 1 kg of battery feed. The properties of recovered cathode materials show good performance; however, they are not as good as the industrial material. Here, with the utilization of the closed-loop recycling process, we report the

successful scaling-up of the process with different EV recycling streams and produce very high quality cathode materials-LiNi<sub>1/3</sub>Mn<sub>1/3</sub>Co<sub>1/3</sub>O<sub>2</sub> (NMC 111). The large scale experiment (7-day) also reveals how the particles are evolved, which has not been reported before. In this work, the end-of-life LIBs come from General Motor Chevrolet Volt (GM), Ford Focus (Ford) and Fiat Chrysler Automobiles 500 e (FCA) vehicles. The batteries used in both GM and Ford's EV batteries use a cathode which consists of LiNi<sub>1-x-y</sub>Mn<sub>x</sub>Co<sub>y</sub>-LiMn<sub>2</sub>O<sub>4</sub> (NMC-LMO), while FCA's battery supplier employs a cathode comprised of LiNi<sub>1-x-y</sub>Mn<sub>x</sub>Co<sub>y</sub>-LiMn<sub>2</sub>O<sub>4</sub>-LiNi<sub>x</sub>Co<sub>y</sub>Al<sub>z</sub>O<sub>2</sub> (NMC-LMO-NCA)<sup>27-32</sup>. The successful scaling-up of the process was confirmed by our own analyses and independent electrochemical test results from A123 Systems. Compared with the commercially sourced cathode material that was used as our control, our recycled cathode shows comparable electrochemical performances and, notably, superior rate capability.

## 2. Experimental Section

### 2.1 Overall Recycling Process

In general, the closed-loop recycling stream can be summarized in **Fig. 1**. End-of-life batteries are first cut, shredded and sieved. Batteries of various form factors, package design (pouch or metal can) and multiple chemistries can be combined in a single feed lot. After removal of the casing, aluminum etc., what remains is the graphite, carbon and cathode powders. The different cathode powders are dissolved together in a leaching solution of sulfuric acid (H<sub>2</sub>SO<sub>4</sub>) and hydrogen peroxide (H<sub>2</sub>O<sub>2</sub>). In this step, some impurities are also dissolved in the leaching solution. In order to synthesize NMC111, impurities such as Cu, Fe, Al are removed by strategically controlling the pH. Inductively coupled plasma optical emission spectrometry (Perkin Elmer Optima 8000 ICP-

OES) is used to determine the concentrations of various metal ions, and nickel sulfate hexahydrate, manganese sulfate monohydrate and cobalt sulfate are added to reach the desired ratio, which is 1:1:1 for Ni, Mn, Co in this study. The co-precipitation reaction will be discussed in detail later. After filtering and drying, precursors ( $\text{Ni}_{1/3}\text{Mn}_{1/3}\text{Co}_{1/3}(\text{OH})_2$ ) mix with  $\text{Li}_2\text{CO}_3$ . Then the mixture is sintered at  $450\text{ }^\circ\text{C}$  for 5 hours and  $900\text{ }^\circ\text{C}$  for 14 hours.



**Figure 1: Scheme of closed-loop recycling process**

## **2.2 The Co-precipitation Reaction – Precursor Synthesis**

After cutting, shredding and sieving to remove foils and cell case or pouch materials, the remaining powders, which are a mixture of carbon, graphite and cathode powder, are leached in acid. After removing the impurities in the leachate, nickel sulfate hexahydrate (GFS Chemicals), manganese sulfate monohydrate (GFS Chemicals) and cobalt sulfate (GFS Chemicals) are added to adjust the ratio of Ni, Mn, Co. This ratio is tested again using ICP, after which the metal sulfate solution undergoes a co-precipitation reaction. Chemical reagents fed into the co-precipitation reactor are (Ni/Mn/Co) metal sulfate solution, ammonia solution (32%, EMD Millipore) and sodium hydroxide (VWR). A 5 L jacketed glass cylinder with customized feed ports is used for the co-precipitation reaction, which is conducted under nitrogen. Process parameters including pH, flow rate and temperature are controlled throughout the reaction. After a certain transient period, the co-precipitation reaction reaches equilibrium, or steady state, and particle size, morphology and tap density remain constant<sup>39</sup>.

At the end of experiment, the suspension is filtered and washed thoroughly to remove residual or absorbed salts. Then, the particles need to be dried in the oven for about 12 hrs at 130 °C. Tap densities are measured manually, whereby a graduated cylinder is tapped constantly until the level stops changing. JEOL JSM 7000 F is used for obtaining SEM images of the particles. X-ray diffraction (XRD) patterns are obtained using PANalytical Empyrean, with highScore software employed to obtain Rietveld refinement.

## **2.3 Cathode Sintering**

To synthesize cathode active material, 1 mol of precursor is mixed with 1.05 mol of  $\text{Li}_2\text{CO}_3$  (VWR). An excess of 5%  $\text{Li}_2\text{CO}_3$  compensates for the Li loss during firing<sup>40</sup>. Before sintering, the mixture must be uniform in color. Otherwise, it needs to be mixed again. Sintering conditions are 450 °C for 5 hours and 900 °C for 14 hours. Both heating and cooling rates are 2 °C/min. After cooling down to room temperature, the cathode powder must undergo grinding to ensure the material does not contain any agglomerates.

## **2.4 Electrochemical Testing**

Cathode powder, conductive carbon (super C65), and Polyvinylidene fluoride (PVDF) dissolved in N-Methyl-2-pyrrolidone (NMP) are mixed uniformly. Then the slurry is cast onto an aluminum foil and dried at 60 °C for 8 hours. 14 mm diameter electrode disks are punched and pressed to reach a desired porosity prior to assembling into coin cells. After being dried in vacuum oven for 8 hours, any excess solvent is removed, and the cathode electrode is ready for coin cell assembly. In the WPI lab, we assemble half coin cells to test the rate performance and full coin cells to test the cycle performance. Half coin cells use a lithium metal anode while full coin cells use a graphite anode. They are both assembled in glove box. The electrolyte used is 1M  $\text{LiPF}_6$  in ethylene carbonate (EC), diethyl carbonate (DEC), and dimethyl carbonate (DMC) (1:1:1). The separator used is a 25um trilayer polypropylene-polyethylene-polypropylene membrane (MTI Corporation). Electrochemical performance tests are conducted with an Arbin instrument (Model BT2043). Both coin cells and single layer pouch cells are also assembled at A123 Systems for independent evaluation following similar cell assembly and testing protocols.

## **3. Results and Discussions**

Parameters optimization of the co-precipitation reaction was accomplished using experiments whose reaction time was 30 hours and in which ~1 kg spent lithium ion batteries were processed. Then parameters were translated to the larger scale experiments, in which 30 kg batteries were used and the reaction time were 168 hours. The ultimate success of the scaling-up of the closed-loop recycling process was verified both by our results and independent electrochemical tests from A123 Systems.

### 3.1 Small-scale Experiment

In the co-precipitation reaction, parameters that need to be optimized include pH number, residence time, reaction time, the feed rates of the ammonia solution and metal sulfate, etc. Here, metal sulfate solution is added in a range of 2.4–3.5 mL/min, and ammonia water is 0.4–0.9 mL/min. NaOH solution is fed automatically and the pH is controlled in a range of 10–11. In the small-scale experiment with a reaction time of 30 hours, samples are taken every five hours to monitor the process. Every sample is filtered and dried for SEM observation and tap density tests. While the as-filtered sample is pink, it turns into black when dried. It is believed that the black powder is a mixture of hydroxide and oxyhydroxide<sup>33</sup>.

Evolution of the precursor particle morphology is observed in the SEM images in **Fig. 2**, and the tap densities detailed in **Fig. 3**. The precursor particles are secondary particles that are spherical in shape, and are aggregates of plate-shaped primary particles. As the reaction progresses, the primary particles keep filling the internal void space available within the secondary particle. Via this mechanism, the precursor particles grow progressively larger and denser. Tap densities in **Fig. 3** supports this trend. At some point, there is no more space for thickening and filling, and particle size achieves steady state and remains constant, beyond which tap density stops increasing significantly. This signals that the co-precipitation reaction has reached equilibrium. In the small-

scale experiment, this occurs at 25 hours. Samples collected after 25 hours can be regarded as the same, which laid the foundation for further scale-up and eventual industrial application. In the later scale-up experiments, it was more evident that the reaction reaches an equilibrium after a transient non-steady state period. It is worth mentioning that particle size and morphology play important roles in electrochemical performances. Uniform, spherical particles improve tap density and further boost the capacity/energy density of the electrodes<sup>34</sup>. Smaller particles are beneficial for cell power performance because of shorter ionic diffusion distance. However, the total higher surface area also adversely impacts performance due to increased contact resistance<sup>35</sup>. Optimized particle size distribution benefits both rate tests and cycle performance, and it is believed  $10 \pm 2 \mu\text{m}$  of D50 is an ideal range for NMC111 based on the size of commercial NMC 111 powder. Here, the 30-hour precursor sample has a tap density of 2.05 g/mL. The high tap density, uniform morphology and suitable size of the precursor particles make them good candidates for sintering into cathode powder.

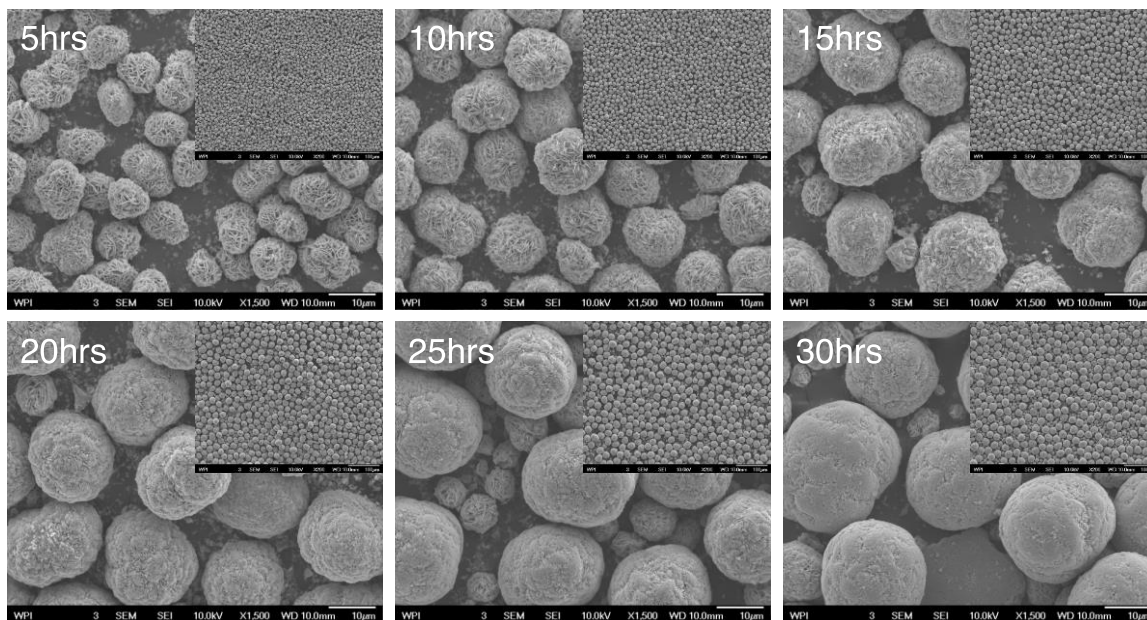


**Figure 2. SEM images of precursors that collected at different time.** For example, 5 hrs is SEM images of 5 hours precursor with a magnification of 1,500 (scale bar: 10  $\mu\text{m}$ ). The top inner right

insert shows the SEM images of the 5 hours precursor with a magnification of 200 (scale bar: 100  $\mu\text{m}$ ), etc.

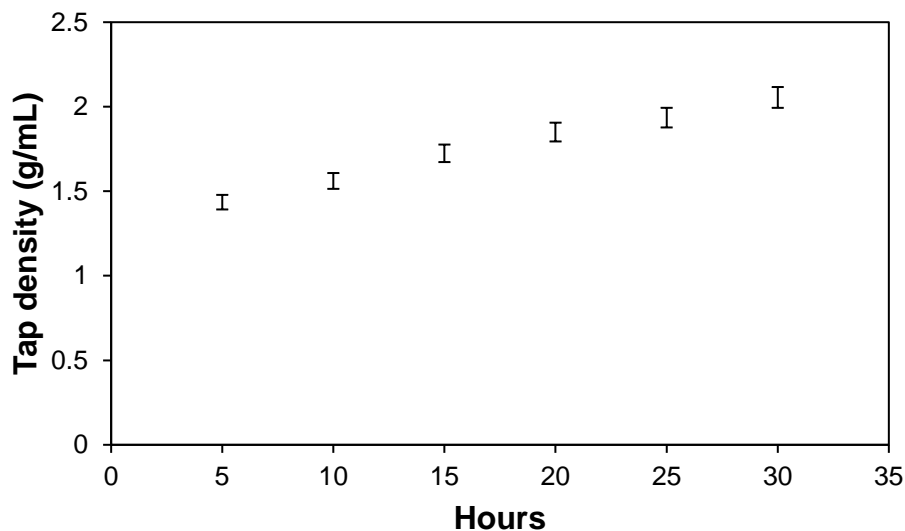


**Figure 3: Tap densities of precursors that collected at different time**

Cathode material is fabricated by sintering the final precursor and lithium carbonate. SEM images are included in **Fig. 4**, and it can be observed that the cathode powder maintains good morphology and the size of the precursor, which highlights the importance of synthesizing high quality precursor. The tap density of the recycled cathode power is as high as 2.75 g/mL, which is beneficial for specific capacity and electrochemical performance, as will be reported later. The crystalline property and purity of the synthesized cathode are confirmed by XRD and ICP-OES, respectively. The XRD pattern and refinement are presented in **Fig. 4** and **Table 2**. The peaks of synthesized cathode are sharp and it is classified as  $\alpha\text{-NaFeO}_2$  structure ( $R\bar{3}m$ ). Distinct separations of (006)/(012) and (018)/(110) are due to the highly ordered layered structure. The  $c/3a$  has a value of 1.6587, which is also an indicator of good layered structure<sup>34</sup>. The XRD pattern difference of synthesized cathode and simulation is marginal, not only from observation but also from the Rwp number (6.50%). The magnitude of ICP-OES tests is in ppm, and both precursor

and cathode powder are dissolved and diluted first. Results are shown in **Table 3**, and ratios of metal ions are exactly 1:1:1:3 (Ni:Mn:Co:Li) with less than 3% measurement error. Moreover, no impurities are detected in ppm order.

Parameters optimization in small-scale experiments was not only successful in generating high quality cathode material, but offers a valuable tool from which the parameters can be translated to inform larger scale experiments. Cathode material synthesized using our closed-loop recycling process exhibits excellent performances, including tap density, particle morphology and size distribution, crystallization and purity tests (XRD and ICP-OES). It not only demonstrates the viability of our recycling method, but also provides parameters for the following scale-up experiments.

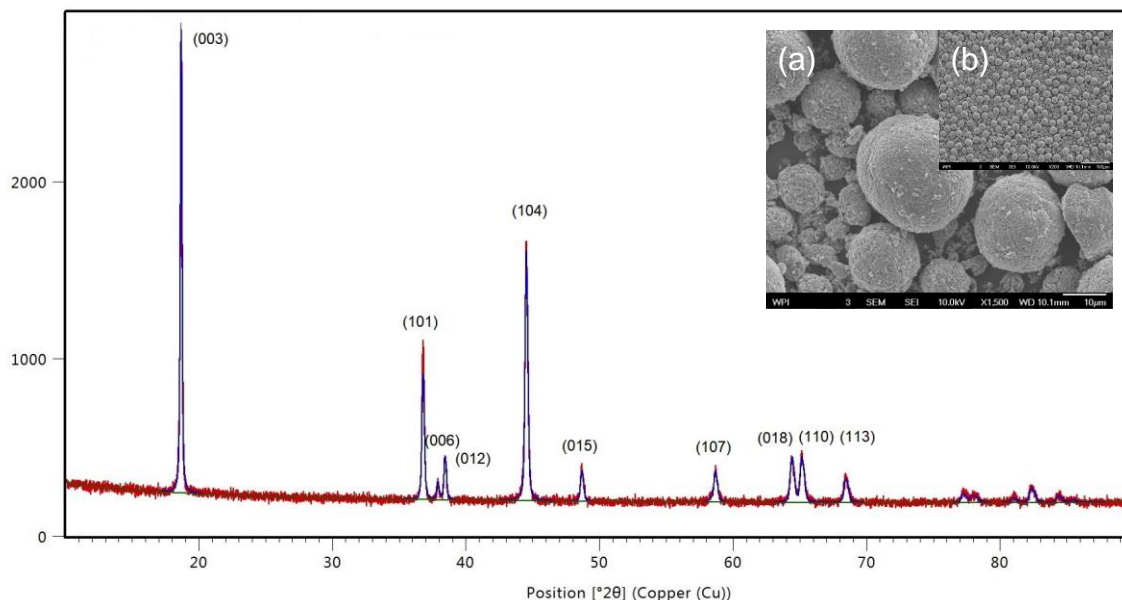


**Figure 4: XRD pattern and Rietveld refinement of cathode- $\text{LiNi}_{1/3}\text{Mn}_{1/3}\text{Co}_{1/3}\text{O}_2$ .** Red line is observed data and blue line is simulation. (a) SEM image of cathode with magnification factor of 1,500 (scale bar: 10  $\mu\text{m}$ ) (b) SEM image of cathode with magnification factor of 200 (scale bar: 100  $\mu\text{m}$ )

**Table 2: Rietveld Refinement of Synthesized  $\text{LiNi}_{1/3}\text{Mn}_{1/3}\text{Co}_{1/3}\text{O}_2$** 

Lattice parameters		Agreement indices		
a (Å)	c (Å)	Rwp (%)	Rp (%)	Re (%)
2.8613	14.2385	6.5004	5.0411	6.5156

**Table 3: Ratio of metal ions tested by ICP-OES. ND: Not detected**

Ratio	NMC 111 Precursor	NMC 111 Cathode
Ni	0.98	1.01
Mn	1.00	1.00
Co	1.00	1.00
Li	ND	3.09
Cu	ND	ND
Fe	ND	ND
Al	ND	ND

### 3.2 Scale-up

Herein, the reaction time is increased to seven days compared with thirty hours in the small experiment. For the adjustments in larger scale experiments, we transferred all the parameters into larger scale experiments in their initial status (168 hrs reaction time) after finding the optimized parameters in smaller scale experiments (30 hrs reaction time). However, in order to accommodate to requirements of particle size distribution, tap density, et al., parameters including pH number, flow rate, etc would be adjusted during the larger scale experiments while monitoring the experiment closely. Therefore, the parameters in larger scale experiments are not exactly the same with those in smaller experiments.

Samples are taken every 24 hours and the experiment is monitored to ensure scaled-up experiments are suited to eventual industrial application. It is well known that industrial-scale co-precipitation processes employ continuous reactions. For example, production runs for 30 days are common, with material being collected daily over the course of the run. The key to successful industrialization is to guarantee every batch of power can be used, and thus every day's precursor is collected for further testing. Tap densities are displayed in **Fig. 5**, and they remain constant from day to day, and as high as 2.00 g/mL. Particle size distribution seems to show some differences over the first three days, as observed in the SEM images in **Fig. 6**. Firstly, the particles have uniform size. With the progress of the experiment, the particles grow larger and new particles are formed. After 3~4 days, the reaction reaches to steady state and at this time the particle size and distribution will not change much with further progress of the experiment. The particles collected after steady state have bimodal size distribution. Although it takes longer to attain equilibrium in large-scale experiment, considering industrialization in the future, three days has marginal influence for a one-month production run. Factors including particle morphology, size distribution, and tap density are monitored and once stable, samples from Day 3 to Day 7 are combined together and sintered into cathode powder. It can be seen by the SEM images presented in **Fig. 6**, that the cathode particles are densely packed and quite spherical, and a tap density of 2.52 g/mL was achieved. Particle size distribution of the synthesized cathode has been characterized by A123 systems and results are shown in **Fig. 7**. Material has a D50 of a value of 11.7  $\mu\text{m}$  and the electrochemical performance is presented in later sections. Although the large-scale experiment in our lab was only carried out for seven consecutive days, it is believed that with a larger reactor and constant supply of reactants, commercialization of our closed-loop recycling process is very promising.

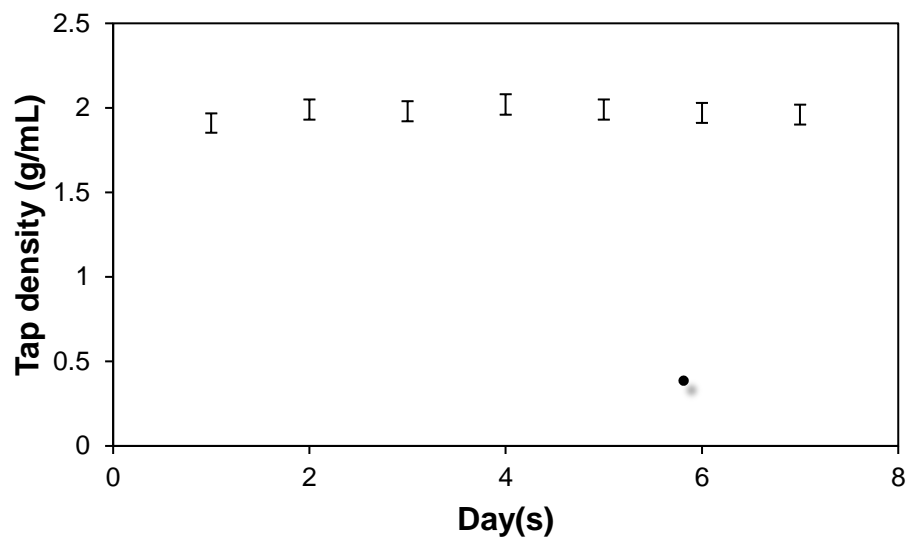


**Figure 5: Tap densities of precursors that collected at different time.**

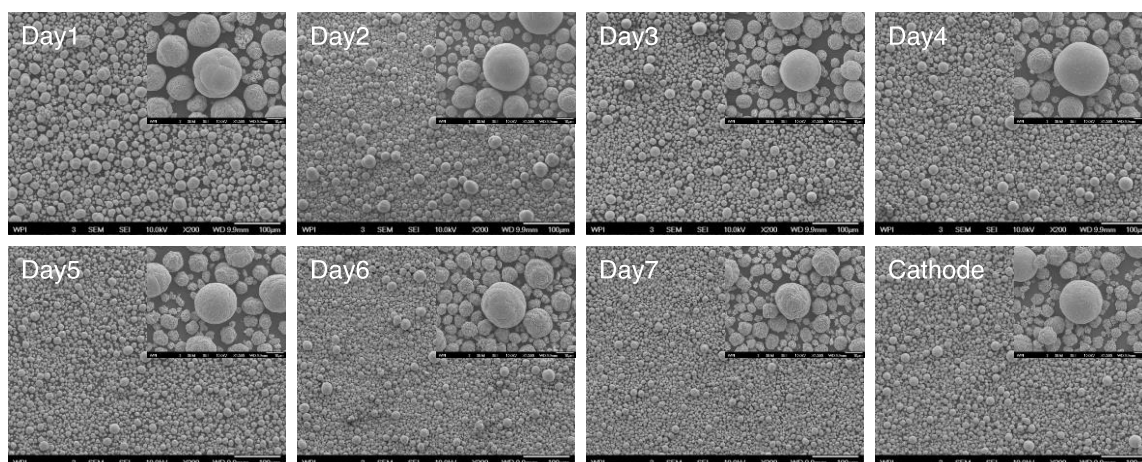


**Figure 6. SEM images of precursors that collected at different range of time and the final cathode (bottom right). For example, Day 1 shows SEM images of Day 1 precursor with a magnification of 200 (scale bar: 100  $\mu\text{m}$ ). The insert for the Day 1 precursor shows the SEM of the same material with a magnification of 1,500 (scale bar: 10  $\mu\text{m}$ ), etc.**

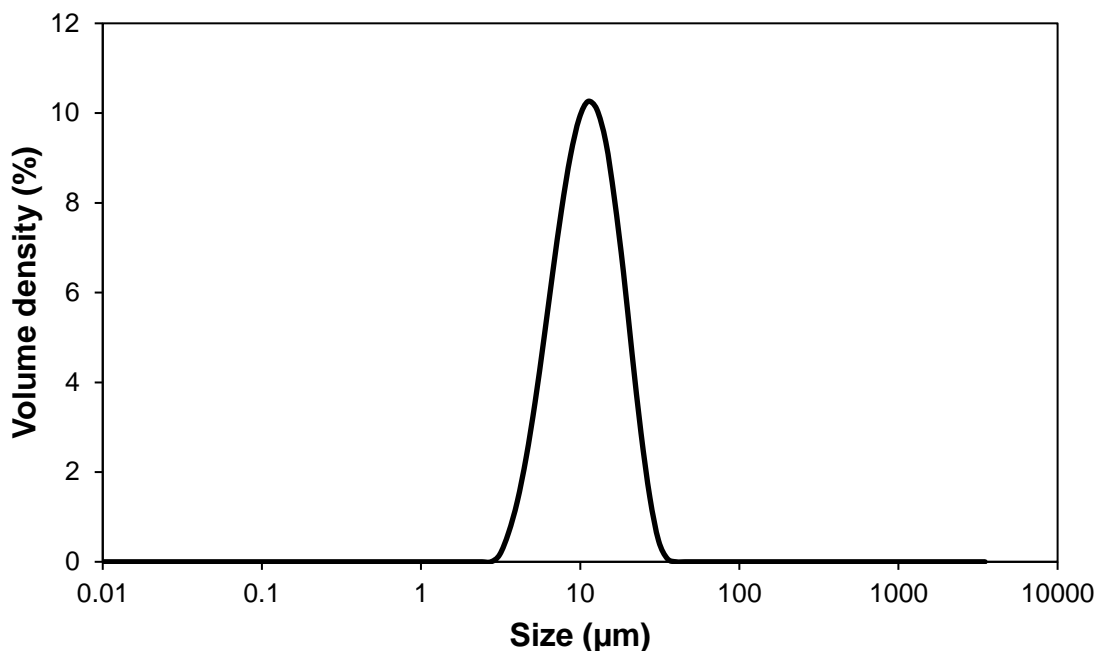


**Figure 7: Size distribution of cathode powder.** D (10) is 6.22 µm, D (50) is 11.7 µm, D (90) is 21.0 µm, D (99.9) is 35.0 µm.

These results demonstrate that our recycling process was successfully scaled up from a spent battery feed of 1 kg to one of 30 kg. The synthesized powder characterization results, including particle size, particle morphology, tap density, purity and crystalline state, and their proximity to results from reference commercial cathode material, suggest that the recycled cathode will deliver comparable electrochemical performance in coin cells and pouch cells. This will be addressed in the next section.

### 3.3 Electrochemical performance

Ultimately the success of our scale-up must be validated by evaluating the electrochemical performance of the recycled cathode material in cells. Accordingly, both half coin cell and full coin cell were assembled in our lab to evaluate rate capability and cycle performance. Results are shown in **Fig. 8**. Specific capacity is 158 mAh/g, 155 mAh/g, 149 mAh/g, 140 mAh/g, 133 mAh/g, 125 mAh/g, 113 mAh/g, 79 mAh/g for 0.1C, 0.2C, 0.5C, 1C, 2C, 3C, 5C, 10C, respectively. The capacity of 158 mAh/g at 0.1C is comparable with commercial NMC 111 capacity. The high rate performance is quite impressive (113 mAh/g and 79 mAh/g for 5C and 10C, respectively). Besides the excellent rate capability results, the cycle life tests, conducted using 0.5C/0.5C cycling, are also promising. The coulombic efficiency stays above 99% for all of the 100 cycles. After 100 cycles, the capacity retention is nearly 100%. There is a slightly specific capacity increase during the cycling. In general, the slight increase of the specific capacity is due to the following reasons: (1) the increased conductivity of electrode materials. (2) the increase of surface area caused by electrode materials' minimal breakage. (3) the continuous activation of electrode materials due to better infiltration of electrolyte. (4) the slight increase of room temperature. Here, the increase of specific capacity was very small (1.55 mAh/g, ~1% of the specific capacity of the material) and we believed the slight increase of room temperature maybe the main reason. The coin cells were tested at room temperature, and there was a slight variation of temperature between daytime and nighttime. Also, the continuous stabilization of interface in coin cells and activation of electrode materials may help the slight capacity increase. Compared with commercial NMC 111 powder, our recycled product is comparable, with better rate capability. Considering the aggregate results including SEM image, tap density, size distribution, purity and crystal structure, one can conclude that the closed-loop recycling process described herein has very promising commercial potential.

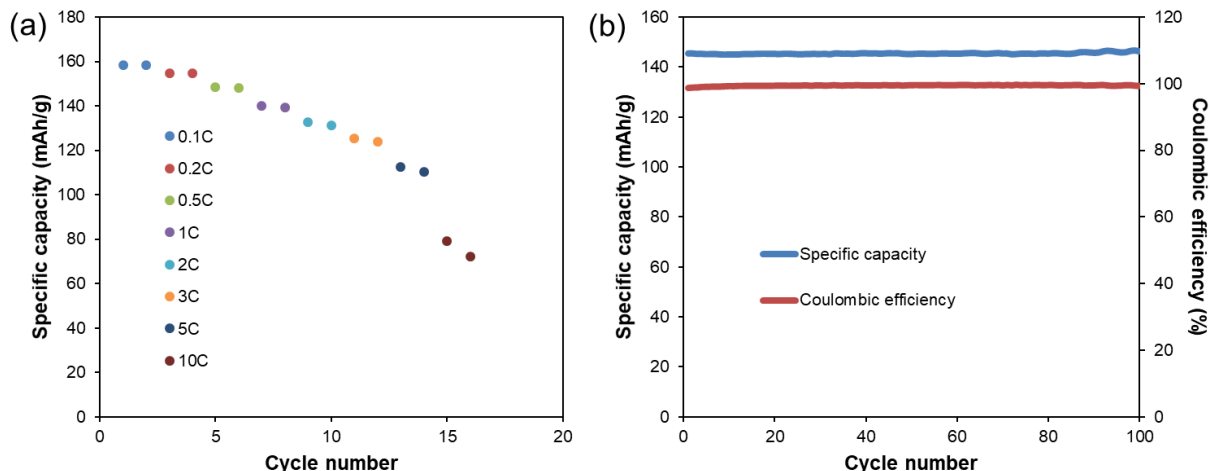


**Figure 8. (a) Rate performance. (b) Cycle performance.**

### 3.4 Independent Testing at A123 Systems

Synthesized cathode powders from the recycling process were sent to A123 Systems for independent electrochemical performance tests. A123 Systems selected a commercially available NMC111 cathode as a control powder, and compared the control powder with WPI synthesized cathode powder (**Fig. 9**) in coin cells and single layer pouch cells (SLPs) that were otherwise identical. Detailed comparison of physical properties between WPI synthesized cathode powder with control cathode powder tested by A123 Systems is depicted in **Table 4**. It was observed that WPI synthesized powder performed better than the control reference at all rate tested up to 10C (**Fig. 9a**). A comparison between WPI synthesized cathode powder and commercial control cathode powder is shown in **Fig. 10**. WPI synthesized cathode is more porous than control cathode, which is especially clear in small particles. Porous cathode particles have more electrolyte uptake and diffusion is easier because ionic diffusion in liquid (diffusion coefficient  $\sim 10^{-6} \text{ cm}^2/\text{s}$ )<sup>36</sup> is faster than that in solid (diffusion coefficient  $\sim 10^{-10} \text{ cm}^2/\text{s}$ )<sup>37</sup>. It explains that at higher rate, WPI

synthesized cathode outperforms control cathode. Specific capacity of WPI synthesized cathode powder has a value 153 mAh/g, 145 mAh/g, 139 mAh/g, 132 mAh/g, 111 mAh/g, 38 mAh/g for 0.2C, 0.5C, 1C, 2C, 5C, 10C, respectively, which is similar to the results in the previous section. Based on those results, the synthesized cathode material from our closed-loop recycling process is well positioned to compete with non-recycled counterparts for Li-ion battery market. Besides coin cell, A123 systems also fabricated single layer pouch (SLP) cell to further study the electrochemical performance of WPI recovered cathode powder.

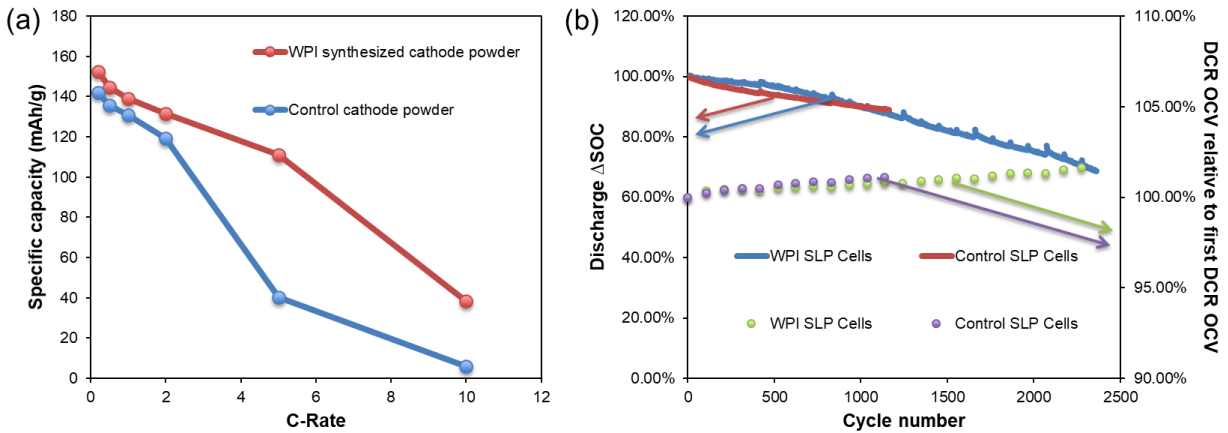


**Figure 9. (a) Rate performance of coin cells. (b) SLP cells cycle performance. (WPI synthesized cathode powder vs. Control cathode powder).**

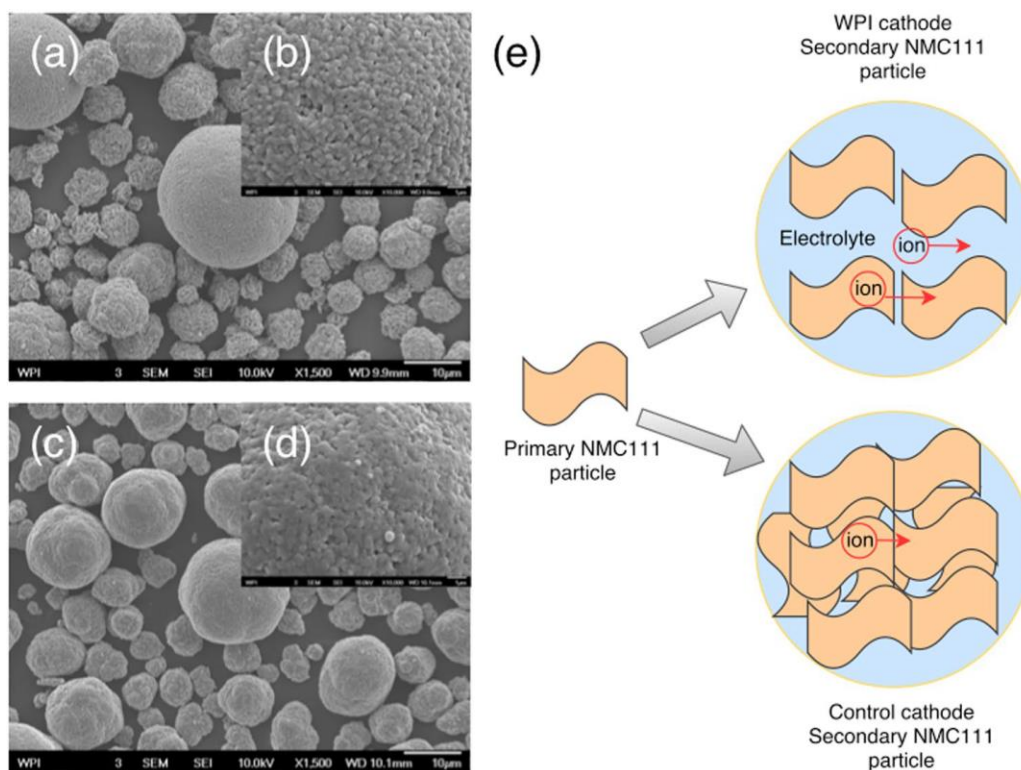


**Figure 10. SEM images of cathode powder (WPI vs. Control).** (a) WPI with magnification factor of 1,500 (scale bar: 10  $\mu\text{m}$ ) (b) WPI with magnification factor of 10,000 (scale bar: 1  $\mu\text{m}$ ) (c) Control with magnification factor of 1,500 (scale bar: 10  $\mu\text{m}$ ) (d) Control with magnification factor of 10,000 (scale bar: 1  $\mu\text{m}$ ) (e) Schematic demonstration of diffusion difference between WPI synthesized cathode and control cathode.

**Table 4: Physical properties comparisons between control cathode powder with WPI synthesized cathode powder.**

Test	Metric	Control Cathode Powder	WPI Synthesized Cathode Powder
Tap density	g/cc	2.84	2.51

D50 PSD	$\mu\text{m}$	9.2	10.2
BET	$\text{m}^2/\text{g}$	0.28	0.65

Pouch cells are widely used in consumer, military and automotive applications because of their simple and lightweight design<sup>38</sup>. The SLP cell is a simple yet representative form factor which largely mimics the multi-layered prismatic cells. Screening battery materials at the SLP level offers a useful research tool for early stage technology development where material quantity may limit the choice of form factors between coin cell and large format pouch cells. Therefore, the electrochemical performance of SLP cells fabricated by A123 Systems has great values and offers insight to inform subsequent work. Results are presented in **Fig. 9(b)**, where control and WPI synthesized cathode show similar trends in both discharge  $\Delta\text{SOC}$  tests and direct current resistance (DCR) tests. After 1000 cycles, 90% of the discharge capacity is retained, and after 1700 cycles, 80% of its discharge capacity remains. Impedance is also comparable for the control and WPI synthesized cathode powders. Independent electrochemical performance tests again yield encouraging results. WPI synthesized cathode powder has comparable or better (for high rates) performance than the commercially sourced control powder. The results suggest that our recycling process is capable of being scaled up. The critical next phase of technology development and large scale validation is presently being conducted by Battery Resourcers, Inc.

#### 4. Conclusions

In this study, it is confirmed that our closed-loop recycling process can handle large format spent batteries that come from different commercial electrified vehicles (GM, Ford and FCA), having

different cathode chemistries. Moreover, recycled cathode powder synthesized by WPI has similar or better performance when compared to equivalent stoichiometry commercial powder. This is validated by electrochemical testing of WPI assembled coin cells, and independent electrochemical testing of coin cells and SLP cells made and tested by A123 Systems. In addition, this recycling process is scalable (30 kg spent batteries are recycled in each experiment), with efforts towards further scale-up underway. The very promising results obtained to date of this timely and important work suggest a viable path towards commercialization exists. Toward this end, scale-up and development work continues at Battery Resourcers and further results can be expected in the near future.

## References:

- 1 *Lithium-ion Battery - Global Market Outlook (2017-2026)*, <<http://www.strategymrc.com/report/lithium-ion-battery-market>> (2018).
- 2 Desjardins, J. *Explaining the Surging Demand for Lithium-Ion Batteries*, <<http://www.visualcapitalist.com/explaining-surging-demand-lithium-ion-batteries/>> (2016).
- 3 Georgi-Maschler, T., Friedrich, B., Weyhe, R., Heegn, H. & Rutz, M. Development of a recycling process for Li-ion batteries. *Journal of Power Sources* **207**, 173-182, doi:<https://doi.org/10.1016/j.jpowsour.2012.01.152> (2012).
- 4 Richa, K., Babbitt, C. W., Gaustad, G. & Wang, X. A future perspective on lithium-ion battery waste flows from electric vehicles. *Resources, Conservation and Recycling* **83**, 63-76, doi:<https://doi.org/10.1016/j.resconrec.2013.11.008> (2014).
- 5 Kang, D. H. P., Chen, M. & Ogunseitan, O. A. Potential Environmental and Human Health Impacts of Rechargeable Lithium Batteries in Electronic Waste. *Environmental Science & Technology* **47**, 5495-5503, doi:10.1021/es400614y (2013).
- 6 Xu, J. *et al.* A review of processes and technologies for the recycling of lithium-ion secondary batteries. *Journal of Power Sources* **177**, 512-527, doi:<https://doi.org/10.1016/j.jpowsour.2007.11.074> (2008).
- 7 Gaines, L. Lithium-ion battery recycling processes: Research towards a sustainable course. *Sustainable Materials and Technologies* **17**, e00068, doi:<https://doi.org/10.1016/j.susmat.2018.e00068> (2018).
- 8 Ren, G.-x. *et al.* Recovery of valuable metals from spent lithium ion batteries by smelting reduction process based on FeO–SiO<sub>2</sub>–Al<sub>2</sub>O<sub>3</sub> slag system. *Transactions of Nonferrous Metals Society of China* **27**, 450-456, doi:[https://doi.org/10.1016/S1003-6326\(17\)60051-7](https://doi.org/10.1016/S1003-6326(17)60051-7) (2017).
- 9 Weng, Y., Xu, S., Huang, G. & Jiang, C. Synthesis and performance of Li[(Ni<sub>1/3</sub>Co<sub>1/3</sub>Mn<sub>1/3</sub>)<sub>1-x</sub>Mgx]O<sub>2</sub> prepared from spent lithium ion batteries. *Journal of*

- Hazardous Materials* **246-247**, 163-172, doi:<https://doi.org/10.1016/j.jhazmat.2012.12.028> (2013).
- 10 Tanong, K., Coudert, L., Mercier, G. & Blais, J. F. Recovery of metals from a mixture of various spent batteries by a hydrometallurgical process. *J Environ Manage* **181**, 95-107, doi:[10.1016/j.jenvman.2016.05.084](https://doi.org/10.1016/j.jenvman.2016.05.084) (2016).
- 11 Larcher, D. & Tarascon, J. M. Towards greener and more sustainable batteries for electrical energy storage. *Nature Chemistry* **7**, 19, doi:[10.1038/nchem.2085](https://doi.org/10.1038/nchem.2085) (2014).
- 12 Leite, D. d. S., Carvalho, P. L. G., de Lemos, L. R., Mageste, A. B. & Rodrigues, G. D. Hydrometallurgical separation of copper and cobalt from lithium-ion batteries using aqueous two-phase systems. *Hydrometallurgy* **169**, 245-252, doi:<https://doi.org/10.1016/j.hydromet.2017.01.002> (2017).
- 13 Pinna, E. G., Ruiz, M. C., Ojeda, M. W. & Rodriguez, M. H. Cathodes of spent Li-ion batteries: Dissolution with phosphoric acid and recovery of lithium and cobalt from leach liquors. *Hydrometallurgy* **167**, 66-71, doi:<https://doi.org/10.1016/j.hydromet.2016.10.024> (2017).
- 14 Guo, X., Cao, X., Huang, G., Tian, Q. & Sun, H. Recovery of lithium from the effluent obtained in the process of spent lithium-ion batteries recycling. *Journal of Environmental Management* **198**, 84-89, doi:<https://doi.org/10.1016/j.jenvman.2017.04.062> (2017).
- 15 Chen, X. *et al.* Organic reductants based leaching: A sustainable process for the recovery of valuable metals from spent lithium ion batteries. *Waste Management* **75**, 459-468, doi:<https://doi.org/10.1016/j.wasman.2018.01.021> (2018).
- 16 Sonoc, A. C., Jeswiet, J., Murayama, N. & Shibata, J. A study of the application of Donnan dialysis to the recycling of lithium ion batteries. *Hydrometallurgy* **175**, 133-143, doi:<https://doi.org/10.1016/j.hydromet.2017.10.004> (2018).
- 17 Meng, Q., Zhang, Y. & Dong, P. Use of electrochemical cathode-reduction method for leaching of cobalt from spent lithium-ion batteries. *Journal of Cleaner Production* **180**, 64-70, doi:<https://doi.org/10.1016/j.jclepro.2018.01.101> (2018).
- 18 Shi, Y., Chen, G. & Chen, Z. Effective regeneration of LiCoO<sub>2</sub> from spent lithium-ion batteries: a direct approach towards high-performance active particles. *Green Chemistry* **20**, 851-862, doi:[10.1039/C7GC02831H](https://doi.org/10.1039/C7GC02831H) (2018).
- 19 Li, J., Wang, G. & Xu, Z. Environmentally-friendly oxygen-free roasting/wet magnetic separation technology for in situ recycling cobalt, lithium carbonate and graphite from spent LiCoO<sub>2</sub>/graphite lithium batteries. *Journal of Hazardous Materials* **302**, 97-104, doi:<https://doi.org/10.1016/j.jhazmat.2015.09.050> (2016).
- 20 Zhan, R., Oldenburg, Z. & Pan, L. Recovery of active cathode materials from lithium-ion batteries using froth flotation. *Sustainable Materials and Technologies* **17**, e00062, doi:<https://doi.org/10.1016/j.susmat.2018.e00062> (2018).
- 21 Lien, L. in *Meeting Abstracts*. 611-611 (The Electrochemical Society).
- 22 Gratz, E., Sa, Q., Apelian, D. & Wang, Y. A closed loop process for recycling spent lithium ion batteries. *Journal of Power Sources* **262**, 255-262, doi:<https://doi.org/10.1016/j.jpowsour.2014.03.126> (2014).
- 23 Sa, Q. *et al.* Synthesis of high performance LiNi<sub>1/3</sub>Mn<sub>1/3</sub>Co<sub>1/3</sub>O<sub>2</sub> from lithium ion battery recovery stream. *Journal of Power Sources* **282**, 140-145, doi:<https://doi.org/10.1016/j.jpowsour.2015.02.046> (2015).
- 24 Zou, H., Gratz, E., Apelian, D. & Wang, Y. A novel method to recycle mixed cathode materials for lithium ion batteries. *Green Chemistry* **15**, 1183-1191, doi:[10.1039/C3GC40182K](https://doi.org/10.1039/C3GC40182K) (2013).
- 25 Heelan, J. *et al.* Current and prospective Li-ion battery recycling and recovery processes. *Jom* **68**, 2632-2638 (2016).
- 26 Sa, Q. *et al.* Synthesis of Diverse LiNi<sub>x</sub>Mn<sub>y</sub>Co<sub>z</sub>O<sub>2</sub> Cathode Materials from Lithium Ion Battery Recovery Stream. *Journal of Sustainable Metallurgy* **2**, 248-256 (2016).
- 27 *BU-1003: Electric Vehicle (EV)*, <[http://batteryuniversity.com/learn/article/electric\\_vehicle\\_ev](http://batteryuniversity.com/learn/article/electric_vehicle_ev)> (2018).

- 28 2016 Chevrolet Volt battery system,  
<[https://media.gm.com/content/dam/Media/microsites/product/Volt\\_2016/doc/VOLT\\_BATTERY.pdf](https://media.gm.com/content/dam/Media/microsites/product/Volt_2016/doc/VOLT_BATTERY.pdf)> (2016).
- 29 SB LiMotive to Provide Lithium-ion Battery Packs for Fiat 500EV,  
<<http://detroit.cbslocal.com/2010/11/08/sb-limotive-to-provide-lithium-ion-battery-packs-for-fiat-500ev/>> (2010).
- 30 Blomgren, G. E. The Development and Future of Lithium Ion Batteries. *Journal of The Electrochemical Society* **164**, A5019-A5025, doi:10.1149/2.0251701jes (2017).
- 31 Warner, J. T. *The Handbook of Lithium-Ion Battery Pack Design: Chemistry, Components, Types and Terminology*. (Elsevier Science, 2015).
- 32 Xiao, Q., Li, B., Dai, F., Yang, L. & Cai, M. Application of Lithium Ion Battery for Vehicle Electrification. *Electrochemical Energy: Advanced Materials and Technologies* (2015).
- 33 Van Bommel, A. & Dahn, J. Synthesis of Spherical and Dense Particles of the Pure Hydroxide Phase Ni $1/3$ Mn $1/3$ Co $1/3$  (OH)  $2$ . *Journal of The Electrochemical Society* **156**, A362-A365 (2009).
- 34 Nam, K.-M., Kim, H.-J., Kang, D.-H., Kim, Y.-S. & Song, S.-W. Ammonia-free coprecipitation synthesis of a Ni–Co–Mn hydroxide precursor for high-performance battery cathode materials. *Green Chemistry* **17**, 1127-1135, doi:10.1039/C4GC01898B (2015).
- 35 Pohjalainen, E., Rauhala, T., Valkeapää, M., Kallioinen, J. & Kallio, T. Effect of Li $4$ Ti $5$ O $12$  Particle Size on the Performance of Lithium Ion Battery Electrodes at High C-Rates and Low Temperatures. *The Journal of Physical Chemistry C* **119**, 2277-2283, doi:10.1021/jp509428c (2015).
- 36 Ong, M. T. *et al.* Lithium Ion Solvation and Diffusion in Bulk Organic Electrolytes from First-Principles and Classical Reactive Molecular Dynamics. *The Journal of Physical Chemistry B* **119**, 1535-1545, doi:10.1021/jp508184f (2015).
- 37 Capron, O. *et al.* On the Ageing of High Energy Lithium-Ion Batteries—Comprehensive Electrochemical Diffusivity Studies of Harvested Nickel Manganese Cobalt Electrodes. *Materials* **11**, 176 (2018).
- 38 BU-301a: *Types of Battery Cells*,  
<[http://batteryuniversity.com/learn/article/types\\_of\\_battery\\_cells](http://batteryuniversity.com/learn/article/types_of_battery_cells)> (2017).
- 39 van Bommel, A. & Dahn, J. R. Analysis of the Growth Mechanism of Coprecipitated Spherical and Dense Nickel, Manganese, and Cobalt-Containing Hydroxides in the Presence of Aqueous Ammonia. *Chemistry of Materials* **21**, 1500-1503, doi:10.1021/cm803144d (2009).
- 40 Cho, J. LiNi $0.74$ Co $0.26$ -xMgxO $2$  Cathode Material for a Li-Ion Cell. *Chemistry of Materials* **12**, 3089-3094, doi:10.1021/cm000153l (2000).
- 41 Zheng, X. *et al.* Spent lithium-ion battery recycling – Reductive ammonia leaching of metals from cathode scrap by sodium sulphite. *Waste Management* **60**, 680-688, doi:<https://doi.org/10.1016/j.wasman.2016.12.007> (2017).
- 42 Barik, S. P., Prabakaran, G. & Kumar, L. Leaching and separation of Co and Mn from electrode materials of spent lithium-ion batteries using hydrochloric acid: Laboratory and pilot scale study. *Journal of Cleaner Production* **147**, 37-43, doi:<https://doi.org/10.1016/j.jclepro.2017.01.095> (2017).
- 43 Li, L. *et al.* Sustainable Recovery of Cathode Materials from Spent Lithium-Ion Batteries Using Lactic Acid Leaching System. *ACS Sustainable Chemistry & Engineering* **5**, 5224-5233, doi:10.1021/acssuschemeng.7b00571 (2017).
- 44 Bahaloo-Horeh, N. & Mousavi, S. M. Enhanced recovery of valuable metals from spent lithium-ion batteries through optimization of organic acids produced by *Aspergillus niger*. *Waste Management* **60**, 666-679, doi:<https://doi.org/10.1016/j.wasman.2016.10.034> (2017).
- 45 Virolainen, S., Fallah Fini, M., Laitinen, A. & Sainio, T. Solvent extraction fractionation of Li-ion battery leachate containing Li, Ni, and Co. *Separation and Purification Technology* **179**, 274-282, doi:<https://doi.org/10.1016/j.seppur.2017.02.010> (2017).

- 46 Yang, Y., Xu, S. & He, Y. Lithium recycling and cathode material regeneration from acid leach liquor of spent lithium-ion battery via facile co-extraction and co-precipitation processes. *Waste Management* **64**, 219-227, doi:<https://doi.org/10.1016/j.wasman.2017.03.018> (2017).
- 47 Chen, X., Fan, B., Xu, L., Zhou, T. & Kong, J. An atom-economic process for the recovery of high value-added metals from spent lithium-ion batteries. *Journal of Cleaner Production* **112**, 3562-3570, doi:<https://doi.org/10.1016/j.jclepro.2015.10.132> (2016).
- 48 Yang, Y., Huang, G., Xie, M., Xu, S. & He, Y. Synthesis and performance of spherical  $\text{LiNi}_x\text{Co}_y\text{Mn}_{1-x-y}\text{O}_2$  regenerated from nickel and cobalt scraps. *Hydrometallurgy* **165**, 358-369, doi:<https://doi.org/10.1016/j.hydromet.2015.11.015> (2016).

## Chapter 3. High Performance Cathode Recovery from Different Electric Vehicle Recycling Streams

### Abstract

For environmental and sustainability reasons, spent Li-ion batteries must be recovered and recycled so that the full promise of an electrified future is realized. Li-ion battery recycling streams pose a serious challenge to all existing recycling technologies because of their unknown and diverse chemistry. In the work described in this paper, four representative recycling streams were used to demonstrate the flexibility of the recycling process developed at Worcester Polytechnic Institute (WPI) to accommodate a variable feed and to generate consistent quality cathode material,  $\text{LiNi}_{1/3}\text{Mn}_{1/3}\text{Co}_{1/3}\text{O}_2$  (NMC111).  $\text{Ni}_{1/3}\text{Mn}_{1/3}\text{CO}_{1/3}(\text{OH})_2$  precursors derived from four recycling streams were produced by a hydroxide coprecipitation method in a continuous stirred tank reactor. It took 2 days for the coprecipitation reaction to reach steady state. A possible evolution of the precursor particles up to the steady state was proposed. Both the precursors and the cathodes from these four different recycling streams exhibit similar morphology, particle size distribution, and tap density. Moreover, these recovered cathode materials display similar electrochemical properties. Surprisingly, these recovered NMC111s have better rate capability than a commercial NMC111 prepared from virgin materials. The different chemical compositions of the incoming recycling streams were shown to have little observed effect on the recovered precursor and resultant cathode material generated by the WPI-developed recycling process with advantages including no sorting, low temperature, and high quality recovered battery materials. Therefore, the

WPI developed process applies to different spent Li-ion battery waste streams and is, therefore, general.

## **1. Introduction**

Because of their many desirable attributes including high energy density, long cycle life, lightweight, and no memory effect, lithium ion (Li-ion) batteries are widely used in an evergrowing list of consumer electronics, electric vehicles, aerospace and defense, industrial, hobby, and other applications. The global Li-ion battery market was valued around USD 31.17 billion in 2016 and is expected to reach USD 67.70 billion by 2020 because of increasing demand for electric vehicles (EV)<sup>1</sup> and other factors. Although Li-ion batteries play an ever-increasing role in our daily lives, a substantial and growing amount of spent Li-ion battery waste is generated each year.<sup>2-4</sup> Irresponsible disposal of spent Li-ion batteries would result in environmental pollution<sup>5</sup> and, hence, would pose a threat to the health of human beings. Moreover, resource availability poses serious constraints for Li-ion batteries.<sup>6</sup> There are potential risks associated with the supply of materials for Li-ion batteries. For sustainability and strategic material considerations, precious resources must not be disposed of as waste. Therefore, to protect the environment, ensure industry sustainability, and harness the full benefits of electrification, it is necessary to develop technologies to recover and recycle spent Li-ion batteries efficiently and economically.<sup>7-9</sup>

Many technologies have been developed to recover and recycle spent Li-ion batteries, including pyrometallurgical, hydrometallurgical, electrochemical, and bioleaching methods.<sup>10-13</sup> Hydrometallurgical processes are considered to be a favorable method for recycling spent Li-ion batteries because of their high recovery yield, high purity of recovered materials, low energy

consumption, and potential zero emissions.<sup>14</sup> A novel closed-loop hydrometallurgical process for recycling spent Li-ion batteries has been developed in our group.<sup>15,16</sup> In this process, spent batteries were crushed. No sorting is needed. The spent batteries can be any size and shape. The pulverized batteries were sieved. Cathode powders were leached, resulting in a leaching solution which was purified. The recovery efficiency was high. The purified solution was adjusted to a desired stoichiometry of Ni, Mn, and Co. The stoichiometry can be 1:1:1, 5:3:2, 6:2:2, 8:1:1, or others. Then, the adjusted solution was employed to synthesize precursor by coprecipitation. Cathode material was produced from the precursor by calcination. The recovered cathode material displayed a very good electrochemical performance. Besides cathode materials, other materials also could be recovered. The no-sorting feature is a significant advantage and addresses one of the key challenges faced by battery recyclers today.

Currently, over 50% of a battery's material cost is associated with the cathode material.<sup>15</sup> Accordingly, a lot of attention has been directed toward efficiently and economically recovering and recycling the cathode material. LiCoO<sub>2</sub> (LCO) is the first generation cathode material used in Li-ion batteries. Recycling LCO in spent Li-ion batteries has been widely investigated.<sup>17,18</sup> Over time, the chemistry of the cathode material has evolved in pursuit of higher energy density, lower cost, and improved abuse tolerance. Today, a broad spectrum of lithium compounds are employed as cathode materials in addition to LCO, including LiMn<sub>2</sub>O<sub>4</sub> (LMO), LiNi<sub>x</sub>Mn<sub>y</sub>Co<sub>z</sub>O<sub>2</sub> (NMC,  $x + y + z = 1$ ), LiNi<sub>0.85</sub>Co<sub>0.1</sub>Al<sub>0.05</sub>O<sub>2</sub> (NCA), LiFePO<sub>4</sub> (LFP), and others. In addition, blending different cathode materials together is a common technique used in making Li-ion batteries for EVs.<sup>19,20</sup> Several commercial automotive battery suppliers have developed Li-ion cells with cathodes composed of a mixture of two or more different active materials. Ford's Focus Electric and General Motor's (GM's) Chevy Volt utilize pouch cell batteries which use a blend of NMC and LMO.<sup>19</sup>

The cathode chemistry in spent Li-ion batteries is occasionally unknown, often with mixed lots of batteries arriving at the recycler's dock. In practice, spent Li-ion batteries come from a variety of sources, including xEVs, consumer electronics, and other applications, and are often the subject of intermediate handling, partial disassembly, repurposing, and so forth. This can obscure provenance and, thereby, introduces significant challenges to the recyclers. It is reasonable to define recycling stream by incoming cathode chemistry given that, in general, a graphite-based anode is used in most commercially available Li-ion batteries. Recycling stream can be either simple or complex. It can be LCO, if the cathode chemistry is only LCO. If blended cathode chemistries are used like NMC and LMO, the recycling stream can be defined as NMC + LMO. If cathode chemistries from various sources are complex, including LCO, NMC, NCA, LMO, and LFP, the recycling stream is LCO + NMC + NCA + LMO + LFP.

Synthesis of cathode materials from various recycling streams has been studied.<sup>21</sup> For example, the  $\text{Li-Ni}_{1/3}\text{Mn}_{1/3}\text{Co}_{1/3}\text{O}_2$  (NMC111) cathode material was synthesized from NMC + LCO and NMC + LCO + LMO recycling streams.<sup>22,23</sup> However, in the literature, there were few studies comparing the cathode material recovered from different recycling streams. The goal of this is to systematically compare both the precursor  $\text{Ni}_{1/3}\text{Mn}_{1/3}\text{Co}_{1/3}(\text{OH})_2$  and the cathode NMC111 synthesized from intentionally different recycling streams. For this purpose, we studied four representative recycling streams. The precursors and cathodes derived from the four different recycling streams were compared in morphology, tap density, particle size distribution, and electrochemical performance.

## 2. Experimental Section

In this study, four different recycling streams of spent Li-ion batteries were employed: NMC + LMO, NMC + LMO + LFP, NMC + NCA + LMO, and NMC + NCA + LMO + LCO + LFP. These recycling streams were obtained from Ford EV batteries, GM EV batteries, Fiat Chrysler Automobiles (FCA) EV batteries, A123 LFP batteries, and consumer electronics batteries. The cathodes derived from these four recycling streams via our process are designated as #1NMC111, #2NMC111, #3NMC111, and #4NMC111, respectively, as shown in **Figure 1**. A commercially procured virgin cathode material, designated #0NMC111, was used for comparison. #0NMC111 is a high-quality commercial cathode from a leading cathode supplier. In each experiment, about 30 kg spent Li-ion batteries was used.

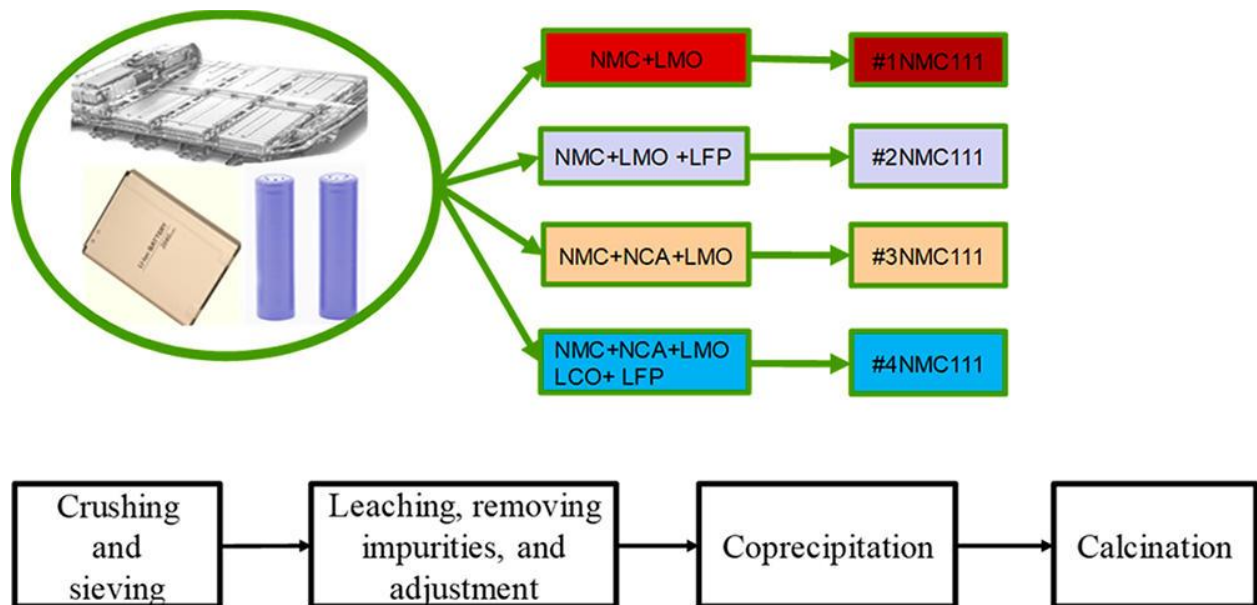


**Figure 1.** Schematic representation of four different recycling streams, and the process to obtain the cathode material NMC111 from spent lithium ion batteries.

The recycling process has been described in detail in a previous paper.<sup>15</sup> Briefly, the process consisted of mechanical treatment of the spent Li-ion batteries, magnetic separation of steel, sieving, density separation, leaching of cathode powders, and removal of impurities in the leaching solution by adjusting pH. H<sub>2</sub>SO<sub>4</sub> and H<sub>2</sub>O<sub>2</sub> were used for the leaching. Before and after removal of impurities, the concentrations of lithium (Li), nickel (Ni), manganese (Mn), cobalt (Co), iron (Fe), aluminum (Al), and copper (Cu) elements in the leaching solution were measured by inductive coupled plasma optical emission spectrometry (ICP-OES). Total carbon analyzer was employed to detect carbon. The recovery efficiencies for Ni, Co, and Mn were over 90%. The molar ratio of Ni:Mn:Co in the leaching solution was adjusted to 1:1:1 by adding NiSO<sub>4</sub>·6H<sub>2</sub>O, MnSO<sub>4</sub>·H<sub>2</sub>O, and CoSO<sub>4</sub>·7H<sub>2</sub>O, as required. The concentration of metal sulfate in the leaching solution was 2.0 M. The concentration and molarity were confirmed by ICP-OES.

Precursor Ni<sub>1/3</sub>Mn<sub>1/3</sub>Co<sub>1/3</sub>(OH)<sub>2</sub> was synthesized by a hydroxide coprecipitation method. The adjusted metal sulfate solution was slowly pumped into a continuous stirred tank reactor (CSTR, 5 L) under nitrogen atmosphere. At the same time, a 5.0 M NaOH solution and appropriate amount of NH<sub>4</sub>OH solution(aq) as chelating agent were also separately metered into the reactor. pH and stirring speed were controlled at desired values. The temperature was controlled at 60 °C. The experiments ran for 7 days each. Samples were collected throughout the process. The precursor was dried overnight.

The recovered Ni<sub>1/3</sub>Mn<sub>1/3</sub>Co<sub>1/3</sub>(OH)<sub>2</sub> and 5% excess Li<sub>2</sub>CO<sub>3</sub> were mixed together thoroughly. The mixture was first calcined at 450 °C for 5 h and then was heated to 900 °C for 15 h in air, to produce the final NMC111 cathode powders.

Scanning electron microscopy (SEM) and laser diffraction instruments were used to analyze morphology and particle size distribution of the precursors and cathode materials. The tap density of these materials was measured. The measurements of particle size distribution and tap density were independently conducted by A123 systems, a leading lithium ion manufacturer in North America.

The electrochemical properties of the cathodes derived from different recycling streams were independently characterized in CR2032 coin cells by A123 systems. Making the cell and all electrochemical tests were carried out in terms of industrial standards. The positive electrode consisted of the active material (recovered NMC111, 94 wt %), carbon black (3.5 wt %), and polyvinylidene difluoride (PVDF) binder (2.5 wt %). The loading level of the active material in the positive electrode was about  $20 \text{ mg cm}^{-2}$ . The mixture was coated onto aluminum foil and was dried under vacuum at  $80 \text{ }^\circ\text{C}$  for 12 h. The cells were assembled in a high-purity argon-filled glovebox with lithium metal as the counter and reference electrode, Celgard 2500 membrane was employed as the separator, and 1.0 M  $\text{LiPF}_6$  in ethylene carbonate (EC) and ethylmethyl carbonate (EMC) (3:7 volume ratio) was used as the electrolyte. The cells were tested in the voltage range from 2.7 to 4.3 V at various constant current rates at room temperature.

### **3. Results and Discussion**

It is vital to precisely control the morphology of  $\text{Ni}_{1/3}\text{Mn}_{1/3}\text{Co}_{1/3}(\text{OH})_2$  particles to produce the desired precursor materials, as they in turn play a large role in determining the morphology and electrochemical properties of the resulting cathode materials. The precursor particles are secondary ones, composed of smaller primary particles. As coprecipitation starts in the CSTR, the primary

particles are formed and agglomerate into secondary particles because of thermodynamic driving forces. In the early stages, these secondary particles are very small and porous. As the reaction proceeds, the secondary particles grow bigger and denser. The growth is likely to be ascribed to insertion of new primary particles and the growing of the existing ones. They also become more and more spherical as a result of grinding as the particles collide.<sup>24</sup> The primary particles comprising the secondary ones thicken until there is no space available for further growth, nor is there adequate room for further insertion of new primary particles. At this stage, relatively uniform and dense particles are obtained. Beyond this stage, new small secondary particles appear, and the existing particles continue their growth. These existing particles most likely cease to grow after a certain time. This may be attributed to a strong hydrodynamic shear force exerted on the larger particles, which inhibits continued surface growth.<sup>25</sup> This mechanism describes the assumed evolution of the secondary particle during its lifetime in the CSTR. Eventually, a stable range of secondary particles from new small agglomerates, growing particles, to growth-terminated larger particles coexist, and the reaction reaches steady state.

**Figure 2** shows the morphology of precursors at different reaction times. At 6 h, the secondary particles are uniform, porous, and small. At 24 h, the secondary particles are uniform and dense. As the reaction continues, the particles continue to grow and become spherical. At 36 h, new small particles emerge, and the existing particles become larger. At 42 h, particles at all evolution stages appear, and fewer larger particles are observed. At 48 h, there is no significant difference compared to particles at 42 h. The biggest particles do not grow during this additional 6 h period, and the reaction reaches steady state. **Figure 3** exhibits the dependence of tap density of the samples for different reaction times. The tap density of the particles increases with the reaction time up to an asymptotic value. This asymptotic behavior also indicates that a steady state is reached after 48 h.

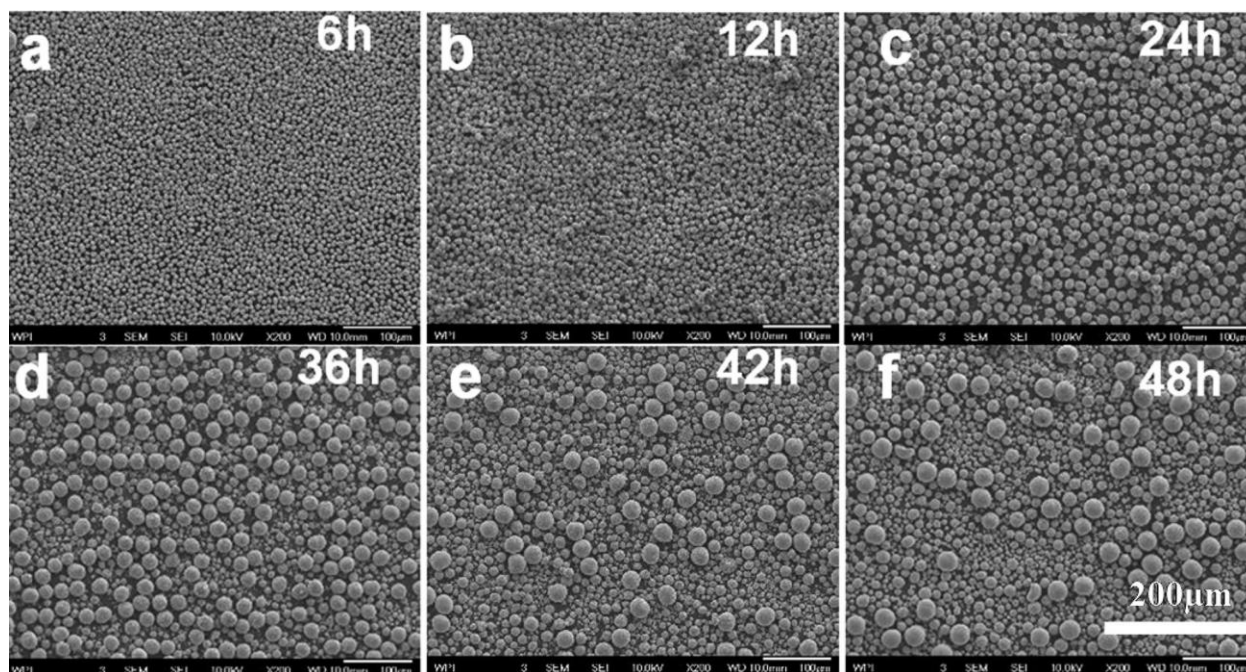


**Figure 2.** SEM images of  $\text{Ni}_{1/3}\text{Co}_{1/3}\text{Mn}_{1/3}(\text{OH})_2$  as a function of reaction time for (a)  $t = 6$  h; (b)  $t = 12$  h; (c)  $t = 24$  h; (d)  $t = 36$  h; (e)  $t = 42$  h; (f)  $t = 48$  h.

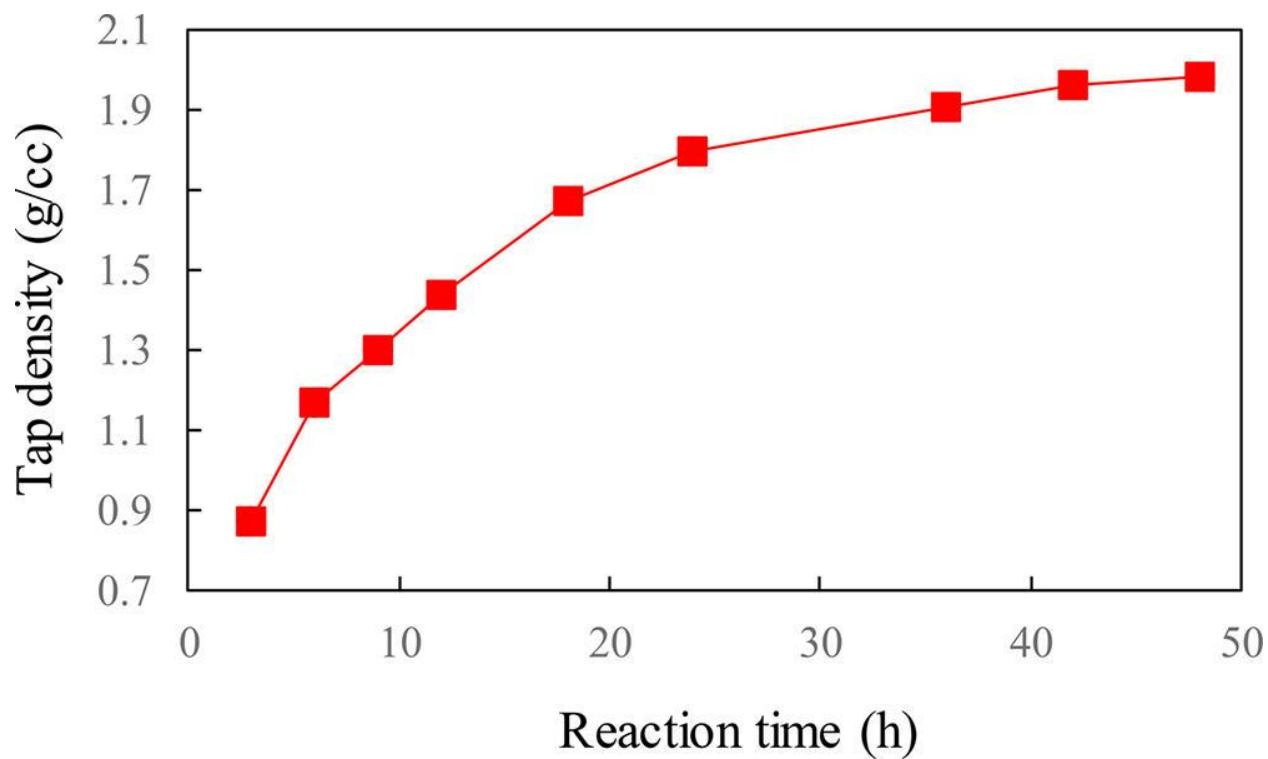


### **Figure 3. Tap densities for the precursor samples at different reaction times.**

For mass production, consistent precursor can reliably be collected after the reaction attains its steady state. In our case, the precursors from each recycling stream were collected after 2 days. The precursors were then collected daily for five additional days. These precursors were labeled Day3, Day4, Day5, Day6, and Day7. The morphology of the representative precursors at Day3, Day5, and Day7 from each recycling stream was analyzed. **Figure 4 a–c** shows the SEM images of the precursors from recycling stream NMC + LMO. The precursors all display features characteristic of steady state. Particle size varies over a full spectrum from less than 1  $\mu\text{m}$  to about 20  $\mu\text{m}$ , and small particles dominate consistently over large ones. The sphericity of the particles increases with size. The largest particles exhibit almost perfect spherical shape. In addition, the packing of the particles becomes denser with increasing size. The morphology and particle size distribution of the precursors harvested on different days is quite similar. Their tap density is almost identical, around 2.1  $\text{g}/\text{cm}^3$  as shown in **Figure 5**. Therefore, as expected, particle morphology, particle size distribution, and tap density remain stable after steady state is reached.

**Figure 4 d–f, g–i, and j–l** shows the SEM images of the precursors from the recycling streams NMC + LMO + LFP, NMC + NCA + LMO, and NMC + NCA + LMO + LCO + LFP. Comparing the precursors from different recycling streams, very slight differences are observed. For instance, the precursor from the recycling streams NMC + LMO and NMC + NCA + LMO has the highest tap density of approximately 2.10  $\text{g}/\text{cm}^3$ . The tap density of the precursor from the recycling stream NMC + LMO + LFP is the lowest, around 2.00  $\text{g}/\text{cm}^3$ . The precursor from the recycling stream NMC + NCA + LMO + LCO + LFP has an intermediate tap density of about 2.0  $\text{g}/\text{cm}^3$ . In addition, all SEM images were not taken selectively. However, it appears that the sizes of the particles from the recycling streams NMC + LMO and NMC + NCA + LMO are slightly larger than those from

the streams NMC + LMO + LFP and NMC + NCA + LMO + LCO + LFP. The very tiny variations in tap density and particle size may be attributed to experimental errors. In spite of these slight differences, the precursors from these four, very different, recycling streams have similar morphology, particle size distribution, and tap density. It is similarly expected that the cathodes prepared by calcining the mixture of the recovered precursors and  $\text{Li}_2\text{CO}_3$  do not significantly vary in morphology, size distribution, and tap density.

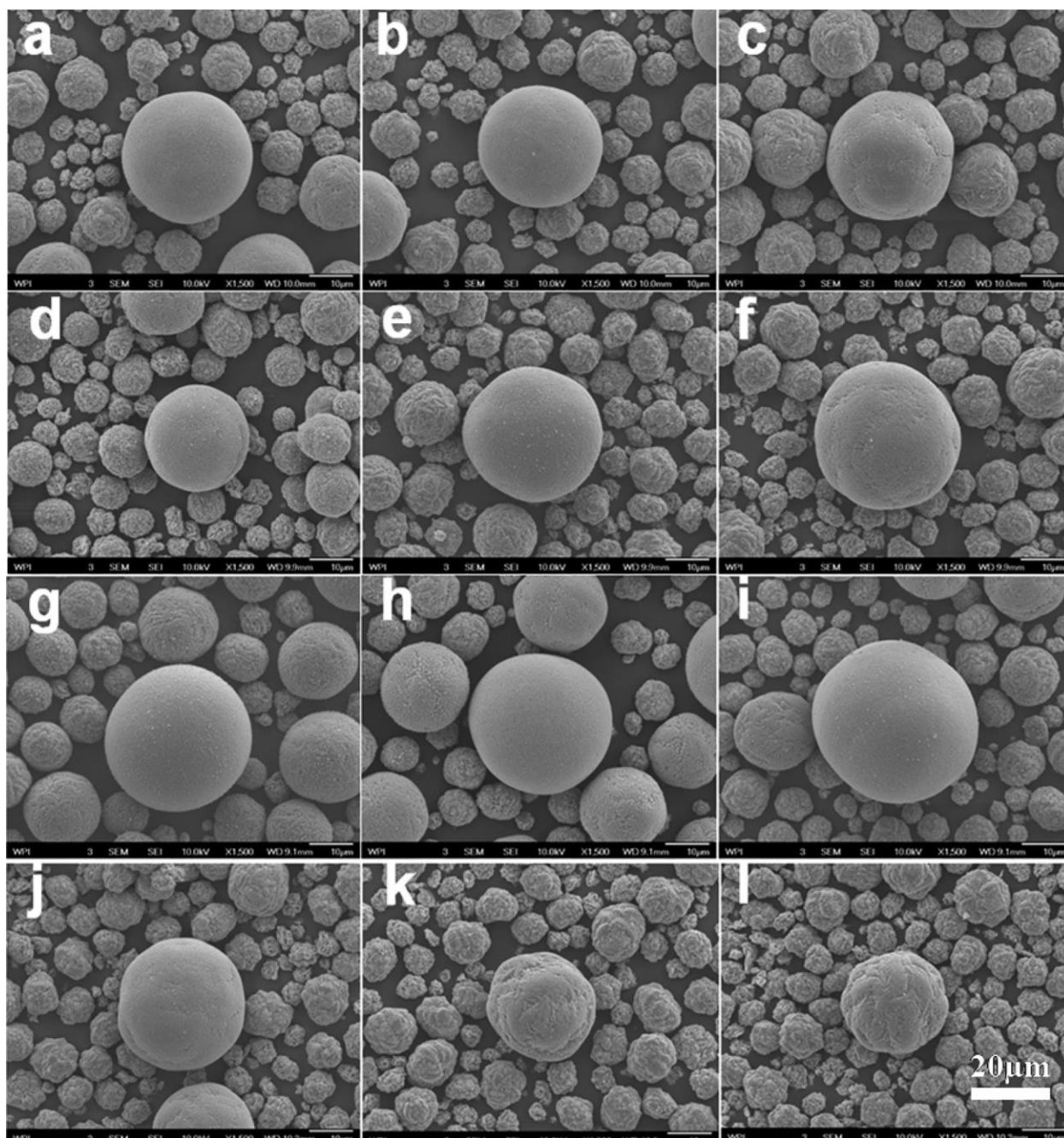


**Figure 4. SEM images of precursors for (a) Day3, (b) Day5, and (c) Day7 derived from recycling stream NMC + LMO; (d) Day3, (e) Day5, (f) Day7 from stream NMC + LMO + LFP; (g) Day3, (h) Day5, (i) Day7 from stream NMC + NCA + LMO; (j) Day3, (k) Day5, (l) Day7 from stream NMC + NCA + LMO + LCO + LFP.**

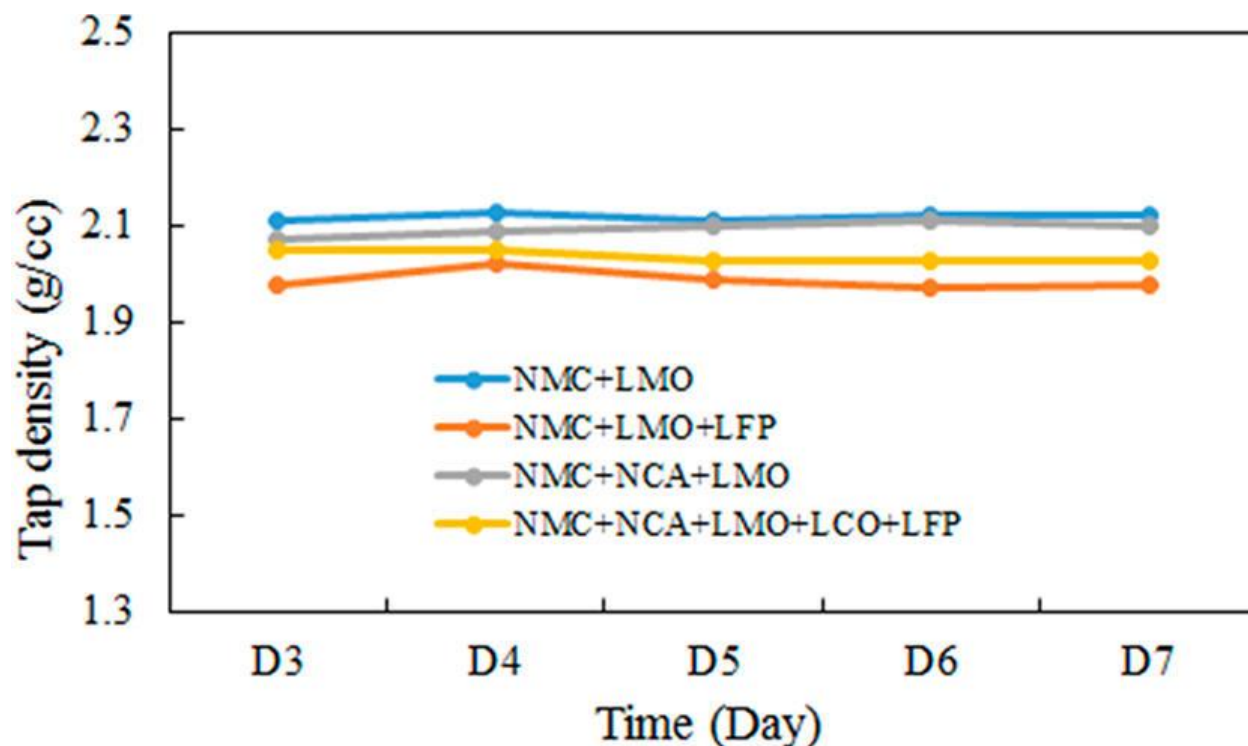


**Figure 5. Tap density of the precursor products of each day from the four different recycling streams.**

For each recycling stream, all of the obtained precursors from Day3 to Day7 were used to synthesize NMC111 cathode. **Figure 6a, b, d, e** shows the morphology of the cathodes from the four streams. They exhibit similar morphology and size distribution as previously seen in precursors. Particles from #1NMC and #3NMC appear slightly larger. **Figure 6f** shows the particle size distributions of the four recovered NMC111 cathodes. The sizes (D50) of #1NMC, #2NMC, #3NMC, and #4NMC are 13.9  $\mu\text{m}$ , 10.7  $\mu\text{m}$ , 11.9  $\mu\text{m}$ , and 9.8  $\mu\text{m}$ , respectively. This variation is expected, correlating according to the morphology of their precursors. The tap density for the four cathodes also is similar, as indicated in **Figure 6c**. #1NMC111 and #2NMC have the same tap density, 2.5  $\text{g}/\text{cm}^3$ , while the tap density of #3NMC is slightly higher at 2.6  $\text{g}/\text{cm}^3$ , and #4NMC has a slightly lower density of 2.5  $\text{g}/\text{cm}^3$ . Therefore, all four recovered cathode materials have

similar morphology, particle size distribution, and tap density. As cathode materials, their electrochemical properties are critical and are described in the following sections along with the commercial control #0NMC.

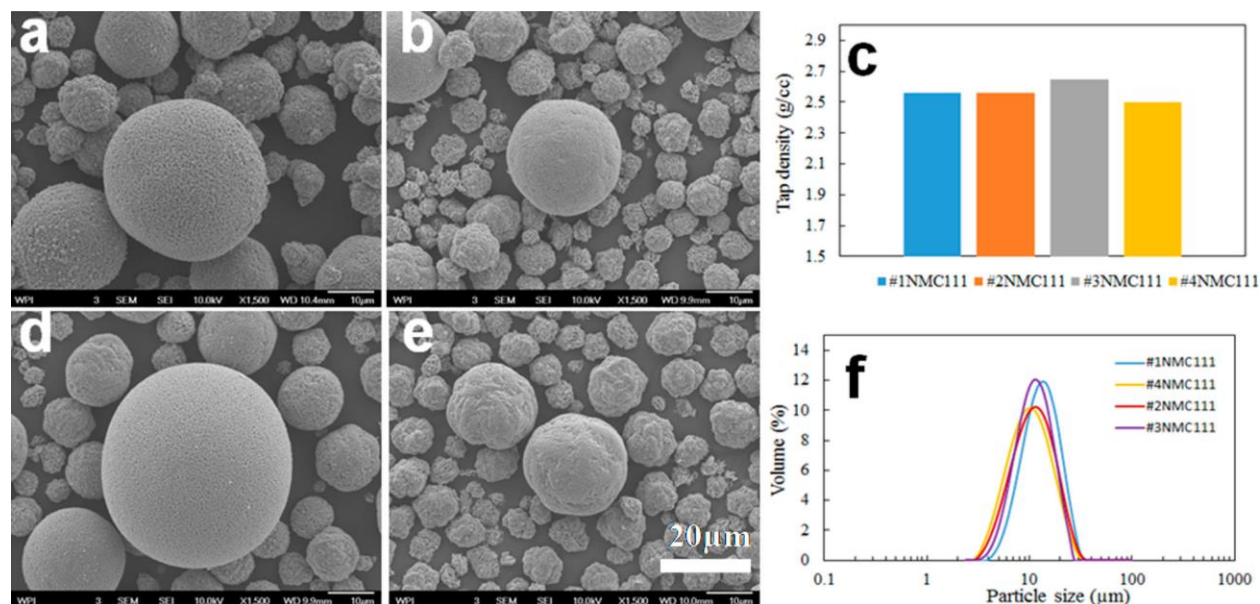


**Figure 6.** SEM images of (a) #1NMC111, (b)#2NMC111, (d) #3NMC111, (e) #4NMC; (c) the tap density for the cathode materials from the four different recycling streams; (f) particle size distribution of the four cathodes.

The electrochemical performances of #1NMC111, #2NMC111, #3NMC111, and #4NMC were obtained by fabricating coin cells with the recovered materials. Equivalent control cells with commercial NMC111 were also made. **Figure 7a** shows the typical discharge curves of #1NMC in the voltage range between 2.7 and 4.3 V versus  $\text{Li}^+/\text{Li}^0$  at the various C-rates. The charging current is 0.5C. As shown in **Figure 7a**, the specific capacity of the cathode decreases with increasing C-rate because of the polarization effect. The specific capacities at 0.2, 0.5, 1, 2, 5, and 10C are around 152.3, 144.2, 137.1, 127.9, 74.7, and 22.2 mAh/g, respectively. #2NMC, #3NMC, and #4NMC also display similar rate performance, as shown in **Figure 7b**. This illustrates that

cathodes synthesized using our recycling process from chemically diverse recycling streams exhibit similar electrochemical performance.

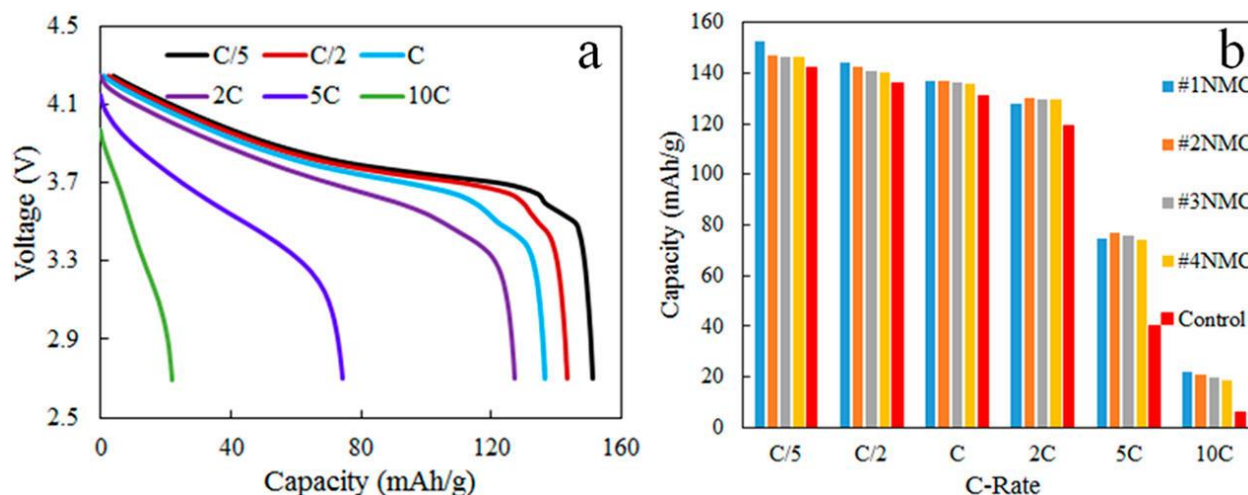


**Figure 7. (a) Discharge curves of #1NMC at various rates; (b) rate performance of #1NMC, #2NMC, #3NMC, #4NMC, and control.**

For comparison, coin cells prepared with commercial (virgin) cathode #0NMC111 were also tested. Specific capacities at 0.2, 0.5, 1, 2, 5, and 10C were measured as 144.5, 136.7, 131.4, 120.8, 46.8, and 7.5 mAh/g, respectively. At rates of 0.2, 0.5, 1, and 2C, the cathodes from the recycling streams exhibit electrochemical performances slightly better than the control #0NMC111. Remarkably, at the highest rates of 5 and 10C, the recovered cathodes have much higher discharge capacity than the commercial one. This comparison shows that the recovered cathodes from all four representative recycling stream consistently exhibit superior rate capability than the commercial control. According to the results of ICP and total carbon analyzer, the control and recovered materials are pure without detectable impurities like Na, Cu, Al, Fe, Mg, S, and C. Therefore, the better rate capability cannot be ascribed to impurities. However, the control has a little higher tap density than the recycled materials, while it has similar particle size with them, 9.7  $\mu\text{m}$ . This

suggests that the control has a little lower porosity. Pore volumes and pore sizes of these materials (recycled and control) were evaluated by BJH method. The cumulative pore volumes of the recycled materials are between 0.000130 and 0.000150 cm<sup>3</sup>/g, and their average pore diameters are between 20.70 and 20.90 Å. The control has lower pore volume 0.000080 cm<sup>3</sup>/g with similar pore size 20.50 Å. Given that the control and recycled materials have similar particle size and are pure, it may be reasonable to attribute the better rate capability to the higher pore volume and, hence, to the higher porosity in the recycled materials.<sup>26</sup> Cycling life of the control and recycled materials is still under independent evaluation. We will report these results in the future.

#### **4. Conclusions**

Four recycling streams of differing compositions were investigated: NMC + LMO, NMC + LMO + LFP, NMC + NCA + LMO, and NMC + NCA + LMO + LCO + LFP. Ni<sub>1/3</sub>Mn<sub>1/3</sub>Co<sub>1/3</sub>(OH)<sub>2</sub> precursors derived from these recycling streams were prepared via hydroxide coprecipitation in a CSTR in a 7 day operation per lot. It took 48 h for the coprecipitation reaction to reach steady state, after which morphology, particle size distribution, and tap density did not significantly change. A possible evolution mechanism of the precursor particles was proposed. The precursors were collected after steady state was reached. All precursors from these four different recycling streams exhibit similar morphology, particle size distribution, and tap density, as do the recovered cathodes synthesized from these precursors. Most important, cathode materials from the different recycling streams display similar electrochemical properties when evaluated in coin cells. Coin cells made using the recovered NMC111s have similar rate capability at low C rates (0.2, 0.5, 1, and 2C) as cells prepared with commercial (virgin) NMC111 and significantly better rate performance at high

rates (5 and 10C). These results demonstrate that the recycling stream composition has minimal effect on the high-quality precursor and cathode material recovered using our closed-loop recycling process with advantages including no sorting, low temperature, and high quality recovered battery materials. Therefore, the closed-loop process applies to multiple spent Li-ion battery waste streams and is, therefore, general.

## References:

- 1 Lithium-Ion Battery Market by Power Capacity Segment, Lithium-Ion Battery Market Has Been Segmented Into 5–25 WH, 48-95 WH, 18–28 KWH, 100–250 KWH And More Than 300 KWH for Include Automotive, Aerospace and Defense, Consumer Electronics, Industrial And Others Application - Global Industry Perspective, Comprehensive Analysis and Forecast, 2016 – 2022; Report Code: ZMR-2165; Zion Market Research: New York, 2017.
- 2 Aral, H.; Vecchio-Sadus, A. Toxicity of lithium to humans and the environment-a literature review. *Ecotoxicol. Environ. Saf.* 2008, 70, 349–356.
- 3 Paulino, J. F.; Busnardo, N. G.; Afonso, J. C. Recovery of valuable elements from spent Li-batteries. *J. Hazard. Mater.* 2008, 150, 843–849.
- 4 Li, L.; Ge, J.; Wu, F.; Chen, R.; Chen, S. Recovery of cobalt and lithium from spent lithium ion batteries using organic citric acid as leachant. *J. Hazard. Mater.* 2010, 176, 288–293.
- 5 Dorella, G.; Mansur, M. B. A study of the separation of cobalt from spent Li-ion battery residues. *J. Power Sources* 2007, 170, 210–215.
- 6 Olivetti, E. A.; Ceder, G.; Gaustad, G. G.; Fu, X. Lithium-ion battery supply chain considerations: analysis of potential bottlenecks in critical metals. *Joule* 2017, 1, 229–243.
- 7 Sun, L.; Qiu, K. Vacuum pyrolysis and hydrometallurgical process for the recovery of valuable metals from spent lithium-ion batteries. *J. Hazard. Mater.* 2011, 194, 378–384.
- 8 Freitas, M.; Garcia, E. M.; Celante, V. G. Electrochemical and structural characterization of cobalt recycled from cathodes of spent Li-ion batteries. *J. Appl. Electrochem.* 2009, 39, 601–607.
- 9 Rabah, M. A.; Farghaly, F. E.; Motaleb, M. A. Recovery of nickel, cobalt and some salts from spent Ni-MH batteries. *Waste Manage.* 2008, 28, 1159–1167.
- 10 Swain, B.; Jeong, J.; Lee, J.; Lee, G.; Sohn, J. Hydrometallurgical process for recovery of cobalt from waste cathodic active material generated during manufacturing of lithium ion batteries. *J. Power Sources* 2007, 167, 536–544.
- 11 Ordoñez, J.; Gago, E. J.; Girard, A. Processes and technologies for the recycling and recovery of spent lithium-ion batteries. *Renewable Sustainable Energy Rev.* 2016, 60, 195–205.
- 12 Garcia, E. M.; Tar, H. A.; Matencio, T.; Domingues, R. Z.; Dos Santos, J. A. F.; Ferreira, R. V.; Loren On, E.; Lima, D. Q.; de Freitas, M. B. J. G. Electrochemical recycling of cobalt from spent cathodes of lithium-ion batteries: Its application as supercapacitor. *J. Appl. Electrochem.* 2012, 42, 361–366.
- 13 Mishra, D.; Kim, D. J.; Ralph, D. E.; Ahn, J. G.; Rhee, Y. H. Bioleaching of metals from spent lithium ion secondary batteries using *Acidithiobacillus ferrooxidans*. *Waste Manage.* 2008, 28, 333–338.

- 14 Li, J.; Wang, G.; Xu, Z. Environmentally-friendly oxygen-free roasting/wet magnetic separation technology for in situ recycling cobalt, lithium carbonate and graphite from spent LiCoO<sub>2</sub>/graphite lithium batteries. *J. Hazard. Mater.* 2016, 302, 97–104.
- 15 Gratz, E.; Sa, Q.; Apelian, D.; Wang, Y. A closed loop process for recycling spent lithium ion batteries. *J. Power Sources* 2014, 262, 255–262.
- 16 Heelan, J.; Gratz, E.; Zheng, Z.; Wang, Q.; Chen, M.; Apelian, D.; Wang, Y. Current and prospective Li-ion battery recycling and recovery processes. *JOM* 2016, 68, 2632–2638.
- 17 Ma, L.; Nie, Z.; Xi, X.; Han, X. Cobalt recovery from cobalt bearing waste in sulphuric and citric acid systems. *Hydrometallurgy* 2013, 136, 1–7.
- 18 Li, L.; Chen, R.; Sun, F.; Wu, F.; Liu, J. Preparation of LiCoO<sub>2</sub> films from spent lithium ion batteries by a combined recycling process. *Hydrometallurgy* 2011, 108, 220–225.
- 19 Chikkannanavar, S. B.; Bernardi, D. M.; Liu, L. A review of blended cathode materials for use in Li-ion batteries. *J. Power Sources* 2014, 248, 91–100.
- 20 Tran, H. Y.; Täubert, C.; Fleischhammer, M.; Axmann, P.; Küppers, L.; Wohlfahrt-Mehrens, M. LiMn<sub>2</sub>O<sub>4</sub> spinel/Li-Ni<sub>0.8</sub>Co<sub>0.15</sub>Al<sub>0.05</sub>O<sub>2</sub> blends as cathode materials for lithium-ion batteries. *J. Electrochem. Soc.* 2011, 158, A556–A561.
- 21 Zeng, X.; Li, J.; Liu, L. Solving spent lithium-ion battery problems in China: opportunities and challenges. *Renewable Sustainable Energy Rev.* 2015, 52, 1759–1767.
- 22 Sa, Q.; Gratz, E.; He, M.; Lu, W.; Apelian, D.; Wang, Y. Synthesis of high performance LiNi<sub>1/3</sub>Mn<sub>1/3</sub>Co<sub>1/3</sub>O<sub>2</sub> from lithium ion battery recovery stream. *J. Power Sources* 2015, 282, 140–145.
- 23 Li, L.; Bian, Y.; Zhang, X.; Guan, Y.; Fan, E.; Wu, F.; Chen, R. Process for recycling mixed-cathode materials from spent lithium-ion batteries and kinetics of leaching. *Waste Manage.* 2018, 71, 362–371.
- 24 van Bommel, A.; Dahn, J. R. Analysis of the growth mechanism of coprecipitated spherical and dense nickel, manganese, and cobalt containing hydroxides in the presence of aqueous ammonia. *Chem. Mater.* 2009, 21, 1500–1503.
- 25 Wu, J.; Bi, L.; Zhang, J. B.; Poncin, S.; Cao, Z. P.; Li, H. Z. Effects of increase modes of shear force on granule disruption in upflow anaerobic reactors. *Water Res.* 2012, 46, 3189–3196.
- 26 Sun, C.; Rajasekhara, S.; Goodenough, J. B.; Zhou, F. Monodisperse porous LiFePO<sub>4</sub> microspheres for a high-power Li ion battery cathode. *J. Am. Chem. Soc.* 2011, 133, 2132–2135.

## Chapter 4. Systematic Comparison of Al<sup>3+</sup> Modified NMC 622 from Recycling Process

### Abstract

Layered oxide cathodes with a high Ni content are promising for high-energy-density lithium-ion batteries. However, parasitic electrolyte oxidation of the charged cathode and mechanical degradation arising from phase transitions significantly deteriorate the cell safety and cycle performance as the Ni content increases. In this study, LiNi<sub>0.6</sub>Mn<sub>0.2</sub>Co<sub>0.2</sub>O<sub>2</sub> (NMC 622) synthesized from a recycling process, and chemically modified with Al<sup>3+</sup> via two simple methods (dry coating and wet coating), was used as a model system to demonstrate the feasibility in large scale. Through XRD, STEM and XPS, we demonstrate the difference of Al<sup>3+</sup> distribution depth and its impact on the surface atomic structure of NMC 622 between the two coating methods. The Al-rich layer was largely concentrated on the surface of secondary particles after the dry coating process, whereas Al penetrated into the secondary particles in the wet coating process. The Al-rich layer from the dry coating process imparted improved structural and thermal stability in accelerated cycling performed at 45 °C between 3.0 and 4.3 V, and the capacity retention of pouch cells with dry coated NMC 622 (D-NMC) cathode increased from 83% to 91% compared to Al-free NMC 622 after 300 cycles. However, for wet coated NMC 622 (W-NMC), the increased surface area accompanying by formation of NiO rock-salt like structure could have negative impacts on the cycling performance. The results demonstrate that careful design of the interfacial layer by surface modification is an effective approach for improving the durability of Ni-rich NMCs.

## 1. Introduction

With a dramatically increasing demand for electric vehicles (EVs), a long driving range of a minimum of 300 miles is desired. Such a demand has motivated enormous research efforts focused on electrode materials, in particular cathode materials with high energy, low cost and good stability for lithium-ion batteries<sup>1</sup>. However, the cathode materials that can be practically applied in the automotive industry in the next 10 years are more likely limited to a small number of compounds. Among them,  $\text{LiNi}_{1-x-y}\text{Co}_x\text{Mn}_y\text{O}_2$  (NMC) with high Ni content ( $1-x-y \geq 0.6$ ) is one of the most promising candidates that meets high capacity and energy requirements<sup>2-7</sup>. However, Ni-rich NMC still suffers from some technical challenges, including severe capacity fading, resistance increasing upon storage and cycling, and inadequate thermal stability<sup>8</sup>. For example, the high concentration of reactive  $\text{Ni}^{4+}$ , when charging Ni-rich NMC, can accelerate electrolyte decomposition, which results in electrolyte depletion and forms a thick layer of divalent insulating NiO with high interfacial cell impedance<sup>5, 9-11</sup>. Furthermore, residual lithium on the surface of Ni-rich NMC materials can react with  $\text{H}_2\text{O}$  or  $\text{CO}_2$  to form insulating LiOH and  $\text{Li}_2\text{CO}_3$  during storage in ambient environment. These unintended products can affect the pH of the material and introduce risk due to the gas formation<sup>8-9, 12-13</sup>. Moreover, trace metal ions on the surface of Ni-rich NMC can be dissolved in the electrolyte due to HF corrosion, leading to premature battery failures<sup>4, 14</sup>. Therefore, the surface chemistry and side reactions have a decisive influence on the performance of Ni-rich NMC cathode materials for Li-ion batteries.

To address these challenges and improve electrochemical performance and safety, many strategies have been proposed including surface modification<sup>15-16</sup>, elemental doping<sup>17</sup>, gradient material<sup>3, 16</sup>, and binder modification<sup>18</sup>. Surface coating is one of the most effective and commonly adopted tactics. The coating materials, such as metal oxides<sup>19-22</sup> ( $\text{Al}_2\text{O}_3$ ,  $\text{MgO}$ ,  $\text{ZrO}_2$ ,  $\text{TiO}_2$ , etc.),

phosphates<sup>23-25</sup> ( $\text{AlPO}_4$ ,  $\text{FePO}_4$ ,  $\text{Co}_3(\text{PO}_4)_2$ ,  $\text{Ni}_3(\text{PO}_4)_2$ , etc.) and fluorides<sup>26</sup> ( $\text{AlF}_3$ , etc.), can play different roles, including physical barriers, electronically conductive media, ionically conductive media or HF scavengers. Among these materials,  $\text{Al}_2\text{O}_3$  is the simplest and most common one due to its numerous advantages and wide spread applications in industrial products. David et al.<sup>27-28</sup> reported that the atomic layer deposition (ALD) of  $\text{Al}_2\text{O}_3$  on NMC 811 improved the cycling performance by 40%. Also, Su et al.<sup>29</sup> and Wise et al.<sup>22</sup> showed that ALD  $\text{Al}_2\text{O}_3$  coated NMC 532 and 442 enabled high-voltage ( $>4.4$  V) cycling stability. Furthermore, nanoscale  $\text{Al}_2\text{O}_3$ - $\text{Ga}_2\text{O}_3$  alloy coating was synthesized on NMC 532 cathode via a “co-pulsing” ALD technique by Laskar and his colleges<sup>30</sup>. In the latter, the coating improved the cycle life of the battery and produced optimal rate performance. Although ALD  $\text{Al}_2\text{O}_3$  coating shows superior electrochemical performance over other coating techniques, its high cost and low coating rate will prevent it from being used in mass production. Hence, to overcome the technical limitations of ALD  $\text{Al}_2\text{O}_3$  coating, other coating techniques have been developed, such as sol-gel<sup>31</sup>, wet coating<sup>32-33</sup> and dry coating<sup>34-35</sup>. Although the electrochemical properties associated with these surface coated cathode materials are promising, lack of common baseline materials make it extremely difficult to compare electrochemical performances reported by various research groups.

In this paper, we systematically studied two facile scalable  $\text{Al}_2\text{O}_3$  coating methods applied to recycled NMC 622, followed by different material and electrochemical characterization methods. Through XRD, STEM and XPS, we determined the difference of  $\text{Al}^{3+}$  distribution depth and its impact on the surface atomic structure of NMC 622 between the two coating methods. The electrochemical performances were characterized in single layer pouch cells and CR2032-type coin half cells, which were independently tested by A123 Systems. The capacity retention of pouch cells with dry coated NMC 622 (D-NMC) cathode increased from 83% to 91% compared to

uncoated NMC 622 after 300 cycles. However, for wet coated NMC (W-NMC) the increased surface area, accompanied by formation of NiO rock-salt like structure, could have adverse impacts on the cycling performance. Those results demonstrate that suitable surface modification is critical for improving the durability of high energy density cathode materials.

## 2. Experimental

### 2.1 Materials Synthesis

Metal sulfate aqueous solution composed of  $\text{NiSO}_4$ ,  $\text{MnSO}_4$  and  $\text{CoSO}_4$  with a concentration of  $2.0 \text{ mol l}^{-1}$  was achieved by recycling end-of-life lithium ion batteries. This was then used to synthesize spherical Ni-rich  $\text{Ni}_{0.60}\text{Mn}_{0.20}\text{Co}_{0.20}(\text{OH})_2$  precursors prepared by a conventional co-precipitation reaction. The recycling process has been described in detail in a previous paper<sup>36</sup>. Ni-rich NMC cathode materials, P-NMC, were prepared by mixing the synthesized  $\text{Ni}_{0.60}\text{Mn}_{0.20}\text{Co}_{0.20}(\text{OH})_2$  precursor with  $\text{Li}_2\text{CO}_3$ , followed by sintering at  $450 \text{ }^\circ\text{C}$  for 5 hrs and then  $850 \text{ }^\circ\text{C}$  for 18 hrs in air. To compensate for the evaporation of Li during calcination at high temperatures, 5 mol% excess Li was used.

$\text{Al}_2\text{O}_3$  modified NMC was prepared by two methods: dry coating and wet coating. The dry coating process involved mechanical mixing of the P-NMC cathode powder with nano-sized  $\text{Al}_2\text{O}_3$ , and then annealing the mixture at  $600 \text{ }^\circ\text{C}$  for 5 hrs to form the stabilizing coating layer. For the wet coating procedure, a prescribed amount of  $\text{Al}(\text{NO}_3)_3 \cdot 9\text{H}_2\text{O}$  was dissolved in distilled water first, P-NMC powder was then dispersed into the above solution, which was stirred for 5 minutes at room temperature. The powder was then recovered by filtration and dried at  $600 \text{ }^\circ\text{C}$  for 5 hrs. The two materials are hereafter designated as D-NMC (dry) and W-NMC (wet). Alumina content was fixed at 0.35wt% in this study, since the lowest effective amount of  $\text{Al}_2\text{O}_3$  is desired in order to

minimize the impact of impedance. Notably, these two processes are considered as simple and readily scalable, both of which are necessary for commercialization.

## 2.2 Materials Characterization

**XPS characterization.** All spectra were calibrated with the C 1s photoemission peak at 284.8 eV to compensate for the charging effect. The peak-fitting and quantitative evaluations were performed with the Casa XPS software. The background was corrected using the Shirley method.

**Powder XRD diffraction.** X-ray diffraction patterns of the polycrystalline powder were collected on a PANalytical Empyrean Series 2 X-ray Diffraction System with Cu K $\alpha$  radiation between 10 and 90° at an increment of 0.02°. Based on the X-ray diffraction data, the structural parameters of the P-NMC, D-NMC and W-NMC were refined using the Rietveld refinement program FullProf<sup>37</sup>.

**SEM, TEM and STEM characterization.** The particle size and morphology were measured by scanning electron microscope (SEM) with an energy-dispersive X-ray analysis (JEOL JSM-7000F electron microscope). Furthermore, to investigate atomic structure and corresponding elements distribution, transmission electron microscopy (TEM) and high-angle annular dark-field scanning transmission electron microscopy (HAADF STEM) measurements were carried out by Probe-corrected FEI Titan Themis 300 S/TEM, equipped with Super-X EDS (energy-dispersive X-ray spectroscopy) system.

**Electrochemical measurement.** The electrochemical testing is independently conducted at A123 Systems.

**Coin Cell:** The cathode electrodes were fabricated from a 94% mixture of P-NMC, D-NMC or W-NMC with a balance of conductive carbon and polyvinylidene fluoride in NMP. The slurries

were mixed benchtop scale using a Thinky mixer model ARE-310. The slurries were then cast onto Aluminum foil using a wet film applicator on a Sheen Automataic Film Applicator model 1-133N. Electrodes were set to a target loading density of 20 mg/cm<sup>2</sup> and pressed to 3.0 g/cc. Cells were then constructed in an Argon glovebox with a 1.15M LiPF<sub>6</sub> EC/EMC/plus additives electrolyte and paired against Li metal. Once constructed, cells were formed at slow rate charge and discharge cycles between 4.3V and 2.5V and then charged at 0.5C to 4.3V and discharged at various C-Rates to 2.5V at room temperature.

**Single Layer Pouch Cell (SLP):** The cathode electrodes were fabricated from a 94.5% mixture of P-NMC, D-NMC or W-NMC with a balance of conductive carbon and polyvinylidene fluoride in NMP. The slurries were mixed benchtop scale using a Thinky mixer model ARE-310. The slurries were then cast onto Aluminum foil using a wet film applicator on a Sheen Automataic Film Applicator model 1-133N. Electrodes were set to a target loading density of 20 mg/cm<sup>2</sup> and pressed to 3.3 g/cc. The cathode electrodes were matched with a water based graphite anode fabricated on A123 systems' pilot scale coater. SLPs were constructed in a dry room environment and filled with a 1.15M LiPF<sub>6</sub> EC/EMC/plus additives electrolyte. Cells were formed at room temperature using slow rate charge and discharge cycles and then cycled in a 45°C temperature chamber at 1C Charge /1C Discharge between 4.2V and 2,5V using a Maccor Series 4000 Battery Tester.

### 3. Results and Discussion

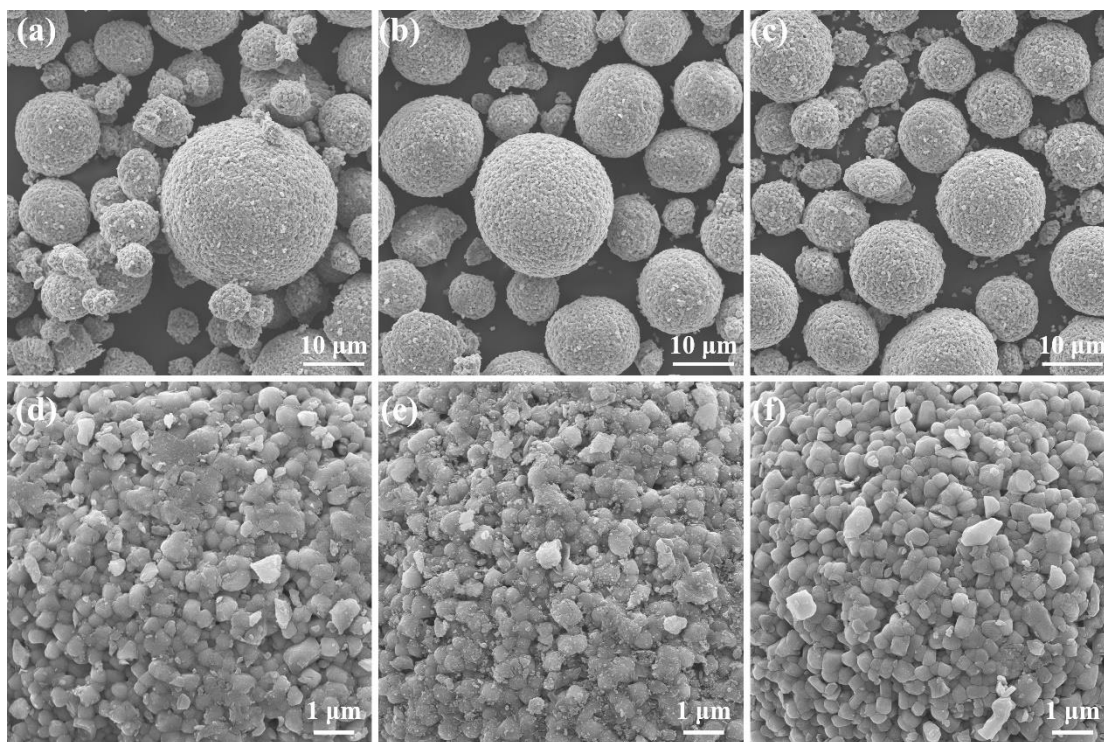


**Fig. 1 SEM images of (a) PNMC, (b) D-NMC and (c) W-NMC samples. (d, e, f) corresponding magnified images.**

**Fig. 1(a), (b) and (c)** show that P-NMC, D-NMC and W-NMC cathode powders retain the original spherical morphology of the secondary particles of  $\text{Ni}_{0.60}\text{Mn}_{0.20}\text{Co}_{0.20}(\text{OH})_2$  shown in **Fig. 2**. Meanwhile, particle size distribution and tap density are consistent before and after  $\text{Al}_2\text{O}_3$  modification, as summarized in **Tab. 1**. In addition, from the magnified images shown in **Fig. 1(d), (e) and (f)**, although the primary particles of each sample are block-like in shape, we could observe that the surface of D-NMC appears to be uniformly covered by some nano-sized particles. The corresponding element distribution mappings are shown in **Fig. 3**. The surfaces corresponding to the different coating techniques are characterized in the following surface chemical analysis.

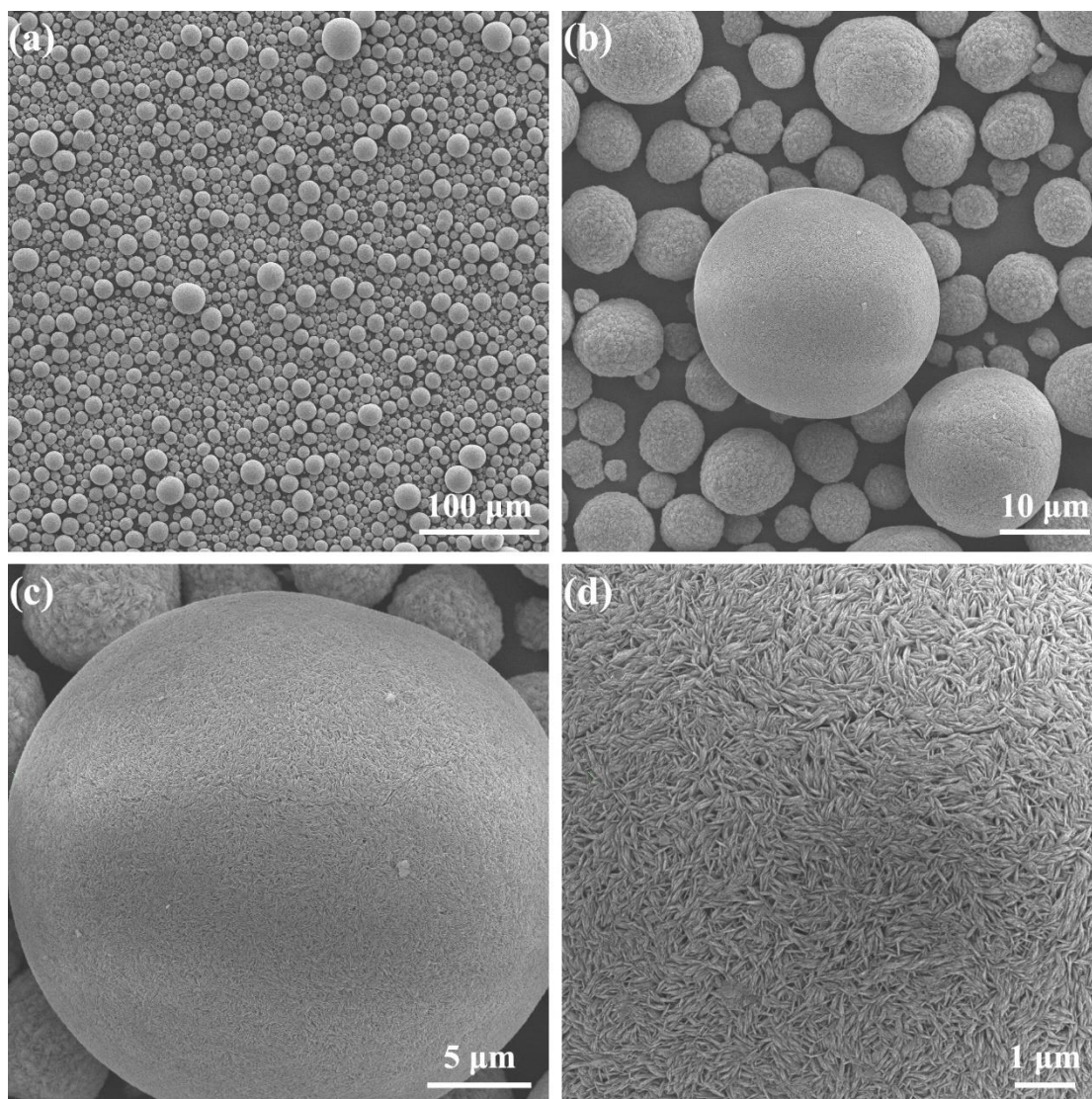


**Fig. 2 SEM images of  $\text{Ni}_{0.60}\text{Mn}_{0.20}\text{Co}_{0.20}(\text{OH})_2$  precursor under different magnifications.**

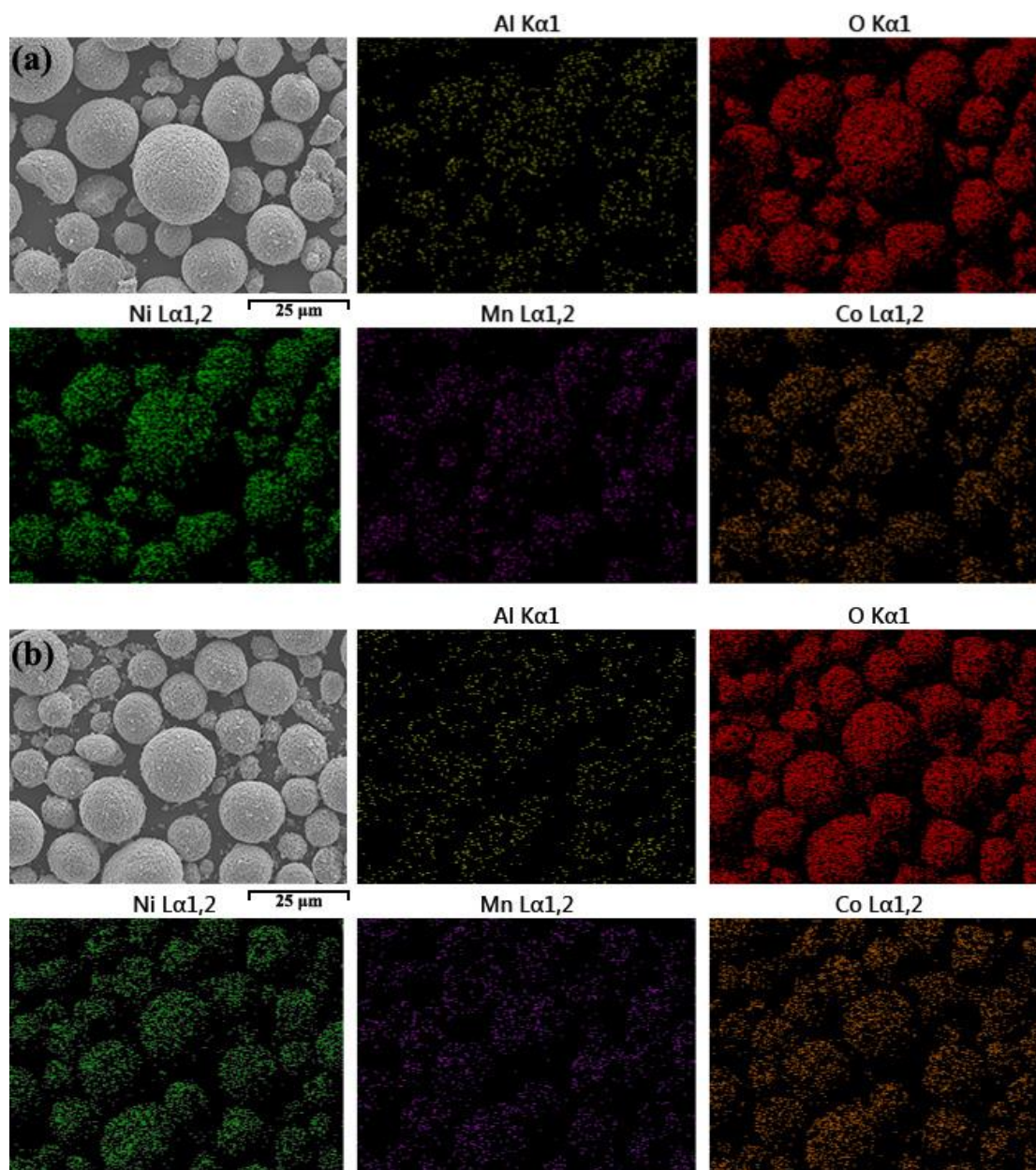


**Fig. 3** SEM image and corresponding EDX elemental mapping images of (a) D-NMC and (b) W-NMC.

**Tab.1** Tap density and particle size distribution of three as-synthesized NMC powders.

Label#	Tap density (gcm <sup>-3</sup> )	D10 (μm)	D50 (μm)	D90 (μm)
NMC	2.66	7.1	12.8	22.1
D-NMC	2.67	6.5	11.6	20.3
W-NMC	2.78	6.7	11.5	19.4

The average chemical composition of the aforementioned three samples, P-NMC, D-NMC and W-NMC, is Li : Ni : Mn : Co = 1.05 : 0.60 : 0.20 : 0.20, Li : Ni : Mn : Co : Al = 0.98 : 0.59 : 0.21 : 0.20 : 0.007 and Li : Ni : Mn : Co : Al = 0.96 : 0.60 : 0.20 : 0.20 : 0.007, respectively, which was determined by inductively coupled plasma mass spectrometry (ICP-MS). The XRD patterns are shown in **Fig. 4**, and all samples have typical diffraction peaks that can be indexed to  $\alpha$ -NaFeO<sub>2</sub> structure of the R-3m space group with no other phases. In general, Ni-rich layered cathodes involve cations disordering between transition-metal sites (octahedral 3a site) and lithium sites (octahedral 3b site), therefore Rietveld refinement is conducted and the results are summarized in **Tab.2**, which shows the a-axis, the c-axis and the fraction of nickel in the lithium layer (%)<sup>38</sup>. For W-NMC, the cation mixing was 4.2%, but was only 3.2% for the P-NMC and D-NMC, indicating that there is no obvious migration of Ni ions during annealing for dry coating. This is because the layered structure of the W-NMC sample becomes unstable during thermal treatment, and more Ni ions migrate to the lithium layer after washing with the aluminum nitrate aqueous solution. Therefore, the washing process makes the nickel-rich cathode more chemically sensitive than non-washed cathodes, leading to subsequent delithiation from the bulk structure during the heat treatment step. These results highlight the importance of carefully considering side effects from the inherent aqueous solution exposure during the wet coating process.

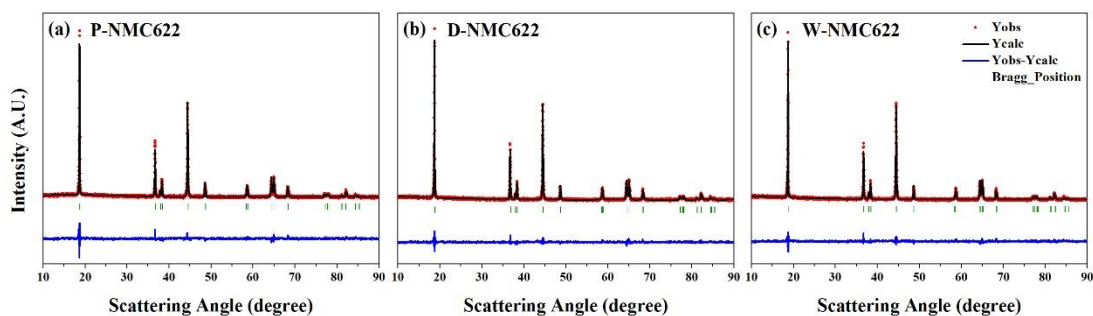


**Fig. 4** Rietveld refinement XRD data of (a) P-NMC, (b) D-NMC and (c) W-NMC samples.

**Table. 2 Powder XRD Rietveld Refinement Results for Different NMC Samples.**

Samples	a ( $\text{\AA} \pm 0.0001$ )	c ( $\text{\AA} \pm 0.0009$ )	Ni <sub>Li</sub> (%)	Bragg R-factor
P-NMC	2.8689	14.2247	3.2	5.06
D-NMC	2.8658	14.2184	3.2	4.26
W-NMC	2.8678	14.2156	4.2	3.65

To assess the effects of the surface modifications on electrochemical performance, three electrodes corresponding to the three NMC sample types were independently tested by A123 Systems, using lithium anodes for half cells and graphite for full cells. In **Fig. 5a**, we observe that W-NMC shows the best rate performance, while D-NMC shows similar rate performance with P-NMC. This can be ascribed to the removal of the inactive layer and higher surface area by washing as shown in **Tab. 3**<sup>40</sup>. For example, the surface areas for P-NMC, D-NMC and W-NMC are 0.21m<sup>2</sup>/g, 0.30m<sup>2</sup>/g and 1.34m<sup>2</sup>/g, respectively. The significantly higher surface area for W-NMC will allow more reaction sites, which leads to the increased rate performance. In order to understand the long term cycling impact of coatings, cycling performance with single layer pouch cells (full cell configuration) was conducted at 1C charge and discharge rate (**Fig. 5b**). The most stable cycle performance (~91% capacity retention after 300 cycles) and highest coulombic efficiency (~99.9%) are achieved by D-NMC. W-NMC has the lowest capacity retention (~80% capacity retention after 300 cycles) and lower coulombic efficiency (99.86%), compared to the P-NMC sample (~83% capacity retention after 300 cycles, 99.87% coulombic efficiency). This indicates that the Al<sup>3+</sup> coating in the wet coated samples appears to be more uniform and appears conformally applied to the surfaces of primary particles on the outer radial portions of the secondary particles (versus dry coated samples). However, the greater associated surface area induces more side reactions, leading to higher degradation during long term cycling<sup>41-42</sup>. An initial benefit in improved rate performance is offset by reduced cycling life of the wet coated samples<sup>43-44</sup>, and these tradeoffs must be fully considered in the actual battery design.

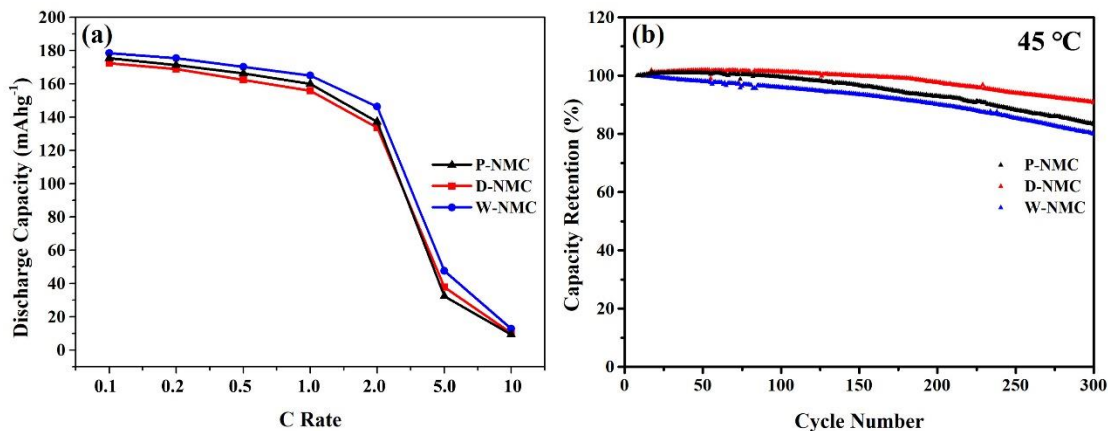


**Fig. 5 (a) Rate performance comparison against a lithium metal anode. (b) Single layer pouch cell cycling performance at discharge rate of 1C against a graphite anode.**

**Tab. 3 Physical properties and first cycling specific capacity of charge and discharge at 0.1C rate.**

Label#	BET (m <sup>2</sup> g <sup>-1</sup> )	Load (mgcm <sup>-2</sup> )	Press Density (g/cc)	FCC(0.1C) (mAhg <sup>-1</sup> )	FDC(0.1C) (mAhg <sup>-1</sup> )	First Cycle Eff (%)
P-NMC	0.21	21.33	2.95	194.8	173.1	88.8
D-NMC	0.30	22.15	2.96	194.8	172.4	88.5
W-NMC	1.34	21.12	2.93	195.8	178.5	91.2

In order to acquire a better understanding of the surface components, XPS was used to interrogate differences in surface chemistry between pristine and Al<sub>2</sub>O<sub>3</sub> modified cathode powders. **Fig. 6a**, corresponding to C1s spectra, is the intensity of binding energy at ~289 eV representing the carbonate group (CO<sub>3</sub><sup>2-</sup>)<sup>44</sup>. This compound should be consistent in O1s spectra, and it is around 531.8 eV, **Fig. 6b**. Therefore, we labeled it with a yellow dashed line in **Figs. 6a** and **b**. It can be seen that the relative intensities at these two positions (289 eV and 531.5 eV) are lower for the Al<sub>2</sub>O<sub>3</sub> modified samples (especially the W-NMC) relative to the P-NMC. The smaller peak intensity means that the Al<sub>2</sub>O<sub>3</sub> or Al(OH)<sub>3</sub> formed after hydrolysis of aluminum nitrate will react

with the residue on the P-NMC particle surface during the annealing process. Generally, some residual lithium compounds in the form of  $\text{Li}_2\text{CO}_3$  and  $\text{LiOH}$  are found on the surface of NMC cathode materials.<sup>39, 45</sup> These residual lithium compounds will react with  $\text{Al}^{3+}$  containing chemicals during the annealing process<sup>29, 46</sup>. The washing process also appears to reduce the amount of residual lithium compounds. This potentially leads to lithium deficient surface layer, which will sacrifice the electrochemical performance of the powder. Therefore, the peak intensity for W-NMC in **Figs. 6a** and **b** after washing is much lower than the P-NMC sample, and the fitting detail of C1s spectra is shown in **Fig. 7**. The results indicate that the  $\text{Li}_2\text{CO}_3$  to  $\text{LiOH}$  ratio is 32%, 28% and 17% for P-NMC, D-NMC and W-NMC, respectively. This is consistent with the results obtained by pH titration (**Tab. 4**). In addition, Al 2p spectra in **Fig. 6c** confirms that the  $\text{Al}_2\text{O}_3$  or  $\text{LiAlO}_2$  diffusion layer exist on the surface of modified samples, and it could be consistent in O1s spectra as marked by the black dashed line<sup>47</sup>.

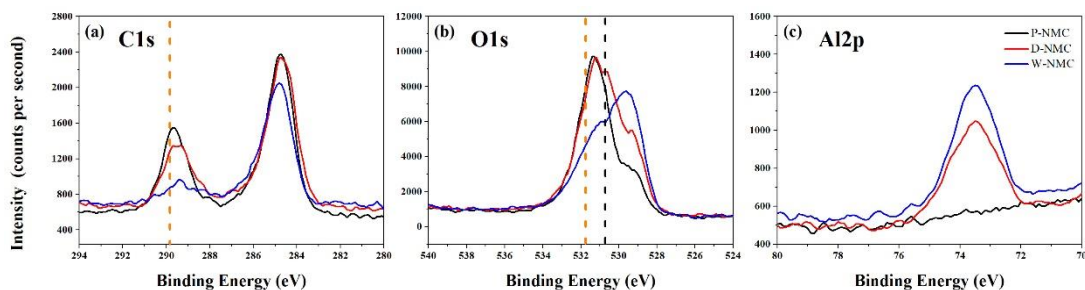


**Fig. 6** XPS spectra (a) C 1s, (b) O1s and (c) Al2p regions of P-NMC, D-NMC and W-NMC cathode powder.

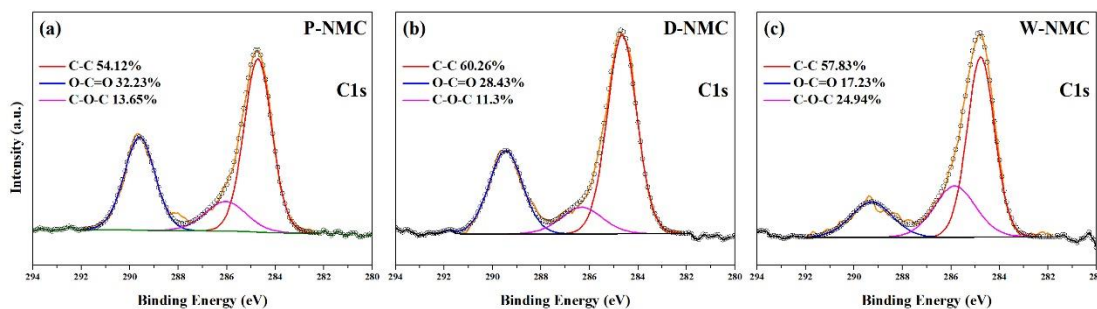


**Fig. 7 Fitted C 1s XPS spectra of (a) P-NMC, (b) D-NMC and (c) W-NMC.**

**Tab. 4 Content of dissolved carbonate and hydroxide compounds in aqueous filtrate measured by pH titration. The values are standardized by weight of NMC powder.**

Label#	Li <sub>2</sub> CO <sub>3</sub> (μmolg <sup>-1</sup> )	LiOH (μmolg <sup>-1</sup> )	Total (μmolg <sup>-1</sup> )
NMC	48	130	178
D-NMC	43	115	158
W-NMC	38	56	94

To understand the difference of the microstructure of the Al<sup>3+</sup> coating layer and the thickness of its diffusion depth in the secondary particle between D-NMC and W-NMC, STEM combined with FIB, and the corresponding fast Fourier transformation (FFT) of the selected area were conducted. In terms of cross sectional imaging of D-NMC, the Al<sup>3+</sup> dominantly distributes on the outer layer of the secondary particle (the region on the right hand of the black dashed line) as indicated in **Fig. 8a**. During the dry coating method, the solid phase of Al<sub>2</sub>O<sub>3</sub> is most likely adsorbed in the pores of the outer surface. Thus, the Al<sup>3+</sup> was detected primarily on the surface of the secondary particle with a coating layer thickness of hundreds of nanometers. For more chemical and structural information of the coating layer on the surface of the outer primary particles, energy-dispersive X-ray spectroscopy (STEM/EDS) was performed. Mapping of the Al, Ni, Mn and Co distribution indicates that the pores and surface of the outer grains were enriched with Al<sup>3+</sup>. The magnified HAADF image of **Fig. 8c** along [110] zone axis (corresponding to the yellow box in **Fig. 8b**) indicates that the surface of D-NMC primary particles retain the same atomic coordination as the R-3m layered structure in the bulk region, and the inset line profile shows the distance between (003) planes is 4.87nm. This is consistent with the corresponding electron diffraction pattern of

region I in **Fig. 8d**. In contrast, the coating layer in region II shows some polycrystalline particles, and this is confirmed by the corresponding electron diffraction pattern of region II in **Fig. 8e**. The inner diffraction ring is most likely an alpha  $\text{Al}_2\text{O}_3$  phase, which usually coexists with the  $\text{LiAlO}_2$  like phase after 600 °C treatment. This is consistent with the XRD patterns shown in **Fig. 9**. Therefore, after dry coating most of the  $\text{Al}^{3+}$  is found on the outer layer of the secondary particles, and distributed uniformly on the outer surfaces of the primary particles. In addition,  $\text{Al}^{3+}$  may be bonded tightly with the surface atoms of NMC622 after annealing.

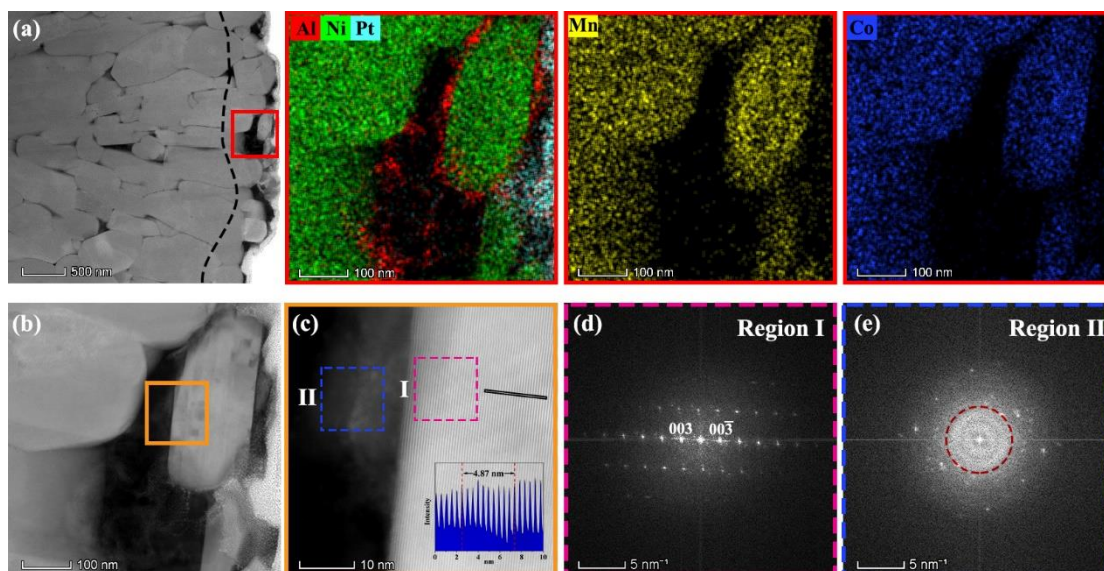


**Fig. 8** (a) STEM-HAADF image of FIB prepared D-NMC secondary particle and the corresponding EDS mapping. (b) STEM-HAADF imaging and (c) atomic level STEM-HAADF imaging of D-NMC primary particle, and corresponding FFT images of (d) region I and (e) region II, corresponding respectively to the pink and blue boxes in panel (c). Inserted line profile corresponds to black lines in panel (c).

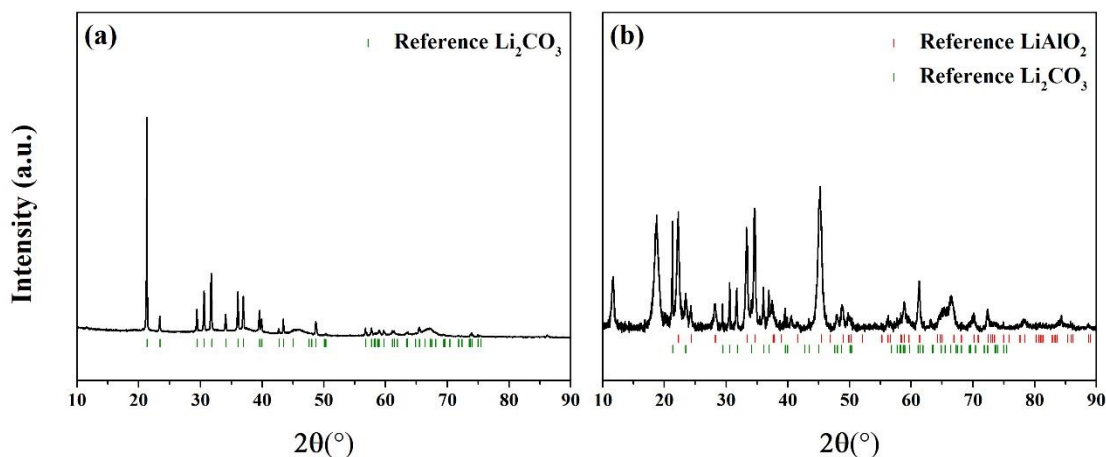


**Fig. 9** XRD patterns of the mixture of  $\text{Li}_2\text{CO}_3$  and  $\text{Al}_2\text{O}_3$  (molar ratio = 1 : 1) (a) before sinter and (b) after sinter in 600 °C for 5 hours.

In contrast, in the wet coating method, the  $\text{Al}^{3+}$  not only distributes at the outer surface of secondary and outward facing primary particles, but it also penetrates into internal grain boundaries (akin to core/shell models) because of the penetration of  $\text{Al}^{3+}$  during the solution treatment<sup>48</sup>. As shown in **Fig. 10a**, Al elements are not localized as they are in the D-NMC sample, indicating that the wet process can achieve a more uniform coating layer relative to the dry powder coating process. Another important observation is that the atomic structure has partially converted from layered structure to rock-salt like structure in the vicinity of some grain boundaries. In general, the distance between (003) planes is around 4.83nm as shown in **Fig. 10d**, which is consistent with the distance 4.87nm as shown in the D-NMC sample. However, especially at the grain boundary positions, the distance between planes narrows down to half, as shown in **Fig. 10e**, which means that some transition metal ions have migrated from the transition metal layers to lithium layers. The lithium loss from the surface resulting from water exposure during washing may facilitate the phase transformation from the layered to rock-salt crystal structure<sup>39</sup>. Hence, even though wet coating results in a uniform coating of  $\text{Al}^{3+}$  on the surfaces of primary particles that are found toward the

outer radial portion of the secondary particles (with some ingress into the outer shell), the coating protection does not compensate for the adverse impacts from the water exposure during washing<sup>49</sup>. The specific surface area of the W-NMC is more than five times that of other two samples (D-NMC and P\_NMC), as shown in **Tab 3**. This means that water has much more opportunity to react the NMC surface layers, and to reduce the residual lithium compounds on the surface of primary particles. This in turn will initiate more micro-crack formation between primary particles and induce surface side reactions, and cation mixing during cycling<sup>50-51</sup>.

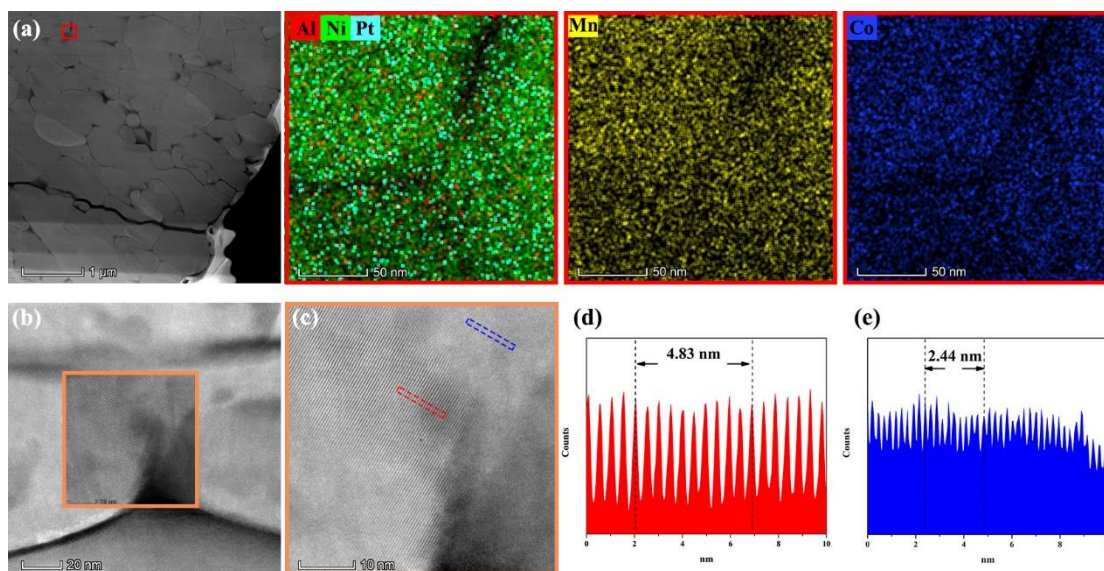


**Fig. 10** (a) STEM-HAADF image of FIB prepared W-NMC secondary particle and the corresponding EDS mapping. (b) STEM-HAADF imaging and (c) atomic level STEM-HAADF imaging of W-NMC primary particle, and (d) (e) line profiles corresponding to red line and blue line in panel (c).

**Fig.11** schematically illustrates the dry coated and wet coated NMC622. For dry coating, the Al compounds are localized on the surface of the secondary particles, which has been shown to stabilize the long term cycle performance. For wet coating, the Al compounds exist on both the

surface of the secondary particles, and as an outer layer on the outermost primary particles (forming a core shell structure). However, although the enlarged surface area due to the wet coating results in improved the first cycle coulombic efficiency, this comes with the penalty of poorer cycle life.

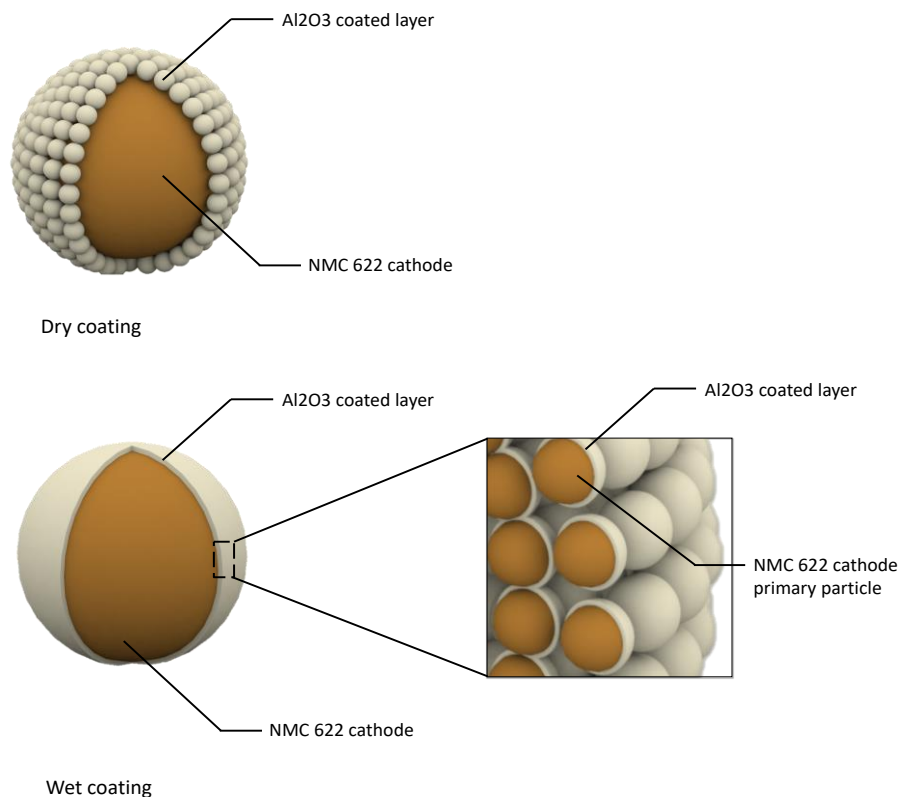


**Fig.11 Schematic illustration of dry and we coating of  $\text{Al}_2\text{O}_3$  on NMC particles**

#### 4. Conclusions

In summary, we systematically studied the surface modification of high-nickel layered  $\text{LiNi}_{0.6}\text{Mn}_{0.2}\text{Co}_{0.2}\text{O}_2$  with  $\text{Al}_2\text{O}_3$  by two methods including: dry coating and wet coating. These coating approaches are simple and scalable processes, and do not use volatile solvents. We

analyzed the methods' relative effectiveness in stabilization of the surface structure using various characterization techniques. For the dry coated samples, it was found that nano-sized polycrystalline  $\text{Al}_2\text{O}_3$  could be located on the outer layer of the secondary particles and its bonding to the surface atoms of the primary particle was confirmed by thermal treatment after mechanical mixing, which was directly identified via STEM/EDX and XPS. Dry coated NMC622 shows enhanced cycle life in single layer pouch cells. In contrast, the wet coating technique results showed that  $\text{Al}^{3+}$  ions penetrated more deeply into inner space and were more homogeneously distributed on the grain boundary regions. However, significant interaction between water (exposure from washing) and NMC powder leads to the generation of rock-salt like structure and cracks, which accounts for the large surface area and severe capacity fading at a high temperature ( $\geq 45$  °C). Each coating technique has different effects upon rate performance and electrochemical stability during cycling, and as such must be fully considered in material and coating system design.

## References:

1. Cano, Z. P.; Banham, D.; Ye, S.; Hintennach, A.; Lu, J.; Fowler, M.; Chen, Z., Batteries and fuel cells for emerging electric vehicle markets. *Nature Energy* 2018, 3 (4), 279-289.
2. Guo, S.; Yuan, B.; Zhao, H.; Hua, D.; Shen, Y.; Sun, C.; Chen, T.; Sun, W.; Wu, J.; Zheng, B.; Zhang, W.; Li, S.; Huo, F., Dual-component  $\text{Li}_x\text{TiO}_2$ @silica functional coating in one layer for performance enhanced  $\text{LiNi}_{0.6}\text{Co}_{0.2}\text{Mn}_{0.2}\text{O}_2$  cathode. *Nano Energy* 2019, 58, 673-679.
3. Sun, Y. K.; Myung, S. T.; Park, B. C.; Prakash, J.; Belharouak, I.; Amine, K., High-energy cathode material for long-life and safe lithium batteries. *Nat Mater* 2009, 8 (4), 320-4.
4. Noh, H.-J.; Youn, S.; Yoon, C. S.; Sun, Y.-K., Comparison of the structural and electrochemical properties of layered  $\text{Li}[\text{Ni}_x\text{Co}_y\text{Mn}_z]\text{O}_2$  ( $x = 1/3, 0.5, 0.6, 0.7, 0.8$  and  $0.85$ ) cathode material for lithium-ion batteries. *Journal of Power Sources* 2013, 233, 121-130.
5. Liu, W.; Oh, P.; Liu, X.; Lee, M. J.; Cho, W.; Chae, S.; Kim, Y.; Cho, J., Nickel-rich layered lithium transition-metal oxide for high-energy lithium-ion batteries. *Angew Chem Int Ed Engl* 2015, 54 (15), 4440-57.
6. Manthiram, A.; Knight, J. C.; Myung, S.-T.; Oh, S.-M.; Sun, Y.-K., Nickel-Rich and Lithium-Rich Layered Oxide Cathodes: Progress and Perspectives. *Advanced Energy Materials* 2016, 6 (1).

7. Xia, Y.; Zheng, J.; Wang, C.; Gu, M., Designing principle for Ni-rich cathode materials with high energy density for practical applications. *Nano Energy* 2018, 49, 434-452.
8. You, Y.; Celio, H.; Li, J.; Dolocan, A.; Manthiram, A., Modified High-Nickel Cathodes with Stable Surface Chemistry Against Ambient Air for Lithium-Ion Batteries. *Angew Chem Int Ed Engl* 2018, 57 (22), 6480-6485.
9. Wu, F.; Tian, J.; Su, Y.; Wang, J.; Zhang, C.; Bao, L.; He, T.; Li, J.; Chen, S., Effect of Ni(2+) content on lithium/nickel disorder for Ni-rich cathode materials. *ACS Appl Mater Interfaces* 2015, 7 (14), 7702-8.
10. Wright, R. B.; Christophersen, J. P.; Motloch, C. G.; Belt, J. R.; Ho, C. D.; Battaglia, V. S.; Barnes, J. A.; Duong, T. Q.; Sutula, R. A., Power fade and capacity fade resulting from cycle-life testing of Advanced Technology Development Program lithium-ion batteries. *Journal of Power Sources* 2003, 119-121, 865-869.
11. Belharouak, I.; Lu, W.; Vissers, D.; Amine, K., Safety characteristics of Li(Ni<sub>0.8</sub>Co<sub>0.15</sub>Al<sub>0.05</sub>)O<sub>2</sub> and Li(Ni<sub>1/3</sub>Co<sub>1/3</sub>Mn<sub>1/3</sub>)O<sub>2</sub>. *Electrochemistry Communications* 2006, 8 (2), 329-335.
12. Lin, F.; Markus, I. M.; Nordlund, D.; Weng, T. C.; Asta, M. D.; Xin, H. L.; Doeff, M. M., Surface reconstruction and chemical evolution of stoichiometric layered cathode materials for lithium-ion batteries. *Nat Commun* 2014, 5, 3529.
13. Cui, S.; Wei, Y.; Liu, T.; Deng, W.; Hu, Z.; Su, Y.; Li, H.; Li, M.; Guo, H.; Duan, Y.; Wang, W.; Rao, M.; Zheng, J.; Wang, X.; Pan, F., Optimized Temperature Effect of Li-Ion Diffusion with Layer Distance in Li(NixMnyCoz)O<sub>2</sub> Cathode Materials for High Performance Li-Ion Battery. *Advanced Energy Materials* 2016, 6 (4).
14. Jin, D.; Song, D.; Friesen, A.; Lee, Y. M.; Ryou, M.-H., Effect of Al<sub>2</sub>O<sub>3</sub> ceramic fillers in LiNi<sub>1/3</sub>Co<sub>1/3</sub>Mn<sub>1/3</sub>O<sub>2</sub> cathodes for improving high-voltage cycling and rate capability performance. *Electrochimica Acta* 2018, 259, 578-586.
15. Kim, H.; Kim, M. G.; Jeong, H. Y.; Nam, H.; Cho, J., A new coating method for alleviating surface degradation of LiNi<sub>0.6</sub>Co<sub>0.2</sub>Mn<sub>0.2</sub>O<sub>2</sub> cathode material: nanoscale surface treatment of primary particles. *Nano Lett* 2015, 15 (3), 2111-9.
16. Hou, P.; Yin, J.; Ding, M.; Huang, J.; Xu, X., Surface/Interfacial Structure and Chemistry of High-Energy Nickel-Rich Layered Oxide Cathodes: Advances and Perspectives. *Small* 2017, 13 (45).
17. Schipper, F.; Dixit, M.; Kovacheva, D.; Talianker, M.; Haik, O.; Grinblat, J.; Erickson, E. M.; Ghanty, C.; Major, D. T.; Markovsky, B.; Aurbach, D., Stabilizing nickel-rich layered cathode materials by a high-charge cation doping strategy: zirconium-doped LiNi<sub>0.6</sub>Co<sub>0.2</sub>Mn<sub>0.2</sub>O<sub>2</sub>. *Journal of Materials Chemistry A* 2016, 4 (41), 16073-16084.
18. Chen, H.; Ling, M.; Hencz, L.; Ling, H. Y.; Li, G.; Lin, Z.; Liu, G.; Zhang, S., Exploring Chemical, Mechanical, and Electrical Functionalities of Binders for Advanced Energy-Storage Devices. *Chem Rev* 2018, 118 (18), 8936-8982.
19. Chen, Y.; Zhang, Y.; Chen, B.; Wang, Z.; Lu, C., An approach to application for LiNi<sub>0.6</sub>Co<sub>0.2</sub>Mn<sub>0.2</sub>O<sub>2</sub> cathode material at high cutoff voltage by TiO<sub>2</sub> coating. *Journal of Power Sources* 2014, 256, 20-27.
20. Kong, J.-Z.; Wang, S.-S.; Tai, G.-A.; Zhu, L.; Wang, L.-G.; Zhai, H.-F.; Wu, D.; Li, A.-D.; Li, H., Enhanced electrochemical performance of LiNi<sub>0.5</sub>Co<sub>0.2</sub>Mn<sub>0.3</sub>O<sub>2</sub> cathode material by ultrathin ZrO<sub>2</sub> coating. *Journal of Alloys and Compounds* 2016, 657, 593-600.
21. Laskar, M. R.; Jackson, D. H.; Xu, S.; Hamers, R. J.; Morgan, D.; Kuech, T. F., Atomic Layer Deposited MgO: A Lower Overpotential Coating for Li[Ni<sub>0.5</sub>Mn<sub>0.3</sub>Co<sub>0.2</sub>]O<sub>2</sub> Cathode. *ACS Appl Mater Interfaces* 2017, 9 (12), 11231-11239.
22. Wise, A. M.; Ban, C.; Weker, J. N.; Misra, S.; Cavanagh, A. S.; Wu, Z.; Li, Z.; Whittingham, M. S.; Xu, K.; George, S. M.; Toney, M. F., Effect of Al<sub>2</sub>O<sub>3</sub> Coating on Stabilizing LiNi<sub>0.4</sub>Mn<sub>0.4</sub>Co<sub>0.2</sub>O<sub>2</sub> Cathodes. *Chemistry of Materials* 2015, 27 (17), 6146-6154.

23. Tan, K.; Reddy, M.; Rao, G.; Chowdari, B., Effect of AlPO-coating on cathodic behaviour of Li(NiCo)O. *Journal of Power Sources* 2005, 141 (1), 129-142.
24. Bai, Y.; Wang, X.; Yang, S.; Zhang, X.; Yang, X.; Shu, H.; Wu, Q., The effects of FePO<sub>4</sub>-coating on high-voltage cycling stability and rate capability of Li[Ni<sub>0.5</sub>Co<sub>0.2</sub>Mn<sub>0.3</sub>]O<sub>2</sub>. *Journal of Alloys and Compounds* 2012, 541, 125-131.
25. Lee, D.-J.; Scrosati, B.; Sun, Y.-K., Ni<sub>3</sub>(PO<sub>4</sub>)<sub>2</sub>-coated Li[Ni<sub>0.8</sub>Co<sub>0.15</sub>Al<sub>0.05</sub>]O<sub>2</sub> lithium battery electrode with improved cycling performance at 55°C. *Journal of Power Sources* 2011, 196 (18), 7742-7746.
26. Sun, Y. K.; Lee, M. J.; Yoon, C. S.; Hassoun, J.; Amine, K.; Scrosati, B., The role of AlF<sub>3</sub> coatings in improving electrochemical cycling of Li-enriched nickel-manganese oxide electrodes for Li-ion batteries. *Adv Mater* 2012, 24 (9), 1192-6.
27. David, L.; Dahlberg, K.; Mohanty, D.; Ruther, R. E.; Huq, A.; Chi, M.; An, S. J.; Mao, C.; King, D. M.; Stevenson, L.; Wood, D. L., Unveiling the Role of Al<sub>2</sub>O<sub>3</sub> in Preventing Surface Reconstruction During High-Voltage Cycling of Lithium-Ion Batteries. *ACS Applied Energy Materials* 2019, 2 (2), 1308-1313.
28. Mohanty, D.; Dahlberg, K.; King, D. M.; David, L. A.; Sefat, A. S.; Wood, D. L.; Daniel, C.; Dhar, S.; Mahajan, V.; Lee, M.; Albano, F., Modification of Ni-Rich FCG NMC and NCA Cathodes by Atomic Layer Deposition: Preventing Surface Phase Transitions for High-Voltage Lithium-Ion Batteries. *Sci Rep* 2016, 6, 26532.
29. Jo, C. H.; Cho, D. H.; Noh, H. J.; Yashiro, H.; Sun, Y. K.; Myung, S. T., An effective method to reduce residual lithium compounds on Ni-rich Li Ni<sub>0.6</sub>Co<sub>0.2</sub>Mn<sub>0.2</sub> O-2 active material using a phosphoric acid derived Li<sub>3</sub>PO<sub>4</sub> nanolayer. *Nano Research* 2015, 8 (5), 1464-1479.
30. Laskar, M. R.; Jackson, D. H.; Guan, Y.; Xu, S.; Fang, S.; Dreibelbis, M.; Mahanthappa, M. K.; Morgan, D.; Hamers, R. J.; Kuech, T. F., Atomic Layer Deposition of Al<sub>2</sub>O<sub>3</sub>-Ga<sub>2</sub>O<sub>3</sub> Alloy Coatings for Li[Ni<sub>0.5</sub>Mn<sub>0.3</sub>Co<sub>0.2</sub>]O<sub>2</sub> Cathode to Improve Rate Performance in Li-Ion Battery. *ACS Appl Mater Interfaces* 2016, 8 (16), 10572-80.
31. Hagh, N. M.; Amatucci, G. G., Effect of cation and anion doping on microstructure and electrochemical properties of the LiMn<sub>1.5</sub>Ni<sub>0.5</sub>O<sub>4-δ</sub> spinel. *J. Power Sources* 2014, 256, 457-469.
32. Xiang, J.; Chang, C.; Yuan, L.; Sun, J., A simple and effective strategy to synthesize Al<sub>2</sub>O<sub>3</sub>-coated LiNi<sub>0.8</sub>Co<sub>0.2</sub>O<sub>2</sub> cathode materials for lithium ion battery. *Electrochemistry Communications* 2008, 10 (9), 1360-1363.
33. Zhao, R.; Liang, J.; Huang, J.; Zeng, R.; Zhang, J.; Chen, H.; Shi, G., Improving the Ni-rich LiNi<sub>0.5</sub>Co<sub>0.2</sub>Mn<sub>0.3</sub>O<sub>2</sub> cathode properties at high operating voltage by double coating layer of Al<sub>2</sub>O<sub>3</sub> and AlPO<sub>4</sub>. *Journal of Alloys and Compounds* 2017, 724, 1109-1116.
34. Du, K.; Xie, H.; Hu, G.; Peng, Z.; Cao, Y.; Yu, F., Enhancing the Thermal and Upper Voltage Performance of Ni-Rich Cathode Material by a Homogeneous and Facile Coating Method: Spray-Drying Coating with Nano-Al<sub>2</sub>O<sub>3</sub>. *ACS Appl Mater Interfaces* 2016, 8 (27), 17713-20.
35. Lee, Y. S.; Shin, W. K.; Kannan, A. G.; Koo, S. M.; Kim, D. W., Improvement of the Cycling Performance and Thermal Stability of Lithium-Ion Cells by Double-Layer Coating of Cathode Materials with Al<sub>2</sub>O<sub>3</sub> Nanoparticles and Conductive Polymer. *ACS Appl Mater Interfaces* 2015, 7 (25), 13944-51.
36. Gratz, E.; Sa, Q.; Apelian, D.; Wang, Y., A closed loop process for recycling spent lithium ion batteries. *Journal of Power Sources* 2014, 262, 255-262.
37. Rodriguezcarvajal, J., Recent Advances In Magnetic-Structure Determination by Neutron Powder Diffraction. *Physica B* 1993, 192 (1-2), 55-69.
38. Zhang, N.; Li, J.; Li, H.; Liu, A.; Huang, Q.; Ma, L.; Li, Y.; Dahn, J. R., Structural, Electrochemical, and Thermal Properties of Nickel-Rich LiNi<sub>x</sub>Mn<sub>y</sub>Co<sub>z</sub>O<sub>2</sub> Materials. *Chemistry of Materials* 2018, 30 (24), 8852-8860.

39. Bichon, M.; Sotta, D.; Dupre, N.; De Vito, E.; Boulineau, A.; Porcher, W.; Lestriez, B., Study of the immersion of  $\text{LiNi}_0.5\text{Mn}_0.3\text{Co}_0.2\text{O}_2$  material in water for aqueous processing of positive electrode for Li-ion batteries. *ACS Applied Materials & Interfaces* 2019.
40. Xu, S.; Du, C. Y.; Xu, X.; Han, G. K.; Zuo, P. J.; Cheng, X. Q.; Ma, Y. L.; Yin, G. P., A Mild Surface Washing Method Using Protonated Polyaniline for Ni-rich  $\text{LiNi}_0.8\text{Co}_0.1\text{Mn}_0.1\text{O}_2$  Material of Lithium Ion Batteries. *Electrochimica Acta* 2017, 248, 534-540.
41. Yan, P.; Zheng, J.; Liu, J.; Wang, B.; Cheng, X.; Zhang, Y.; Sun, X.; Wang, C.; Zhang, J.-G., Tailoring grain boundary structures and chemistry of Ni-rich layered cathodes for enhanced cycle stability of lithium-ion batteries. *Nature Energy* 2018, 3 (7), 600-605.
42. Park, J. H.; Park, J. K.; Lee, J. W., Stability of  $\text{LiNi}_0.6\text{Mn}_0.2\text{Co}_0.2\text{O}_2$  as a Cathode Material for Lithium-Ion Batteries against Air and Moisture. *Bulletin of the Korean Chemical Society* 2016, 37 (3), 344-348.
43. Li, J.; Cameron, A. R.; Li, H.; Glazier, S.; Xiong, D.; Chatzidakis, M.; Allen, J.; Botton, G. A.; Dahn, J. R., Comparison of Single Crystal and Polycrystalline  $\text{LiNi}_0.5\text{Mn}_0.3\text{Co}_0.2\text{O}_2$  Positive Electrode Materials for High Voltage Li-Ion Cells. *Journal of The Electrochemical Society* 2017, 164 (7), A1534-A1544.
44. Zheng, J.; Yan, P.; Estevez, L.; Wang, C.; Zhang, J.-G., Effect of calcination temperature on the electrochemical properties of nickel-rich  $\text{LiNi}_0.76\text{Mn}_0.14\text{Co}_0.10\text{O}_2$  cathodes for lithium-ion batteries. *Nano Energy* 2018, 49, 538-548.
45. Cho, D. H.; Jo, C. H.; Cho, W.; Kim, Y. J.; Yashiro, H.; Sun, Y. K.; Myung, S. T., Effect of Residual Lithium Compounds on Layer Ni-Rich  $\text{LiNi}_0.7\text{Mn}_0.3\text{O}_2$ . *Journal of the Electrochemical Society* 2014, 161 (6), A920-A926.
46. Liu, S.; Zhang, C.; Su, Q.; Li, L.; Su, J.; Huang, T.; Chen, Y.; Yu, A., Enhancing Electrochemical Performance of  $\text{LiNi}_0.6\text{Co}_0.2\text{Mn}_0.2\text{O}_2$  by Lithium-ion Conductor Surface Modification. *Electrochimica Acta* 2017, 224, 171-177.
47. Chen, B.; Ben, L.; Yu, H.; Chen, Y.; Huang, X., Understanding Surface Structural Stabilization of the High-Temperature and High-Voltage Cycling Performance of  $\text{Al}^{3+}$ -Modified  $\text{LiMn}_2\text{O}_4$  Cathode Material. *ACS Applied Materials & Interfaces* 2018, 10 (1), 550-559.
48. Xu, G.-L.; Liu, Q.; Lau, K. K. S.; Liu, Y.; Liu, X.; Gao, H.; Zhou, X.; Zhuang, M.; Ren, Y.; Li, J.; Shao, M.; Ouyang, M.; Pan, F.; Chen, Z.; Amine, K.; Chen, G., Building ultraconformal protective layers on both secondary and primary particles of layered lithium transition metal oxide cathodes. *Nature Energy* 2019.
49. Gao, H.; Cai, J.; Xu, G.-L.; Li, L.; Ren, Y.; Meng, X.; Amine, K.; Chen, Z., Surface Modification for Suppressing Interfacial Parasitic Reactions of a Nickel-Rich Lithium-Ion Cathode. *Chemistry of Materials* 2019, 31 (8), 2723-2730.
50. Kim, J.; Lee, H.; Cha, H.; Yoon, M.; Park, M.; Cho, J., Prospect and Reality of Ni-Rich Cathode for Commercialization. *Advanced Energy Materials* 2018, 8 (6), 1702028.
51. Park, J. H.; Choi, B.; Kang, Y. S.; Park, S. Y.; Yun, D. J.; Park, I.; Ha Shim, J.; Park, J. H.; Han, H. N.; Park, K., Effect of Residual Lithium Rearrangement on Ni-rich Layered Oxide Cathodes for Lithium-Ion Batteries. *Energy Technology* 2018, 6 (7), 1361-1369.

## **Chapter 5. Systematic Electrochemical Comparisons between Recycled NMC Powder with Commercially Controlled Powder**

### **Abstract**

Recycled materials are usually deemed as inferior when in comparison to virgin materials, rendering it as a backup solution for vehicle use or merely as in a sustainability standpoint. There are argues about whether recycled materials should be directly used in brand-new vehicles, mainly having concerns regarding its performances. Giving the benefits of less energy usage and hazard emissions obtained in manufacturing recycled materials, if the electrochemical performances of recycled materials are verified by strict industrial measurements, there is no doubt that recycled materials will become competitive in the market. Here, recycled cathode powder produced from WPI closed-loop recycling stream has such superior behavior and it is verified in various cell formats, ranging from coin cell, single layer pouch cell, 1Ah cell to 11Ah cell. In the evaluation of 1Ah cells, the recovered NMC111 remains above 80% after 4,300 cycles and it performs better than results obtained using commercial cathode powder (3,100 cycles). Compared with virgin materials in rate performance, recycled materials perform superiorly in every cell format. Incorporated with the aforementioned environmental and economic benefits, it is confident to say recycled materials is not necessarily worse, and WPI recycled materials is proven to outperform commercially available equivalent.

### **1. Introduction**

Due to its possession of long cycle life and high energy density, lithium ion batteries are widely employed in our daily lives, such as consumer electronics, electric vehicles and energy storage systems. Especially in recent years, people have the tendency to choose electric vehicles where large format of lithium ion battery packs are equipped, and the sale of electric vehicles keeps increasing. It is anticipated that in 8 to 10 years, the quantity of spent lithium ion batteries will become un-negligible, and thus, mature and efficient recycling processes need to exist now.

However, there exist concerns of recruiting recycled materials in the market, and the questions arises from whether recycled materials can compete with virgin materials in cost, yield and performance. Academia and industry are making great efforts to optimize the recycling process, in order to reduce the cost and increase the yield simultaneously. When mass production is realized in the near future, it is believed the cost can be further minimized and the yield can be maximized. Above all, the electrochemical performance of recycled power plays a decisive role if recycled materials want to make an impact and this verification must be fulfilled by trustworthy testing. Since most of the research work of recycling is still conducted in lab size and the testing results are usually associated with coin cells, which is a relatively simple cell format and thus lacks reliability, industry has less confidence to use recycled materials. In order to verify the electrochemical performance of recycled battery materials, long-time and reliable testing need to be conducted. Also, side-by-side comparison with virgin materials is essential to deliver meaningful messages.

In the recent years, different LIB recycling processes have been developed. Pyrometallurgical recycling is a high-temperature smelting process and recent innovations appear in new slag systems' inventions, after-slag treatment and in-situ reduction roasting. The first two aim at increasing the recycling efficiency, and with the adoption of novel slag system and after-slag

treatment, manganese and lithium can be selectively recycled.<sup>1-3</sup> In-situ reduction roasting is an emerging and appealing technology since it requires no additives, and end-of-life batteries can be directly recovered and transformed into commodities via pyrolysis.<sup>4-7</sup> Hydrometallurgy recycling contains leaching and subsequent separation, and academic research are designed to optimize the involved various steps. Leaching dissolves metals from spent batteries and researchers increase its leaching efficiency through alkali leaching, acid leaching and bio-leaching.<sup>8-21</sup> Following leaching, an effective and efficient separation needs to exist to guarantee the purities of recycled materials and it is fulfilled by continuous innovations in solvent extraction, chemical precipitation electrolysis and ion exchange.<sup>22-33</sup> Direct recycling rejuvenates spent batteries primarily via physical separations and it thus avoids chemical breakdown of materials. The academic progresses are focused on the re-lithiation methods: solid-state sintering, hydrothermal process, electrochemical process and chemical process.<sup>34-39</sup> The recovered materials can restore its original structure and show competitive performance compared with virgin materials. However, current research in LIB recycling has two challenges: 1) Much research is still in very small lab scale, which leads to the economic analysis not very useful. Thus, scale-up ability of recycling process itself needs to be verified; 2) The recycled materials (mainly cathode) are mainly evaluated with coin cells. Thus, reliable testing in larger-format cells needs to exist.

In order to overcome the two challenges above, the Worcester Polytechnic Institute (WPI) team in the Department of Mechanical Engineering has developed a closed-loop lithium ion battery recycling process, which combines the benefits of hydrometallurgical and direct recycling technologies.<sup>16,27-31,40-43</sup> Our previous work has demonstrated our recycling process can be successfully scaled up.<sup>30,31,43</sup> Here, through the in-depth collaborations with academia and industrial partners, we evaluated our recycled materials in different cell format ranging from coin

cell, single layer pouch cell, 1Ah cell to 11Ah cell (**Figure 1**) and successfully overcame the second challenge reside in testing. In this paper, we will present the best industrial-level testing results of recycled materials so far and compare it with the virgin equivalent. Series of industrial plug-in hybrid electric vehicle (PHEV) tests are applied to our recycled materials and recycled materials not only pass all the aggressive industrial tests, but also precede the commercial counterparts in some tests.

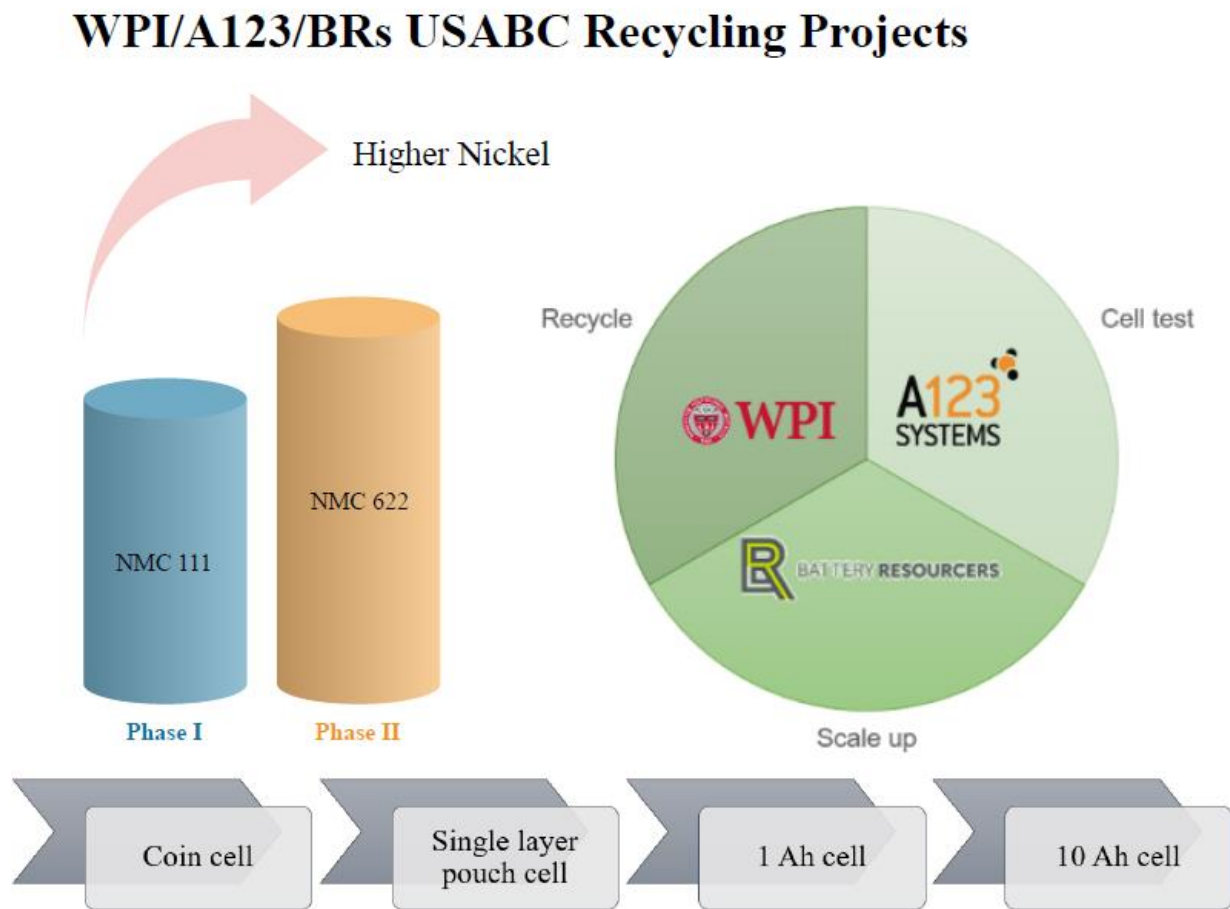


**Figure 1: WPI/A123/BRs USABC Recycling Projects**

## 2. Experiments

### 2.1 WPI Recycling Process

In the WPI process (**Figure 2**), spent batteries of various chemistries, form factors, and packaging can be combined into a single feedstock. Spent batteries are first discharged to avoid unintended thermal runaway during processing. Next, discharged batteries are cut, shredded, and sieved; steel cases, current collectors (Al, Cu), electronics circuits, plastics, and pouch materials (Al foils) are removed and recycled. The shredded batteries are sieved and separated, and current collectors, steel, plastics, etc., are recovered. The treated remaining black mass is composed of graphite, carbon, active material, some residues of Al, Cu, and Fe. After that, a hydrometallurgical process is implemented, and precious metals (Ni, Mn, Co), as well as lower-value metals (Cu, Fe, Al) found in LIBs, are dissolved in the leaching solution. Meanwhile, graphite, carbon, and undissolved metals are filtered out. First, impurities in the leachate including Cu, Fe and Al are removed through a series of pH adjustments, leaving the NMC metal ions. Next, the ratio of Ni, Mn, Co is tailored to the desired ratio by adding virgin metal sulfates as needed. The ability to fabricate various NMCs (responding to market demand) is a key advantage of the WPI recycling technology versus competing processes. Subsequently, the adjusted metal sulfate solution undergoes the co-precipitation reaction, and NMC hydroxide precursor powder is produced. After calcination with recovered lithium carbonate, recovered NMC cathode powder is ready for use in ‘new’ batteries, enabling a closed loop approach.

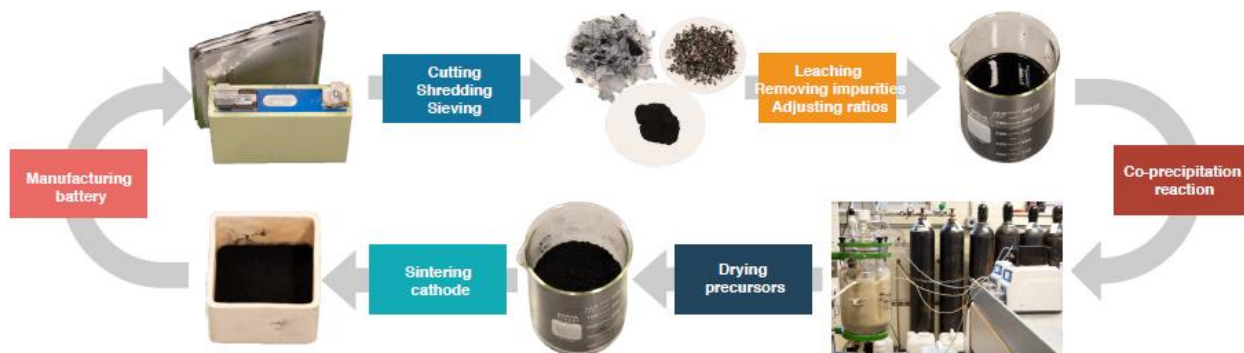


**Figure 2: WPI developed closed-loop recycling process**

## 2.2. Materials Characterization

*SEM*: Scanning electron microscope (SEM) images were taken using JEOL JSM 7000 F to obtain information of particle size and particle morphology.

*XRD*: X-ray diffraction (XRD) patterns of the materials were gained using PANalytical Empyrean with Cu K $\alpha$  radiation (45 kV, 40 mA).

*ICP*: Inductively coupled plasma optical emission spectrometry (Perkin Elmer Optima 8000 ICP-OES) was used to obtain the concentration of metal ions in materials.

## 3. Results and Discussions

### 3.1 Materials Characterization

Prior to the construction of cells, recycled cathode powder is assessed by its physical parameters and the characteristics being monitored include composition, tap density, particle size distribution (PSD), surface area. Cathode powders are dissolved in acid and the composition is tested by ICP-

OES. Control powder has a composition of  $\text{Li}_{0.99}\text{Ni}_{0.35}\text{Mn}_{0.31}\text{Co}_{0.34}\text{O}_2$  and recycled powder is  $\text{Li}_{1.03}\text{Ni}_{0.34}\text{Mn}_{0.33}\text{Co}_{0.33}\text{O}_2$ . In **Table 1**, SLP powder is employed in SLP cell, and 1Ah1 to 1Ah3 powder are fabricated as 1Ah cells, whilst 11Ah1 and 11Ah2 are built into 11Ah cell formats. Generally, recycled materials have a lower tap density and higher surface area while maintaining a similar particle size when comparing with control materials. From SEM observations (**Figure 3a and 3b**), recycled materials possess good morphology as control powder and it is composed by spheres of different sizes. XRD pattern of recycled powder perfectly matches standard NMC 111 materials and a good crystallinity is proved.

**Table 1: Powder characterization**

Test	Metric	Control	SLP	1Ah1	1Ah2	1Ah3	11Ah1	11Ah2
Tap density	g/cc	2.84	2.16	2.31	2.36	2.51	2.45	2.52
D50 PSD	$\mu\text{m}$	9.2	9.38	11.6	14.1	10.2	11.7	11.2
BET	$\text{m}^2/\text{g}$	0.28	0.56	0.53	0.36	0.65	0.40	0.43
Cumulative pore Vol	$\text{cm}^3/\text{g}$	0.000080	-	0.000132	0.000092	0.000163	0.000240	0.000150
Avg pore Diameter	$\text{\AA}$	20.502	-	20.865	20.721	20.833	21.352	20.929

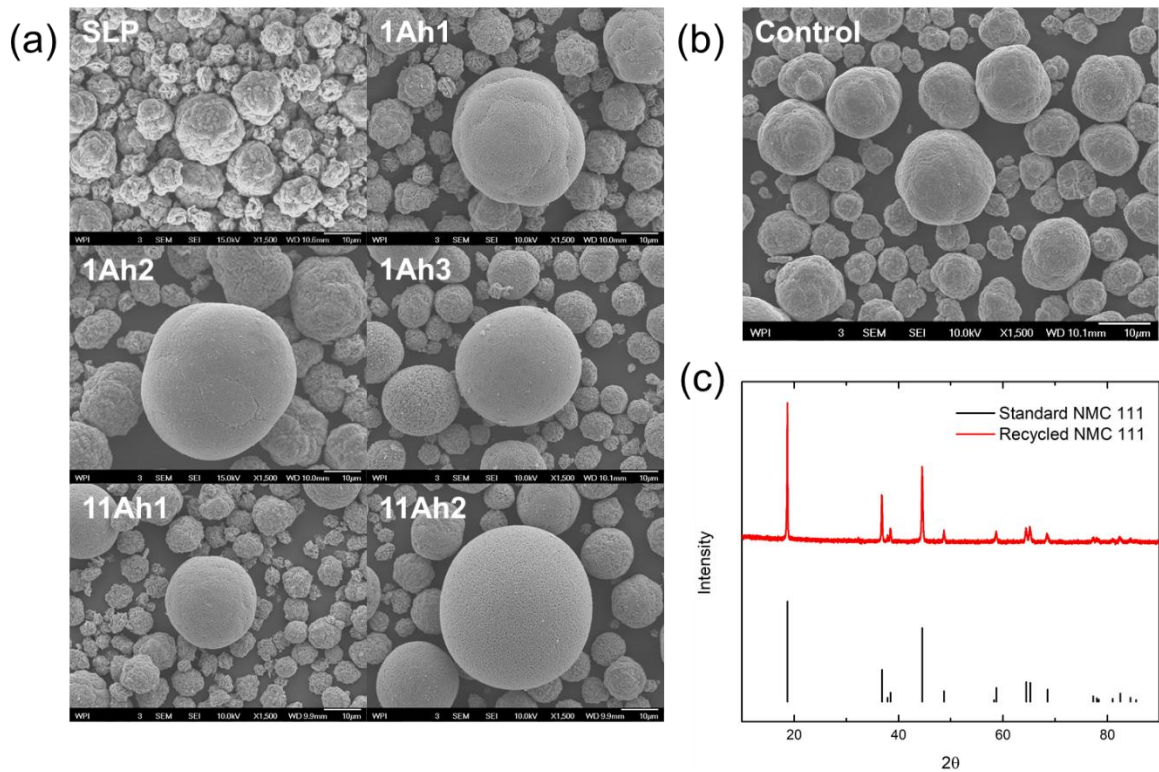


**Figure 3: (a) SEM images of recycled materials used in various cells (scale bar: 10μm). (b) SEM image of control materials (scale bar: 10μm). (c) XRD pattern of recycled NMC 111 in comparison with standard NMC 111 pattern.**

Upon physical characteristics assessments, recycled materials are formed into cells and the electrochemical performance are systematically evaluated. In order to deliver the message that recycled materials can compete with virgin one and it indeed has practical usage in industry, a top-level commercial control powder is adopted for side-by-side comparison. The recycled cathode powder is assembled in various formats, including coin cell, single layer pouch cell (SLP), 1Ah cell and 11Ah cell, and undergoes corresponding series tests. Coin cell is a simple format to evaluate the quality of battery material and is frequently assembled in laboratory. SLP cell imitates

the multi-layer prismatic pouch cell and is a simple but valuable tool to screen materials before more complicated form factors are built. 1Ah and 11Ah cell are representative form factors and can be utilized in vehicles straight.

The testing of 1Ah and 11Ah cells follows the USABC'S PHEV protocol.<sup>44</sup> Generally, testing is made up by three regions, which is characterization, life testing and reference performance testing (RPT). Characterization testing is aimed at constructing the baseline properties, such as self-discharge, static capacity, hybrid pulse power characterization (HPPC) and cold crank. Life testing tends to track the dynamic behavior at various condition, like temperature and state of charge (SOC), and consists of cycle life and calendar life. RPT is performed periodically along with life testing and to monitor the degradation relative to the baseline.<sup>44</sup>

### 3.2. Coin Cell

Coin cells are firstly fabricated for electrochemical evaluations of recycled powder. Coin cell electrode has an industrial-level loading density ( $20 \text{ mg/cm}^2$ ) and press density ( $3.0 \text{ g/cm}^3$ ), which is much higher than what reported in literature. This strict loading standard makes our coin cell data representative and trustworthy. **Figure 4** summarizes the specifications that need to be examined and the recycled powder compare favorable to the control samples, especially at higher rate. At 1C and 2C, capacity differences between recycled and control material is still minimal, whilst, it exceeds the commercial counterpart by 88% to 170% at 5C rate. This significant enhancement is vital for fast-charging applications and it directs a way to commercialize recycled material. The underlying reason is speculated to be the lower tap density and higher porosity.<sup>30,31</sup>

SLP powder shows abnormal behavior at 1C and 2C, however, it is believed this is due to the coin cell fabrication, not materials itself. The SLP data in the next section can also prove this statement.

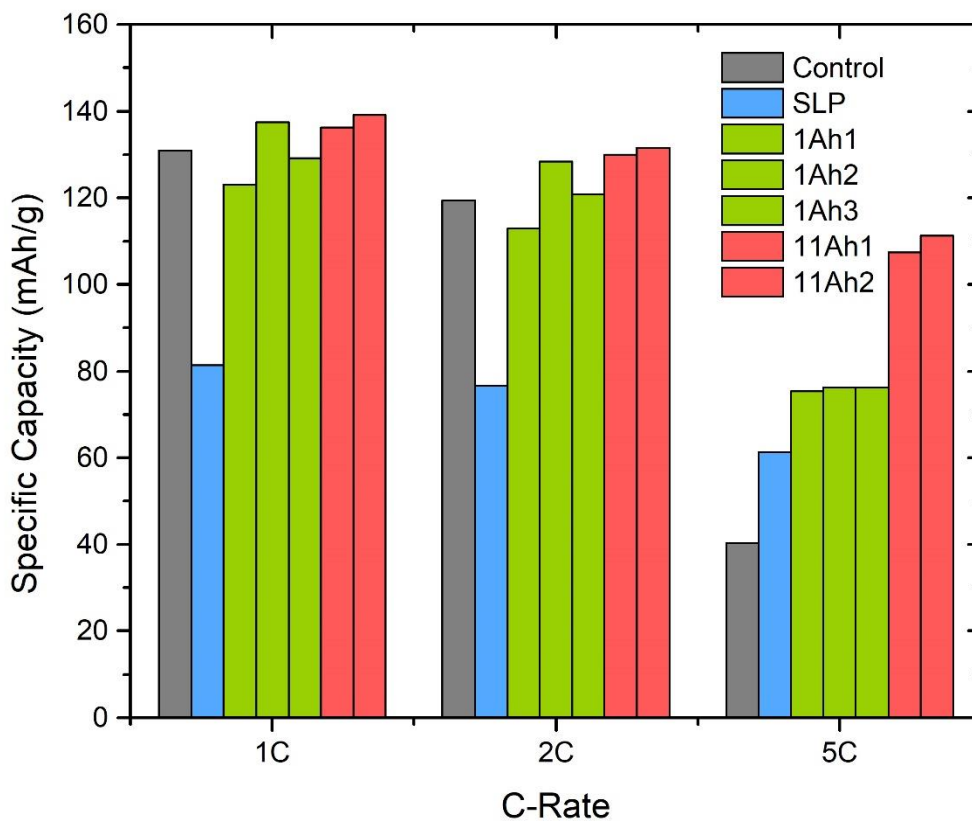


**Figure 4: Comparison of control vs. recycled powder in coin cell performances in rate capability (control-gray, SLP-blue, 1Ah-green, 11Ah-red).**

### 3.3. Single Layer Pouch Cell

Similar to coin cells, the SLP electrode are set to have a high loading density of 20 mg/cm<sup>2</sup> and press density of 3.3 g/cm<sup>3</sup>. SLP cells are cycled at 23°C in a voltage window of 2.7V to 4.2V. In

each cycle, the cell is charged at 1C and then discharged at 2C at a typical testing protocol of PHEV. **Figure 5** shows the electrochemical performance comparison between control and recycled powder in SLP cell, in which control powder has three lots (in gray) and recycled powder has 6 lots (in blue). All cells are showing reasonable and similar performance during cycling, and recycled powder retains 80% of its capacity after ~1200 cycles averagely.<sup>31</sup> During the cycling tests, cells are regularly going through state of health (SOH) check and the direct current resistance (DCR) is recorded. Considering the DCR growth, a significantly higher growth in control cells indicates a worse stability for control cells. Results of SLP cells supports the 1Ah cell builds of recycled powder in the next step.

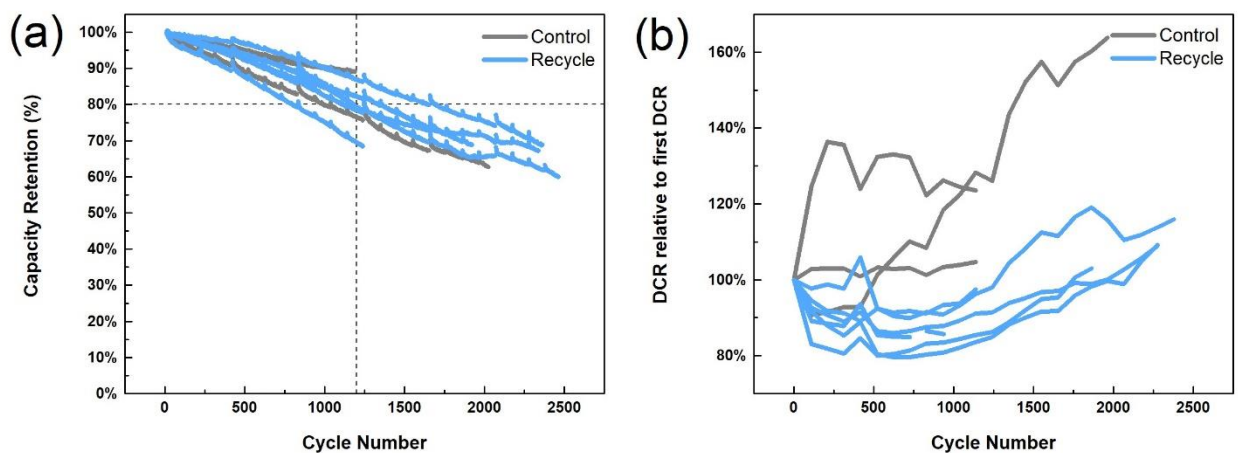


**Figure 5: Comparison of control vs. recycled powder in SLP cell performances (control-gray vs. recycled-blue). (a) Capacity retention (%) vs. Cycle number (b) DCR relative to first DCR vs. Cycle number**

### 3.4. 1Ah Cell

1Ah cell is a prototypical format for industry adoption, thus, employing recycled materials in 1Ah cell and the corresponding measurements is more trustable comparing to coin cell and SLP cell results. The results include the beginning-of-life (BOL) testing, life testing and RPT testing.

### **3.4.1 Beginning-of-life Testing**

BOL testing is carried out when the characterization of the test article begins, and it consists of self-discharge test, static capacity, HPPC and cold crank. These series of tests establish a baseline performance from which the deterioration is tracked.

All of the self-discharge rate fall on a region of 3.7 to 8.4 mAh/day, and among them, control materials shows a higher self-discharge rate on average than recycled products. The discharge curves of various articles overlap with each other and demonstrate nearly identical properties. The capacity of each build is recorded and slightly variations are shown.

The HPPC test involves discharge and regen pulses and it tends to identify the dynamic power capability in the defined voltage range. Vehicles may be exposed to extremely cold surroundings and whether battery can sustain a certain capacity or voltage threshold is especially important. Cold crank tests simulate such condition and tends to measure the cell capability at a specific temperature and SOC accordingly. This test is crucial for hybrid electric vehicle since battery is used to propel vehicle itself.

HPPC and cold crank tests are conducted and the results are displayed in **Figure 6**. The discharge resistance, regen resistance and open circuit voltage (OCV) of HPPC test share a similar trend among all of the test samples. As the depth of discharge (DOD) progresses, resistance fluctuates a little and suddenly increases a lot when DOD is approaching 100%. Synchronously, pulse power capability in HPPC of separate materials shows an overall similar tendency as the DOD advances.

The discharge power capability gradually shrinks and regen power capability increases step by step with a small drop near 100% DOD. Cold crank testing is depicted below and all of the cells pass the tests and sustain above the 2.2 V voltage limit. Cells with WPI recycled materials have an average voltage of 2.9V and control one has a value of 2.85V as a comparison.

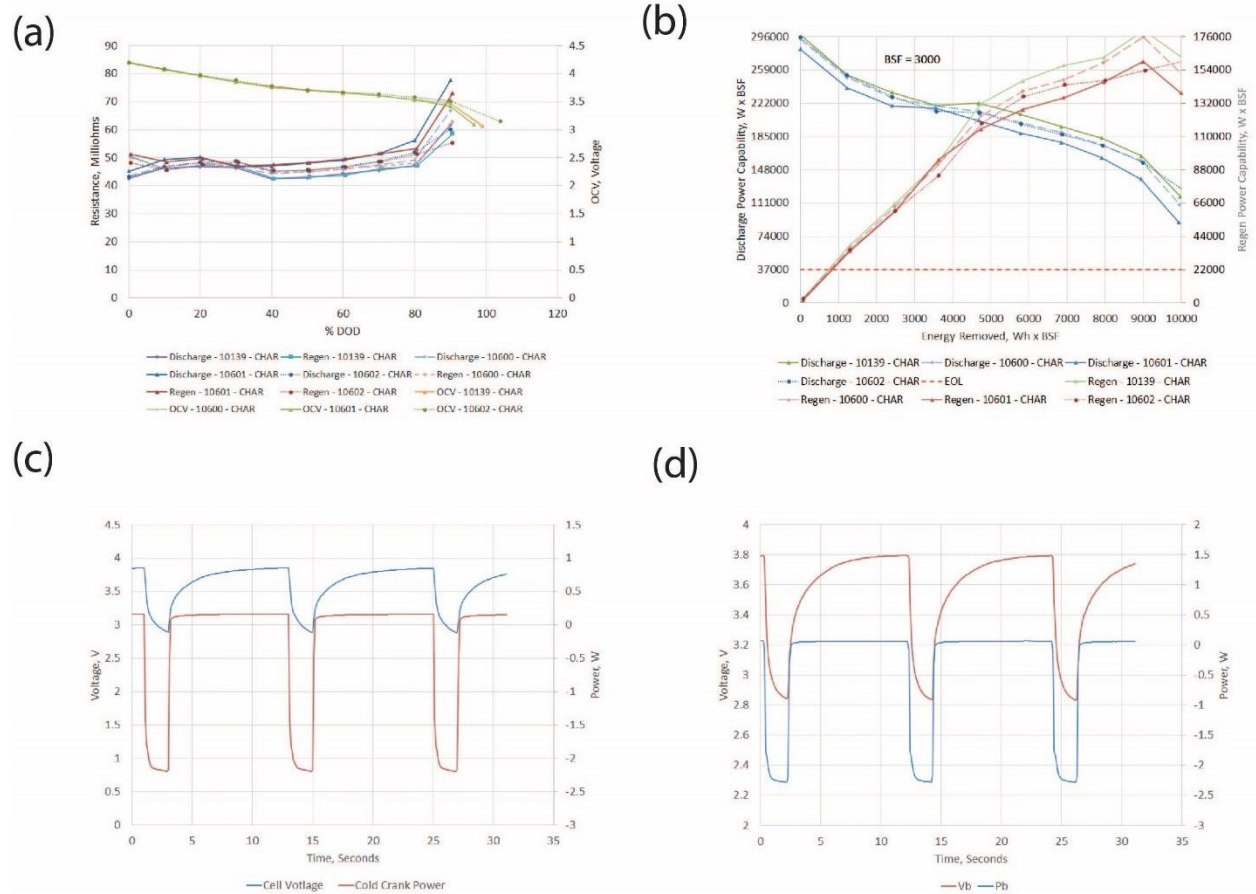


**Figure 6: HPPC and cold crank testing of 1Ah cells. (a) HPPC-resistance (b) HPPC-pulse power capability. (c) Cold crank tests of cells with WPI recycled powder. (d) Cold crank tests of cells with control powder.**

### 3.4.2 Life Testing

Cycle life applies a continuous and defined charge/discharge pattern to tested subject and monitors its capacity retention before end-of-life status reaches, within a specific voltage window. Temperature can be arisen above room temperature and a meaningful result can be obtained with a shorter testing duration. Calendar life testing is operated by applying a pulse once per day and then reposing the tested object under OCV monitoring. Unlike cycle life testing which requires constant execution, calendar life testing mimics a minimal usage of battery and establish the degradation rate correspondingly, and moreover, it is conducted at an elevated temperature in order to expedite the decay process. Here, a 50 °C is chosen to accelerate the deterioration while avoiding unpleasant failure mechanisms.

**Figure 7a** shows the cycle performance of 1Ah cells with recovered NMC111 made from 3 different, diverse EV input streams and control powders and it includes 7-batch of recycled material and 2-batch of control powder. Insert of Figure 2 located in the lower-right region demonstrates the actual 1Ah cell that is fabricated. Cells were fabricated and tested at 45°C between 2.7V-4.15V with each cycle of 1C charge and 2C discharge. The recovered NMC111 shows very consistent results, and after ~4,000 cycles, the cells' capacity retention remains above 80%. These results are better than results obtained using commercial cathode powder (black lines), whose end-of-life (EOL) cycle number is around 3,100. The astonishing improvement of recycle powder from control material further clear any hesitation of recruiting recycled cathode powder in the market.

The calendar life performance is tested at 50°C and the results are depicted in **Figure 7b**. 600, 601 and 602 are three different lots of 1Ah cell that build, and in every lot 4 different cells are tested. 601 and 602 performs better than the control powder while 600 decays at a higher rate. Overall, the recycled material has similar performance comparing to commercial powder and it decays in

a reasonable range. After 300-day of calendar life testing, recycled material can sustain a capacity retention ranging from 86% to 90%.

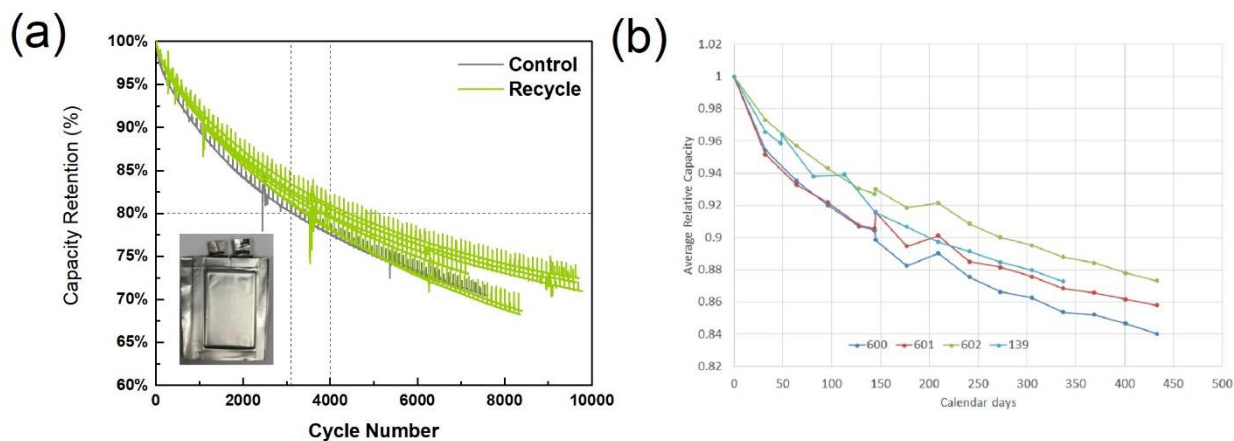


**Figure 7: (a) Cycle life testing. Capacity retention of control powder (in gray) and recycled powder (in green) in 1Ah cells. (b) Calendar life testing. 600, 601 and 602 are cells equipped with WPI recycled powder, while 139 is commercial control powder.**

### 3.4.3 RPT Testing

RPT testing is performed periodically and intends to gauge the extent and rate of degradation as the life testing proceeds, and the interval between each RPT is around 32 days for this calendar life RPT testing. The results from RPTs are typically compared with value get from the beginning of life (referred to as RPT0) and the changes are recorded.

HPPC testing is conducted on recycled and control samples, and the corresponding RPTs results associated with resistance and pulse power capability are demonstrated in **Figure 8**. The resistance

and discharge power are tested when 5.8kWh are removed. Three recycled batches exhibit a resistance increase of 29.0%, 39.4% and 29.9% at RPT10, while control lot yields a 22.8% increase at RPT7. According to **Figure 9**, the discharge power reduction is 23.9%, 29.2% and 24.0% for recycled powder at RPT10, and 19.8% is related to control powder at RPT7.

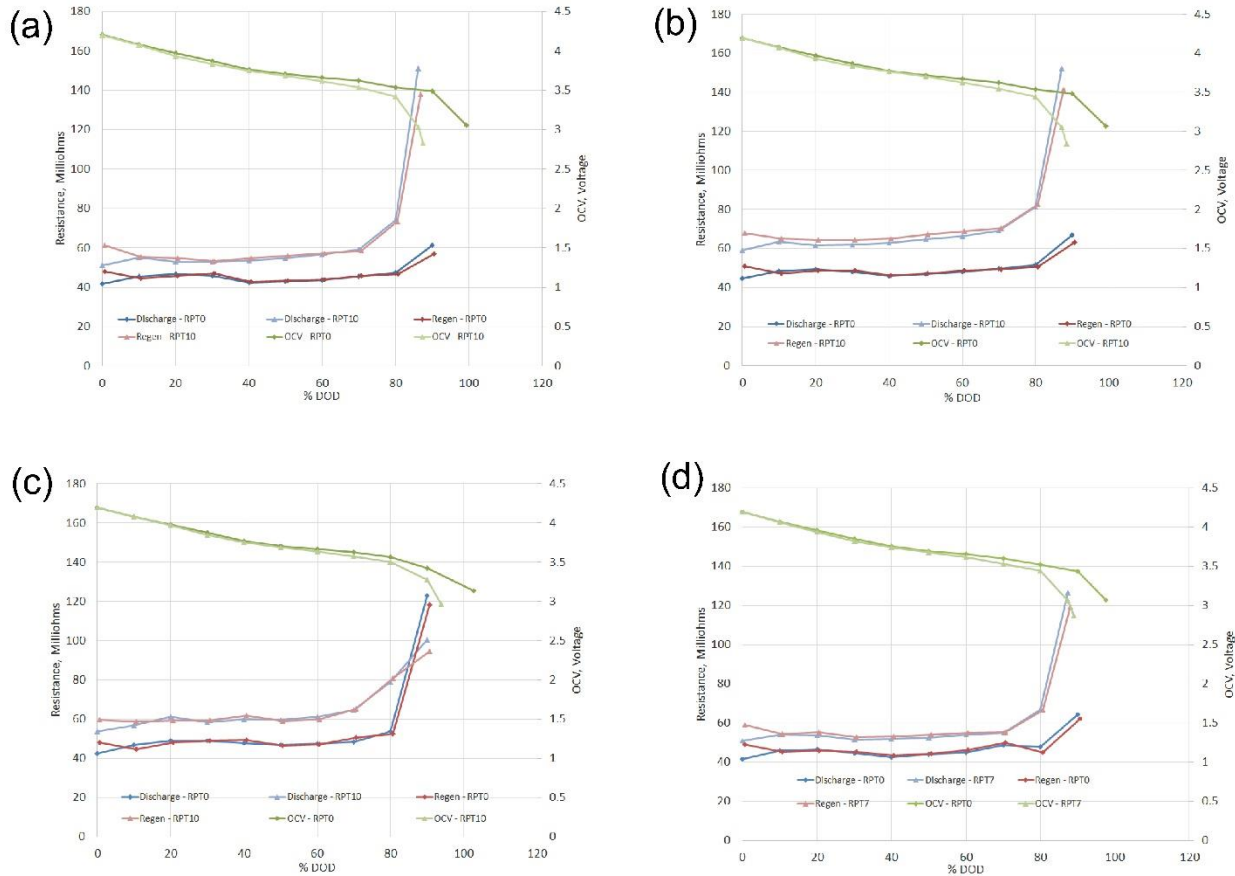


**Figure 8: Calendar life RPT HPPC testing. (a-c) HPPC-resistance results from three recycled lot. (d) HPPC-resistance results from one control lot.**

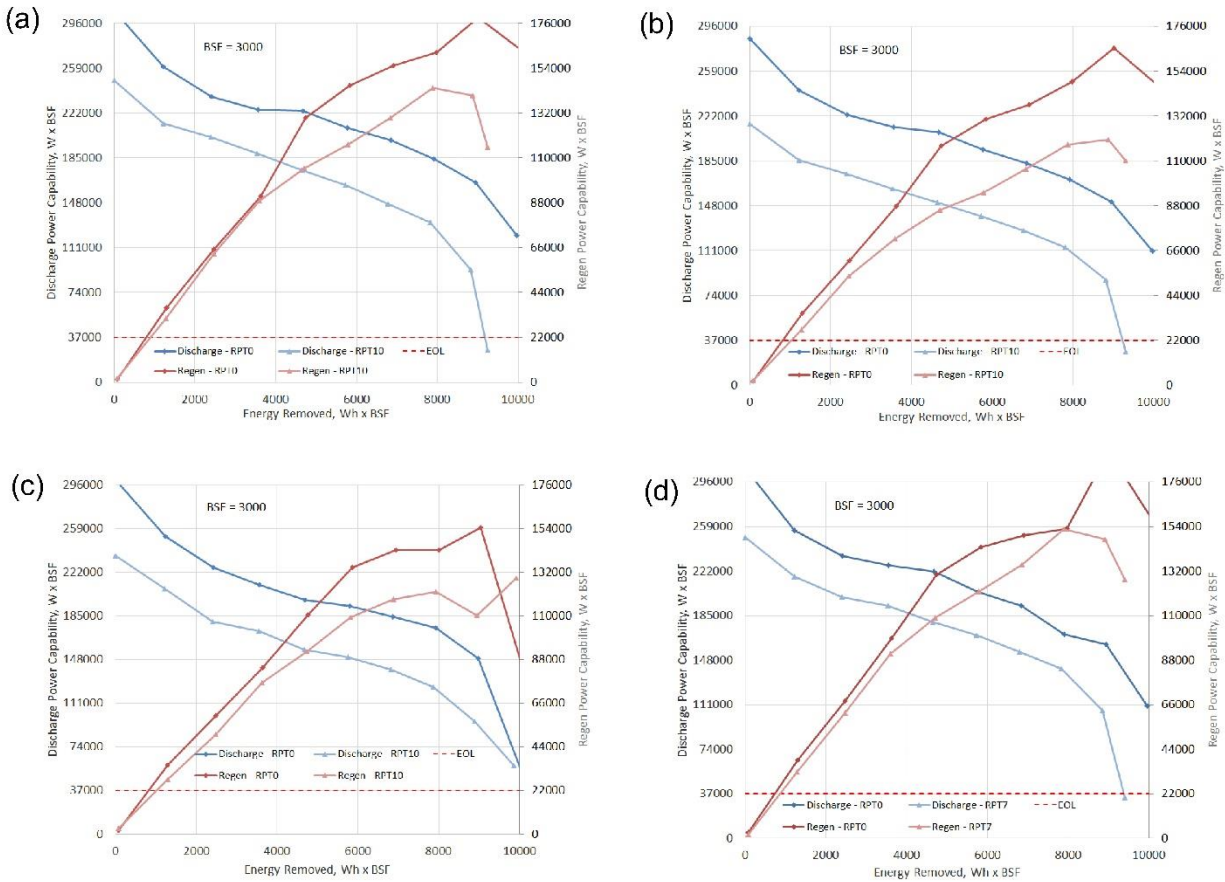


**Figure 9: Calendar life RPT HPPC testing. (a-c) HPPC-pulse power capability results from three recycled lot. (d)HPPC-pulse power capability results from one control lot.**

### 3.5. 11Ah Cell

To drive a longer distance, xEVs require to be equipped with a battery that has a higher capacity, hence, 11Ah cells are built to analyze the recycle powder. Following USABC’S PHEV testing protocol,<sup>44</sup> 11Ah cells are screened via rate performance, cycle performance, HPPC and cold crank.

#### 3.5.1 Beginning-of-life Testing

The self-discharge rate is similar among recycled materials (42mAh/day) and control powder (45mAh/day). Analogous to 1Ah cell, the discharge curves are showing no difference among recycle and commercial powder, and the deviation between builds is minor. Cold crank testing of two recycle powder and one control powder has no significant difference and they all pass the voltage limit.

HPPC testing results tested by ANL are shown in **Figure 10**. Overall, various batches share an alike trend over the DOD range. In addition, the variation between batches is slight.

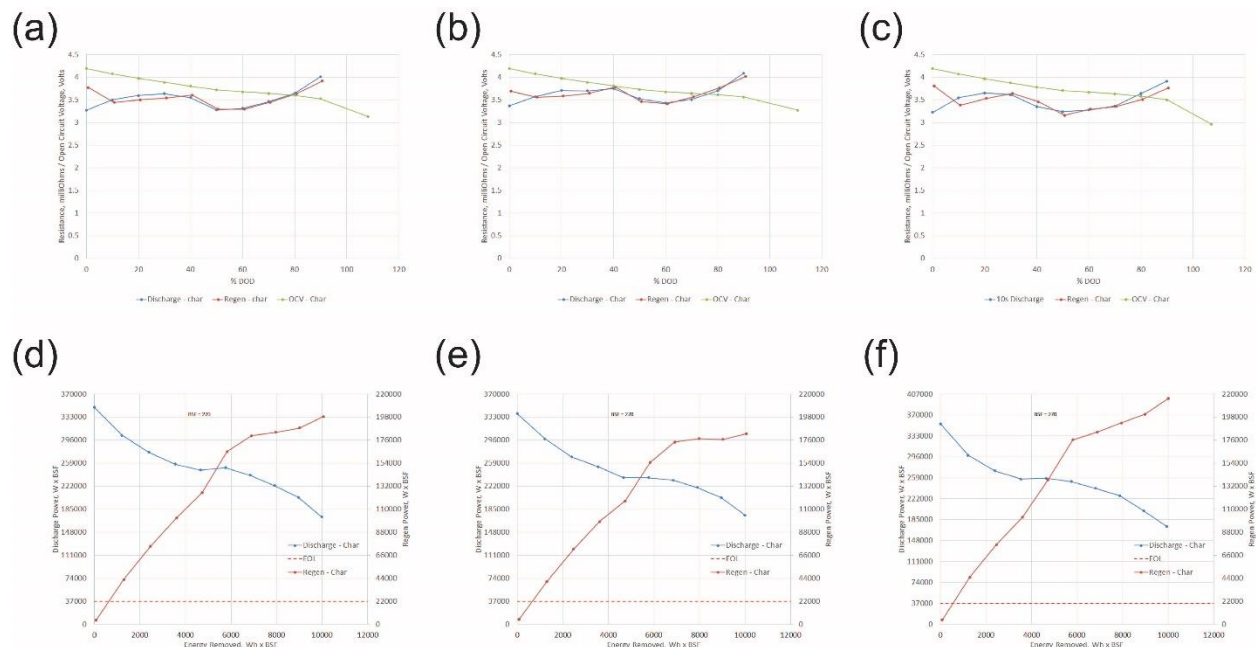


**Figure 10: HPPC testing of 11Ah cells. (a-c) HPPC-resistance of two recycled lot and one control. (d-f) HPPC-pulse power capability of two recycled lot and one control.**

A123 Systems also evaluates 11Ah cells with HPPC and cold crank testing. This HPPC test is initiated when 11Ah cells are in a degree of 100% state-of-charge (SOC) and then cells are

discharged to next 10% decrement relative to SOC and followed by a default rest period to return cells to equilibrium status. Between each SOC datapoint, a pair of 30-second discharge and regen pulses are executed and immediate feedback of resistance are collected. Here, two series of temperature (25°C versus 0°C) are chosen to determine the influence of ambient temperature. The discharge resistances are plotted at each 10% decrement in **Figure 11** between 0% SOC and 100% SOC.

HPPC tests are performed on 11Ah cells with WPI recycled powder to validate its application in PHEVs. At 25°C, the cells are discharged at 5C current for 30 second, and then charged at 3.75C for 30 seconds. The resistances are tested from 100% to 0% state of charge (SOC). At 0°C, the discharge current keeps the same (5C), and the charge current changes to 1.5C in order to reduce the dendrite formation.

The result of WPI recycled cathode powder is very consistent and it is illustrated in **Figure 11**. It is shown that at lower temperature, the DCR is higher due to the rate limitation of kinetics. And at lower SOC, the DCR also is larger. When performed at 25°C, both resistances have 3 mOhm at 1 second and 3.9 mOhm at 10 seconds at 50% SOC DCR. While at 0°C, green lot expresses a slightly higher DCR than red one. And at 50% SOC DCR and 1 second, green lot has a DCR of 9.3 mOhm while red one has a number of 8.5 mOhm. And at 50% SOC DCR and 10 seconds, green lot has a DCR of 10.4 mOhm while red one has a number of 9.6 mOhm.

Here, the cold crank tests are performed on cells with WPI recycled powder and commercially available 26Ah product that has similar chemistry at -30 °C and 15% SOC. The commercially available 26Ah product is here to act as reference cell, even the capacity is different from 11Ah cells packed with WPI recycled powder. The comparison is still valid due to the similar chemistry.

It includes three 2-second pulses and 10-second rest between pulses. The three repeated runs are pictured in **Figure 11**. Two 11Ah cells show equivalent performance as the reference cells and all cells maintain above 2.7V after three consecutive pulses, although pulses gradually decrease the voltage as the test proceed. and WPI cells share similar performance with commercial product.

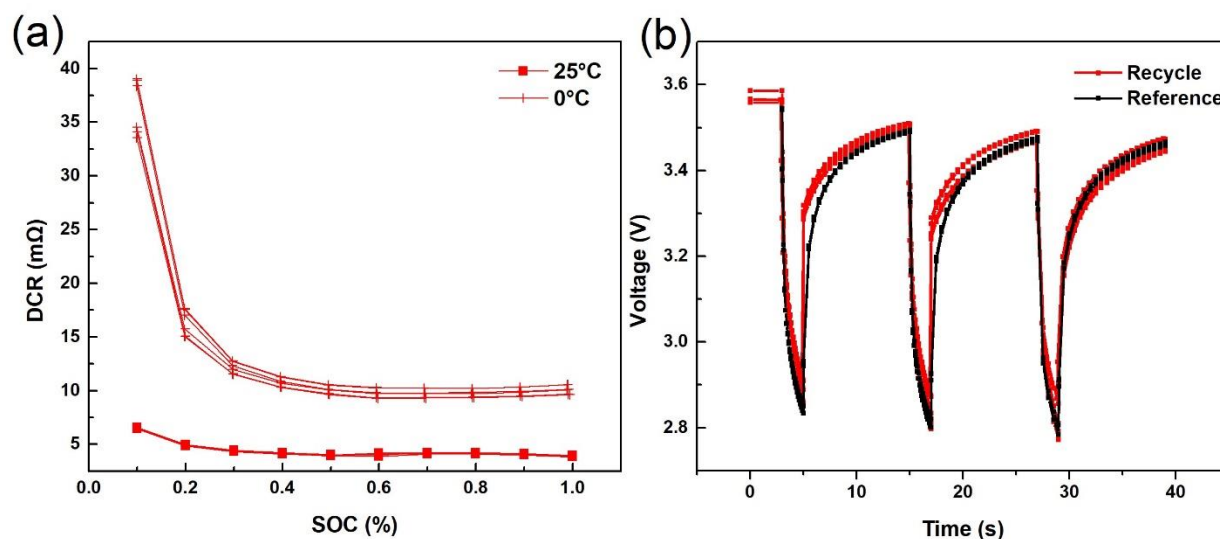


**Figure 11: (a) 11Ah HPPC test. 10s discharge resistance at 25°C and 0°C. 1s discharge resistance at 25°C and 0°C. (b) 11Ah cold crank tests. Cells with WPI recycled powder are in red, and commercial product are in black.**

Rate performance tests are conducted at 25°C within a voltage window of 2.7V to 4.15V. The cells are charged at 1C and then discharged at 1C, 2C, 3C, 5C, 7C, 9C respectively. Reference cell is a commercially available 26Ah cell with similar chemistry as recycle powder, and the result of comparison is shown in **Figure 12**. Two batches of WPI synthesized recycle cathode are included in this figure and both of them present superior rate performance than the reference cell at every rate, and it agrees with coin cell test once again. In particular, at 5C, cell maintains over 60% of

discharge capacity relative to the 1C discharge capacity, and at 9C, the capacity is approaching 30%.

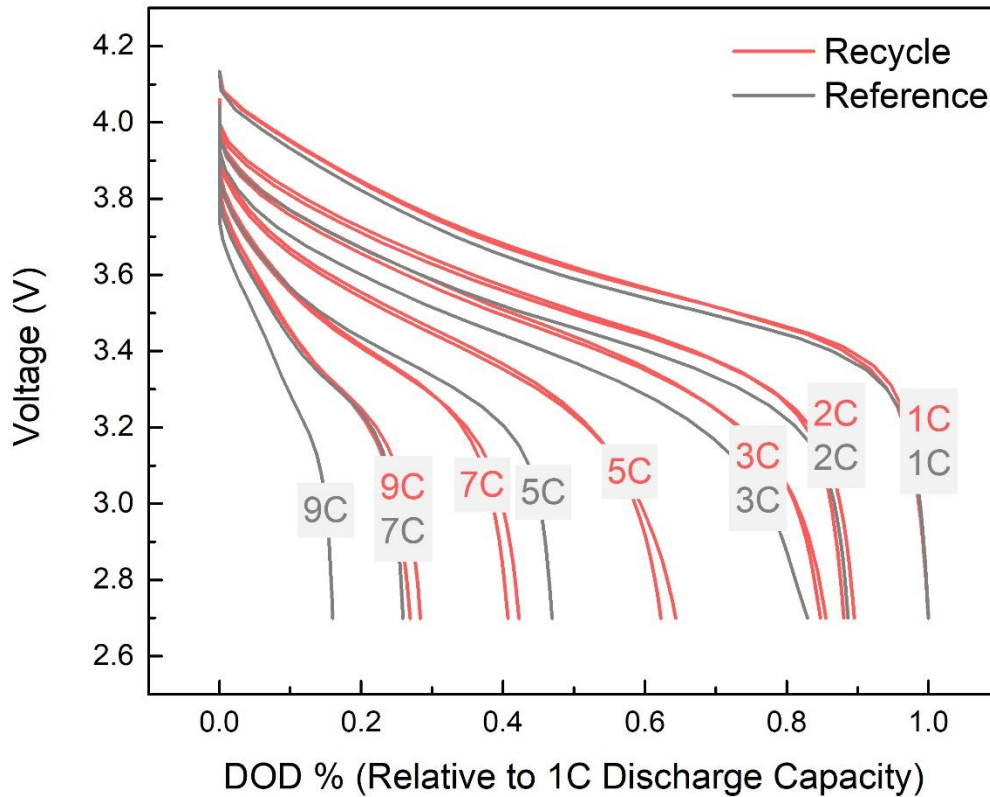


**Figure 12: 11 Ah rate performance. Recycled powder is in red, and reference is in grey.**

### 3.5.3 Life Testing

Cycle life testing is conducted at 30°C and shown in **Figure 13a**. It is conducted at 45°C with 1C charge and 2C discharge between 2.7V-4.15V. Control group shows a slightly better cycle performance than WPI powder, and one cell retains 87% capacity at 1000 cycles. Cells with WPI

recycled powder remains 85%-83% capacity around 1000 cycles, and the cycle life of 11Ah cell is ~40% of its 1Ah cell. After 2000 cycles, there is abrupt decay in capacity associated with recycled material, and similar condition happens to one control group after 3500 cycles, but this abnormal performance is ascribed to anode adhesion. Another control group also experiences this rapid decay in capacity at 800 cycles, and at that point, the capacity retention is 85%. With that, no determination between control and WPI material can be made.

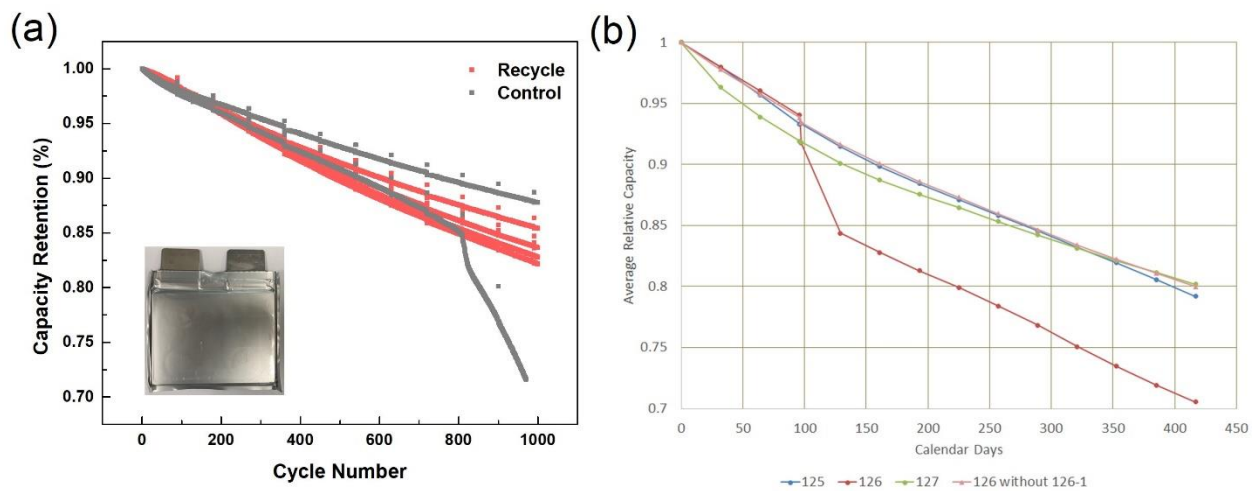


**Figure 13: Cycle life and calendar life of 11Ah cells. (a) Cycle life. Recycled is in red, and control is in grey. (b) Calendar life. Recycled is in red and blue, and control is in green.**

### 3.5.4 RPT Testing

During calendar life testing, HPPC testing is conducted periodically and the resistance and pulse power capability results are exhibit in **Figure 14**. At RPT 8, 1202 and 1182 cycles are completed for two recycle batches, and control batch accomplishes 1205 cycles. The discharge resistance is

increased by 58.3% and 43.8% of two recycled powder, and 35.8% for commercial counterpart. Since RPT0, there are 38.1%, 46.5% and 27.8% average decrease in power accordingly.

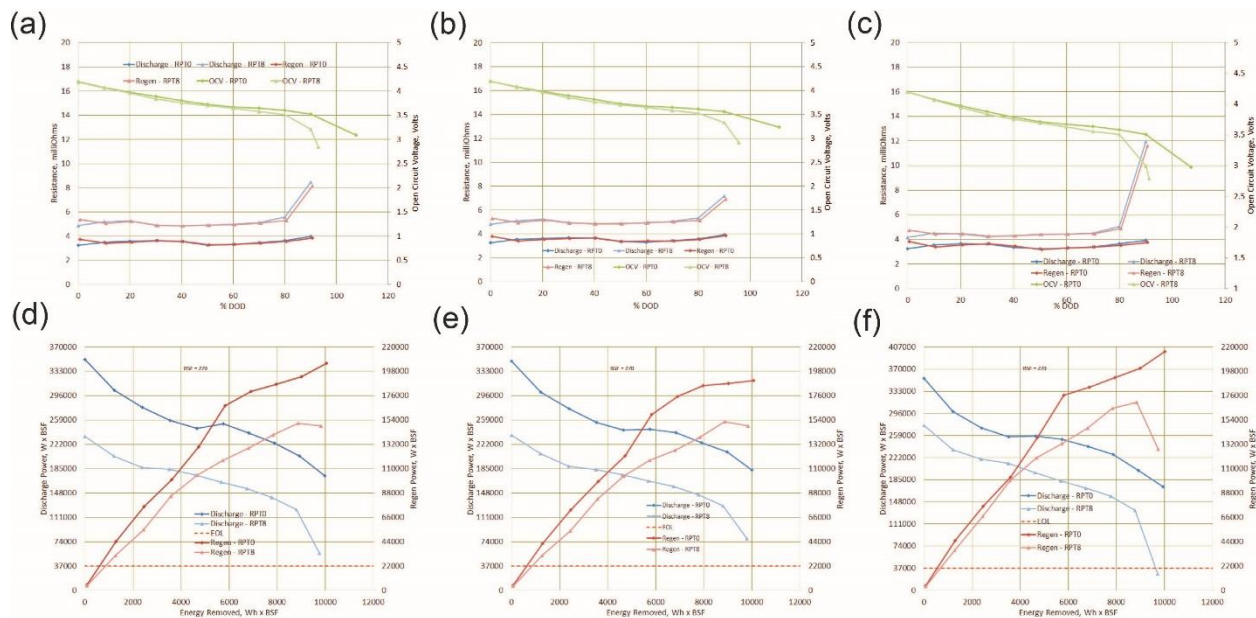


**Figure 14: Calendar life RPT HPPC testing of 11Ah cell. (a-c) HPPC-resistance results from two recycled lot and one control. (d-f) HPPC-pulse power capability results from two recycled lot and one control.**

### 3.6. Why Better Rate and Cycle Performance

In principle, good rate and good cycle performance cannot be achieved simultaneously and researchers need to balance the tradeoff. Improved rate performance indicated a better diffusion path, and it always results in a compromised cycle performance due to the larger exposed surface area and severer side reactions. However, with an optimized electrode geometry, our recycled materials demonstrated a combined good rate and cycle performance and this trait is accomplished by the porous structure of itself. As evident in **Table 1**, having a similar particle size with control

cathode, the recycled cathode has a lower tap density, and thus result in a higher surface area and a larger cumulative pore volume. We believe this porous structure provides a shorter diffusion path for lithium ion transport and gives rise to the faster charge transfer and better rate performance as a result. In consideration for the cycle test, this porous structure also promotes the performance working as a buffer function. The degradation of battery materials during cycling is always accompanied by the pulverization of cathode particles<sup>45,46</sup> and many researchers are seeking methods to depress this phenomenon, such as coating and doping. Our recycled materials, equipped with natural and advantageous porous structure, can mitigate the tension between the primary particles (inter-granular) and within primary particles (intra-granular). Hence, with less cracking formed, the cycle performance precedes the control equivalent.

#### **4. Conclusions**

Academia and industry have doubts of recruiting recycled materials into the fabrication of new battery packs mainly due to the uncertainty of its electrochemical performance, uncompetitive price and still low yield. The cost and yield can be resolved by optimizing recycling process and scale-up, which can be achieved when a plenty of lithium ion batteries become waste. Prior to the mass production, the electrochemical performance of recycled materials needs to be verified and the results should be compared with superior commercial virgin materials.

In this literature, we show the best results of recycled materials so far in a long-term and reliable testing with various cell formats, which consists of coin cell, single layer pouch cell, 1Ah cell and 11Ah cell. When in contrast with an outstanding virgin material, our WPI-synthesized recycled material not only meets all of the rigorous industrial-level testing requirements, it also shows better

behavior in some tests. The 1Ah cell of recycled NMC 111 has a life-time of 4,300 cycles while virgin equivalent cannot surpass 3,100 cycles. Due to the higher porosity, recycled materials perform much better than the control powder, especially at higher rate. This superior rate performance opens up a highway of recruiting recycled materials in the area of fast charging.

Through this trustworthy testing and the corresponding, I believe there won't be any concerns regarding recycled materials' performance. To smoothly be adopted by industry, continuous developments of reducing cost, increasing yields and improving performance should be conducted.

## References:

1. Georgi-Maschler, T., Friedrich, B., Weyhe, R., Heegn, H. & Rutz, M. Development of a recycling process for Li-ion batteries. *Journal of Power Sources* 207, 173-182, doi:<https://doi.org/10.1016/j.jpowsour.2012.01.152> (2012).
2. Guoxing, R. et al. in *Advances in Molten Slags, Fluxes, and Salts: Proceedings of the 10th International Conference on Molten Slags, Fluxes and Salts 2016*. (eds Ramana G. Reddy, Pinakin Chaubal, P. Chris Pistorius, & Uday Pal) 211-218 (Springer International Publishing).
3. Dang, H. et al. Recycled Lithium from Simulated Pyrometallurgical Slag by Chlorination Roasting. *ACS Sustainable Chemistry & Engineering* 6, 13160-13167, doi:10.1021/acssuschemeng.8b02713 (2018).
4. Li, J., Wang, G. & Xu, Z. Environmentally-friendly oxygen-free roasting/wet magnetic separation technology for in situ recycling cobalt, lithium carbonate and graphite from spent LiCoO<sub>2</sub>/graphite lithium batteries. *Journal of Hazardous Materials* 302, 97-104, doi:<https://doi.org/10.1016/j.jhazmat.2015.09.050> (2016).
5. Xiao, J., Li, J. & Xu, Z. Novel Approach for in Situ Recovery of Lithium Carbonate from Spent Lithium Ion Batteries Using Vacuum Metallurgy. *Environmental Science & Technology* 51, 11960-11966, doi:10.1021/acs.est.7b02561 (2017).
6. Xiao, J., Li, J. & Xu, Z. Recycling metals from lithium ion battery by mechanical separation and vacuum metallurgy. *Journal of Hazardous Materials* 338, 124-131, doi:<https://doi.org/10.1016/j.jhazmat.2017.05.024> (2017).
7. Mao, J., Li, J. & Xu, Z. Coupling reactions and collapsing model in the roasting process of recycling metals from LiCoO<sub>2</sub> batteries. *Journal of Cleaner Production* 205, 923-929, doi:<https://doi.org/10.1016/j.jclepro.2018.09.098> (2018).
8. Zheng, X. et al. Spent lithium-ion battery recycling – Reductive ammonia leaching of metals from cathode scrap by sodium sulphite. *Waste Management* 60, 680-688, doi:<https://doi.org/10.1016/j.wasman.2016.12.007> (2017).
9. Chen, Y. et al. Thermal treatment and ammoniacal leaching for the recovery of valuable metals from spent lithium-ion batteries. *Waste Management* 75, 469-476, doi:<https://doi.org/10.1016/j.wasman.2018.02.024> (2018).

10. Barik, S. P., Prabakaran, G. & Kumar, L. Leaching and separation of Co and Mn from electrode materials of spent lithium-ion batteries using hydrochloric acid: Laboratory and pilot scale study. *Journal of Cleaner Production* 147, 37-43, doi:<https://doi.org/10.1016/j.jclepro.2017.01.095> (2017).
11. He, L.-P., Sun, S.-Y., Song, X.-F. & Yu, J.-G. Leaching process for recovering valuable metals from the LiNi<sub>1/3</sub>Co<sub>1/3</sub>Mn<sub>1/3</sub>O<sub>2</sub> cathode of lithium-ion batteries. *Waste Management* 64, 171-181, doi:<https://doi.org/10.1016/j.wasman.2017.02.011> (2017).
12. Li, H. et al. Recovery of Lithium, Iron, and Phosphorus from Spent LiFePO<sub>4</sub> Batteries Using Stoichiometric Sulfuric Acid Leaching System. *ACS Sustainable Chemistry & Engineering* 5, 8017-8024, doi:10.1021/acssuschemeng.7b01594 (2017).
13. Gao, W. et al. Lithium Carbonate Recovery from Cathode Scrap of Spent Lithium-Ion Battery: A Closed-Loop Process. *Environmental Science & Technology* 51, 1662-1669, doi:10.1021/acs.est.6b03320 (2017).
14. Zeng, X., Li, J. & Shen, B. Novel approach to recover cobalt and lithium from spent lithium-ion battery using oxalic acid. *Journal of Hazardous Materials* 295, 112-118, doi:<https://doi.org/10.1016/j.jhazmat.2015.02.064> (2015).
15. Sun, L. & Qiu, K. Organic oxalate as leachant and precipitant for the recovery of valuable metals from spent lithium-ion batteries. *Waste Management* 32, 1575-1582, doi:<https://doi.org/10.1016/j.wasman.2012.03.027> (2012).
16. Sa, Q. et al. Synthesis of high performance LiNi<sub>1/3</sub>Mn<sub>1/3</sub>Co<sub>1/3</sub>O<sub>2</sub> from lithium ion battery recovery stream. *Journal of Power Sources* 282, 140-145, doi:<https://doi.org/10.1016/j.jpowsour.2015.02.046> (2015).
17. Zheng, R. et al. A closed-loop process for recycling LiNi<sub>x</sub>Co<sub>y</sub>Mn<sub>(1-x-y)</sub>O<sub>2</sub> from mixed cathode materials of lithium-ion batteries. *Green Energy & Environment* 2, 42-50, doi:<https://doi.org/10.1016/j.gee.2016.11.010> (2017).
18. Yao, L., Feng, Y. & Xi, G. A new method for the synthesis of LiNi<sub>1/3</sub>Co<sub>1/3</sub>Mn<sub>1/3</sub>O<sub>2</sub> from waste lithium ion batteries. *RSC Advances* 5, 44107-44114, doi:10.1039/C4RA16390G (2015).
19. Zhang, X. et al. Innovative Application of Acid Leaching to Regenerate Li(Ni<sub>1/3</sub>Co<sub>1/3</sub>Mn<sub>1/3</sub>)O<sub>2</sub> Cathodes from Spent Lithium-Ion Batteries. *ACS Sustainable Chemistry & Engineering* 6, 5959-5968, doi:10.1021/acssuschemeng.7b04373 (2018).
20. Bahaloo-Horeh, N. & Mousavi, S. M. Enhanced recovery of valuable metals from spent lithium-ion batteries through optimization of organic acids produced by *Aspergillus niger*. *Waste Management* 60, 666-679, doi:<https://doi.org/10.1016/j.wasman.2016.10.034> (2017).
21. Horeh, N. B., Mousavi, S. M. & Shojaosadati, S. A. Bioleaching of valuable metals from spent lithium-ion mobile phone batteries using *Aspergillus niger*. *Journal of Power Sources* 320, 257-266, doi:<https://doi.org/10.1016/j.jpowsour.2016.04.104> (2016).
22. Wang, F., Sun, R., Xu, J., Chen, Z. & Kang, M. Recovery of cobalt from spent lithium ion batteries using sulphuric acid leaching followed by solid-liquid separation and solvent extraction. *RSC Advances* 6, 85303-85311, doi:10.1039/C6RA16801A (2016).
23. Virolainen, S., Fallah Fini, M., Laitinen, A. & Sainio, T. Solvent extraction fractionation of Li-ion battery leachate containing Li, Ni, and Co. *Separation and Purification Technology* 179, 274-282, doi:<https://doi.org/10.1016/j.seppur.2017.02.010> (2017).
24. Pinna, E. G., Ruiz, M. C., Ojeda, M. W. & Rodriguez, M. H. Cathodes of spent Li-ion batteries: Dissolution with phosphoric acid and recovery of lithium and cobalt from leach liquors. *Hydrometallurgy* 167, 66-71, doi:<https://doi.org/10.1016/j.hydromet.2016.10.024> (2017).
25. Guo, X., Cao, X., Huang, G., Tian, Q. & Sun, H. Recovery of lithium from the effluent obtained in the process of spent lithium-ion batteries recycling. *Journal of Environmental Management* 198, 84-89, doi:<https://doi.org/10.1016/j.jenvman.2017.04.062> (2017).
26. Yang, Y., Xu, S. & He, Y. Lithium recycling and cathode material regeneration from acid leach liquor of spent lithium-ion battery via facile co-extraction and co-precipitation processes. *Waste Management* 64, 219-227, doi:<https://doi.org/10.1016/j.wasman.2017.03.018> (2017).

27. Sa, Q. et al. Synthesis of Diverse  $\text{LiNi}_x\text{Mn}_y\text{Co}_z\text{O}_2$  Cathode Materials from Lithium Ion Battery Recovery Stream. *Journal of Sustainable Metallurgy* 2, 248-256, doi:10.1007/s40831-016-0052-x (2016).
28. Gratz, E., Sa, Q., Apelian, D. & Wang, Y. A closed loop process for recycling spent lithium ion batteries. *Journal of Power Sources* 262, 255-262, doi:https://doi.org/10.1016/j.jpowsour.2014.03.126 (2014).
29. Zou, H., Gratz, E., Apelian, D. & Wang, Y. A novel method to recycle mixed cathode materials for lithium ion batteries. *Green Chemistry* 15, 1183-1191, doi:10.1039/C3GC40182K (2013).
30. Zheng, Z. et al. High Performance Cathode Recovery from Different Electric Vehicle Recycling Streams. *ACS Sustainable Chemistry & Engineering* 6, 13977-13982, doi:10.1021/acssuschemeng.8b02405 (2018).
31. Chen, M. et al. Closed Loop Recycling of Electric Vehicle Batteries to Enable Ultra-high Quality Cathode Powder. *Scientific Reports* 9, 1654, doi:10.1038/s41598-018-38238-3 (2019).
32. Li, L. et al. Process for recycling mixed-cathode materials from spent lithium-ion batteries and kinetics of leaching. *Waste Management* 71, 362-371, doi:https://doi.org/10.1016/j.wasman.2017.10.028 (2018).
33. Li, L. et al. Sustainable Recovery of Cathode Materials from Spent Lithium-Ion Batteries Using Lactic Acid Leaching System. *ACS Sustainable Chemistry & Engineering* 5, 5224-5233, doi:10.1021/acssuschemeng.7b00571 (2017).
34. Shi, Y., Chen, G. & Chen, Z. Effective regeneration of  $\text{LiCoO}_2$  from spent lithium-ion batteries: a direct approach towards high-performance active particles. *Green Chemistry* 20, 851-862, doi:10.1039/C7GC02831H (2018).
35. Shi, Y., Chen, G., Liu, F., Yue, X. & Chen, Z. Resolving the Compositional and Structural Defects of Degraded  $\text{LiNi}_x\text{Co}_y\text{Mn}_z\text{O}_2$  Particles to Directly Regenerate High-Performance Lithium-Ion Battery Cathodes. *ACS Energy Letters* 3, 1683-1692, doi:10.1021/acseenergylett.8b00833 (2018).
36. Song, X. et al. Direct regeneration of cathode materials from spent lithium iron phosphate batteries using a solid phase sintering method. *RSC Advances* 7, 4783-4790, doi:10.1039/C6RA27210J (2017).
37. Li, X., Zhang, J., Song, D., Song, J. & Zhang, L. Direct regeneration of recycled cathode material mixture from scrapped  $\text{LiFePO}_4$  batteries. *Journal of Power Sources* 345, 78-84, doi:https://doi.org/10.1016/j.jpowsour.2017.01.118 (2017).
38. Chen, S. et al. Renovation of  $\text{LiCoO}_2$  with outstanding cycling stability by thermal treatment with  $\text{Li}_2\text{CO}_3$  from spent Li-ion batteries. *Journal of Energy Storage* 8, 262-273, doi:https://doi.org/10.1016/j.est.2016.10.008 (2016).
39. Ganter, M. J., Landi, B. J., Babbitt, C. W., Anctil, A. & Gaustad, G. Cathode refunctionalization as a lithium ion battery recycling alternative. *Journal of Power Sources* 256, 274-280, doi:https://doi.org/10.1016/j.jpowsour.2014.01.078 (2014).
40. Heelan, J. et al. Current and Prospective Li-Ion Battery Recycling and Recovery Processes. *JOM* 68, 2632-2638, doi:10.1007/s11837-016-1994-y (2016).
41. Chen, M., Ma, X., Chen, B., Arsenault, R., Karlson, P., Simon, N. and Wang, Y., 2019. Recycling end-of-life electric vehicle lithium-ion batteries. *Joule*.
42. Ma, X., Chen, M., Chen, B., Meng, Z. and Wang, Y., 2019. High-Performance Graphite Recovered from Spent Lithium-Ion Batteries. *ACS Sustainable Chemistry & Engineering*, 7(24), pp.19732-19738.
43. Chen, B., Ma, X., Chen, M., Bullen, D., Wang, J., Arsenault, R. and Wang, Y., 2019. Systematic Comparison of  $\text{Al}^{3+}$  Modified  $\text{LiNi}_0.6\text{Mn}_0.2\text{Co}_0.2\text{O}_2$  Cathode Material from Recycling Process. *ACS Applied Energy Materials*, 2(12), pp.8818-8825.
44. Battery Test Manual for Plug-In Hybrid Electric Vehicles, INL/EXT-14-32849, Rev 3, September 2014.

45. Xu, Z., Rahman, M.M., Mu, L., Liu, Y. and Lin, F., 2018. Chemomechanical behaviors of layered cathode materials in alkali metal ion batteries. *Journal of Materials Chemistry A*, 6(44), pp.21859-21884.
46. Xia, S., Mu, L., Xu, Z., Wang, J., Wei, C., Liu, L., Pianetta, P., Zhao, K., Yu, X., Lin, F. and Liu, Y., 2018. Chemomechanical interplay of layered cathode materials undergoing fast charging in lithium batteries. *Nano energy*, 53, pp.753-762.

## **Chapter 6. Summary and Recommendations for Future Work**

### **1. Summary**

Lithium-ion batteries (LIBs) are occupied in our daily life, from consumer electronics, energy storage systems to electric vehicles. The recent prosperous market in electric transportation induce enormous interests and this high demand of LIBs will translate into a substantial waste in the end. Therefore, in order to accommodate the incoming end-of-life LIBs, an efficient and mature recycling process needs to be developed. Over the last several years, Prof. Wang's group at Worcester Polytechnic Institute has developed a highly efficient closed-loop recycling process. During my Ph.D. studies, I was focused on recovering high quality cathode materials from end-of-life EV LIBs and the following parts are a brief summary of the research.

First, we summarized the recent innovations in LIBs recycling and provided outlook and suggestions for the future development. The three options for handling end-of-life LIBs, including remanufacturing, repurposing, and recycling, were analyzed. Remanufacturing and repurposing are extending the life of batteries, and recycling closes the loop by returning materials back to the value chain. Pyrometallurgy, hydrometallurgy, and direct recycling are the three recycling processes for spent LIBs. Then we reviewed the most recent improvements both in academia and industry. However, none of the current recycling technologies is perfect, and if they want to make an impact, the challenges need to be overcome. By providing insights and suggestions in this perspective paper, the direction for improvement of lithium-ion battery recycling becomes clear. We hope that with the mutual efforts from academia, industry, and governments, recycling will play a significant role from both ecologic and economic points of view.

There exist several concerns of recruiting recycled materials into industry: scale-up ability, flexibility, trustworthy testing. Hence, the following projects were here to clear the doubt towards our closed-loop recycling process. Scale-up ability was first verified by experiment and the corresponding results were as followed. Instead of dealing with a few grams of end-of-life batteries which is very common in papers, 30kg of spent LIBs from electric vehicles were employed and seven-day experiments were conducted with over 4kg of cathode produced. The recovered cathode powder showed similar performance to commercial powder, and even better at some tests. All of the comparisons were evaluated in coin cells and industrial-level pouch cells. It demonstrated our closed-loop recycling process had the ability to scale up and the further scaling-up development was conducted in Battery Resources. For the flexibility of this recycling process, it was confirmed by intentionally changing the incoming feed of LIBs packs - General Motors, Fiat Chrysler Association, and Ford. As we all know, there were five common cathode materials and manufacturers intent to use a mixture. It leaves a puzzle for LIBs recyclers since the inner chemistry is unknown when battery pack is received. As the results revealed in our experiments, the generated cathode powder was consistent in quality and showed similar physical properties (morphology, particle size distribution, surface area, tap density et al.), electrochemical performance. Here, with intentionally designed experiment, we showed the different incoming chemical compositions had little effect on the recovered powder and proved the good flexibility of our closed-loop recycling process. The rest concern resides in the reliable performance testing. Coin cells were mostly utilized in labs to evaluate the electrochemical performances, however, coin cells were relatively simple and lacked credibility. Therefore, industrial-level cell format and testing need to conduct to deliver meaningful messages to the audience. Here, recycled cathode powder had such superior behavior and the testing was conducted in various industrial-level cell

formats (coin cell, single layer pouch cell, 1Ah cell, 11Ah cell). Especially, in the evaluation of 1Ah cells, the recovered NMC111 remains above 80% after 4,300 cycles and it performs better than results obtained using commercial cathode powder (3,100 cycles). When it comes to the rate performance, recycled materials performed superiorly in every cell format. To sum up, we have proved the scale-up ability and flexibility of our closed-loop recycling process. The performance of our recovered materials was also evaluated in industrial-level cell formats and testing protocols and the side-by-side comparisons with commercial equivalent was conducted. Incorporated with the obvious environmental and economic benefits, we hope it will clear any hesitation to utilize recycled materials in industry.

Layered oxide cathodes with a high nickel content are popular recently because of its high energy density. However, there also exists some serious problems with these materials and coating is a common method to protect the materials during cycling. In our recycling process, we employed two scalable coating method (dry coating and wet coating) on NMC 622 and tried to understand the underling mechanisms. Characterizations include XRD, STEM and XPS were utilized the and the differences of these two coating methods were revealed. Wet coating provided a deep and homogeneous covering and demonstrated a better rate performance. However, it behaved the worst in cycle evaluations and the reason was the exposure to aqueous solution. Even though dry coating provided a discrete covering, it still gave reasonable protection to cathode materials and performed the best among them. Therefore, for improving the durability of Ni-rich NMCs, surface modification method should be chosen wisely and carefully.

## **2. Future Work**

It has shown that our recycled materials have advantageous performance compared with its commercial counterpart, however, the underlying mechanism is still unknown. We have several hypotheses, such as porosity and impurity, however, all of these hypotheses need to be verified either by modeling simulation or post-mortem analysis.

In addition, with the excellent flexibility of our recycling process, different cathode materials can be synthesized and evaluated, such as single-crystal NMCs and lithium, manganese-rich material.

In LIBs, cathode materials account for over 40% of the materials cost, thus, it is reasonable and economical feasible to recycle cathode materials. However, in order to achieve the highest efficiency and become more profitable, other materials in the LIBs need to be recycled. Our group has developed methods to successfully recover anode materials from filter-cake and lithium from leaching solution. The electrolyte, separator, and ammonia (waste solution from co-precipitation reaction) can also be recovered and incorporated into this whole recycling stream.

## Chapter 7. Publications and Presentations

### 1. Publications

- ❖ Chen, M., Ma, X., Chen, B., Arsenault, R., Karlson, P., Simon, N. and Wang, Y., 2019. Recycling End-of-Life Electric Vehicle Lithium-Ion Batteries. *Joule*.
- ❖ Chen, M.\*, Zheng, Z., Wang, Q., Zhang, Y., Ma, X., Shen, C., Xu, D., Liu, J., Liu, Y., Gionet, P. and O'Connor, I., 2019. Closed Loop Recycling of Electric Vehicle Batteries to Enable Ultra-high Quality Cathode Powder. *Scientific reports*, 9(1), p.1654.
- ❖ Zheng, Z., Chen, M.\*, Wang, Q., Zhang, Y., Ma, X., Shen, C., Xu, D., Liu, J., Liu, Y., Gionet, P. and O'Connor, I., 2018. High Performance Cathode Recovery from Different Electric Vehicle Recycling Streams. *ACS Sustainable Chemistry & Engineering*, 6(11), pp.13977-13982.
- ❖ Chen, B., Ma, X., Chen, M.\*, Bullen, D., Wang, J., Arsenault, R. and Wang, Y., 2019. Systematic Comparison of Al<sup>3+</sup> Modified LiNi<sub>0.6</sub>Mn<sub>0.2</sub>Co<sub>0.2</sub>O<sub>2</sub> Cathode Material from Recycling Process. *ACS Applied Energy Materials*, 2(12), pp.8818-8825.
- ❖ Ma, X., Chen, M., Chen, B., Meng, Z. and Wang, Y., 2019. High-Performance Graphite Recovered from Spent Lithium-Ion Batteries. *ACS Sustainable Chemistry & Engineering*, 7(24), pp.19732-19738.
- ❖ Heelan, J., Gratz, E., Zheng, Z., Wang, Q., Chen, M., Apelian, D. and Wang, Y., 2016. Current and prospective Li-ion battery recycling and recovery processes. *JOM*, 68(10), pp.2632-2638.
- ❖ Zhang, R., Zheng, Y., Yao, Z., Vanaphuti, P., Ma, X., Bong, S., Chen, M., Liu, Y., Feng, C., Yang, Z., Wang, Y.. Systematic study of Al impurity for NCM622 cathode materials. In review.
- ❖ Chen, M., Wang, Y.. Systematic Electrochemical Comparisons between Recycled NMC Powder with Commercially Controlled Powder. To be submitted.

\*represents first co-coauthor

## 2. Presentations

- ❖ 2019 MRS Fall Meeting and Exhibit (Oral presentation)

Title: NMC Cathode Materials with Outstanding Performance Generated by a Closed-Loop Recycling Process

- ❖ 2018 MRS Fall Meeting and Exhibit (Oral presentation)

Title: Closed Loop Recycling of Electric Vehicle Batteries to Enable Ultra-high Quality Cathode Powder

- ❖ 2018 255th ACS National Meeting (Invited talk)

Title: Closed loop recycling process for lithium ion batteries

- ❖ 2018 Cabot Student Material Research Forum (Poster)

Title: Growth Mechanism of  $\text{LiNi}_{1/3}\text{Mn}_{1/3}\text{Co}_{1/3}\text{O}_2$  Precursor Particles

- ❖ 2017 MRS Fall Meeting and Exhibit (Poster)

Title: Growth Mechanism of  $\text{LiNi}_{1/3}\text{Mn}_{1/3}\text{Co}_{1/3}\text{O}_2$  Precursor Particles